Density Model for Melon-Headed Whale (*Peponocephala electra*) for the U.S. Gulf of Mexico: Supplementary Report

Duke University Marine Geospatial Ecology Lab*

Model Version 1.4 - 2015-10-01

Citation

When referencing our methodology or results generally, please cite our open-access article:

Roberts JJ, Best BD, Mannocci L, Fujioka E, Halpin PN, Palka DL, Garrison LP, Mullin KD, Cole TVN, Khan CB, McLellan WM, Pabst DA, Lockhart GG (2016) Habitat-based cetacean density models for the U.S. Atlantic and Gulf of Mexico. Scientific Reports 6: 22615. doi: 10.1038/srep22615

To reference this specific model or Supplementary Report, please cite:

Roberts JJ, Best BD, Mannocci L, Fujioka E, Halpin PN, Palka DL, Garrison LP, Mullin KD, Cole TVN, Khan CB, McLellan WM, Pabst DA, Lockhart GG (2015) Density Model for Melon-Headed Whale (*Peponocephala electra*) for the U.S. Gulf of Mexico Version 1.4, 2015-10-01, and Supplementary Report. Marine Geospatial Ecology Lab, Duke University, Durham, North Carolina.

Copyright and License

Revision History

Version	Date	Description of changes
1	2015-01-22	Initial version.
1.1	2015-02-02	Updated the documentation. No changes to the model.
1.2	2015-03-06	Updated the documentation. No changes to the model.
1.3	2015-05-14	Updated calculation of CVs. Switched density rasters to logarithmic breaks. No changes to the model.
1.4	2015-10-01	Updated the documentation. No changes to the model.

*For questions, or to offer feedback about this model or report, please contact Jason Roberts (jason.roberts@duke.edu)

Survey Data

Survey	Period	Length (1000 km)	Hours	Sightings
SEFSC GOMEX92-96 Aerial Surveys	1992-1996	27	152	0
SEFSC Gulf of Mexico Shipboard Surveys, 2003-2009	2003-2009	19	1156	6
SEFSC GulfCet I Aerial Surveys	1992-1994	50	257	4
SEFSC GulfCet II Aerial Surveys	1996-1998	22	124	0
SEFSC GulfSCAT 2007 Aerial Surveys	2007-2007	18	95	0
SEFSC Oceanic CetShip Surveys	1992-2001	49	3102	18
SEFSC Shelf CetShip Surveys	1994-2001	10	707	1
Total		195	5593	29

Table 2: Survey effort and sightings used in this model. Effort is tallied as the cumulative length of on-effort transects and hours the survey team was on effort. Sightings are the number of on-effort encounters of the modeled species for which a perpendicular sighting distance (PSD) was available. Off effort sightings and those without PSDs were omitted from the analysis.

Period	Length (1000 km)	Hours	Sightings
1992-2009	195	5592	29
1998-2009	62	2679	14
% Lost	68	52	52

Table 3: Survey effort and on-effort sightings having perpendicular sighting distances. % Lost shows the percentage of effort or sightings lost by restricting the analysis to surveys performed in 1998 and later, the era in which remotely-sensed chlorophyll and derived productivity estimates are available. See Figure 1 for more information.

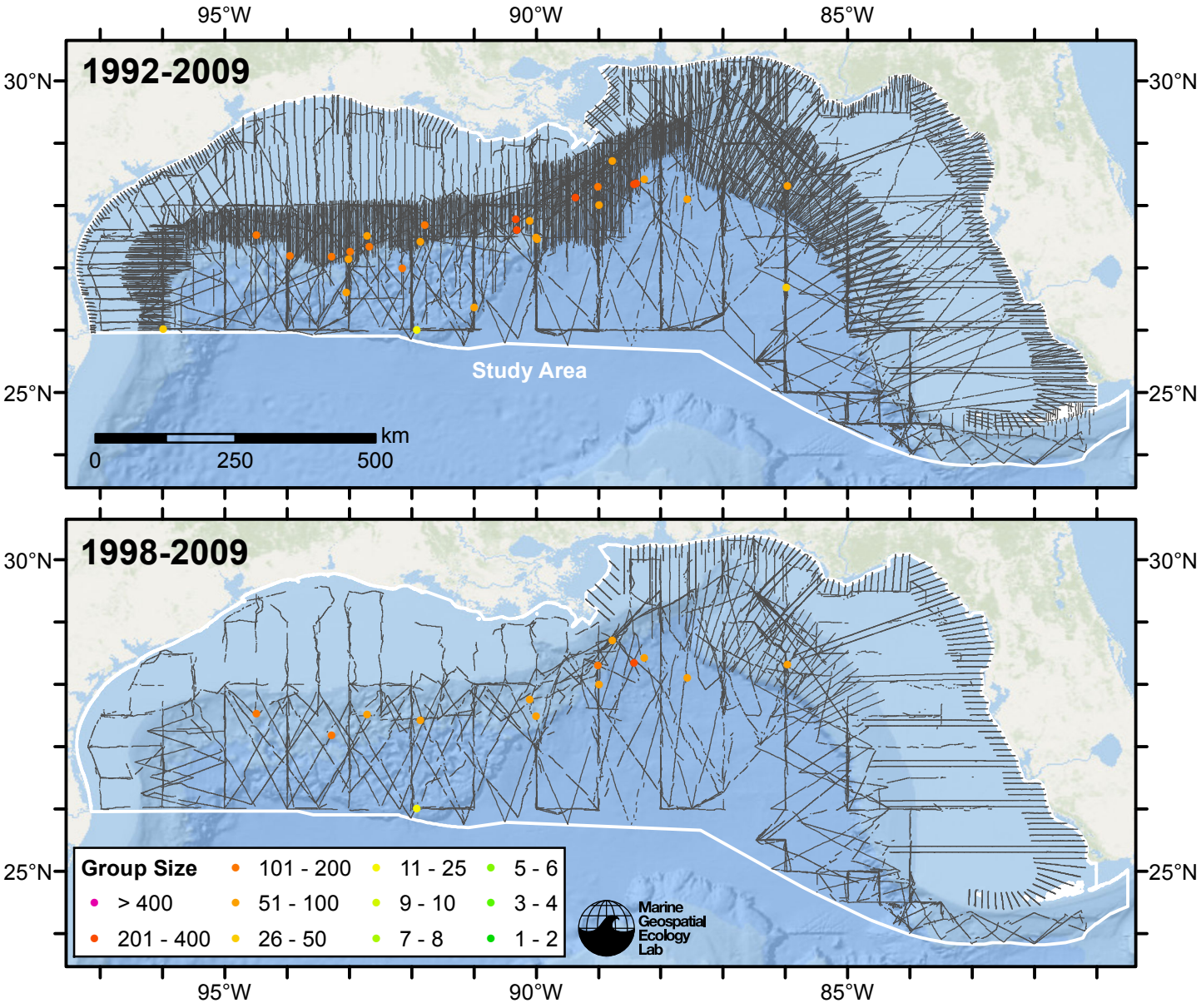

Figure 1: Melon-headed whale sightings and survey tracklines. The top map shows all surveys. The bottom map shows surveys performed in 1998 or later. the era in which remotely-sensed chlorophyll and derived productivity estimates are available. Models fitted to contemporaneous (day-of-sighting) estimates of those predictors only utilize these surveys. These maps illustrate the survey data lost in order to utilize those predictors. Models fitted to climatogical estimates of those predictors do not suffer this data loss.

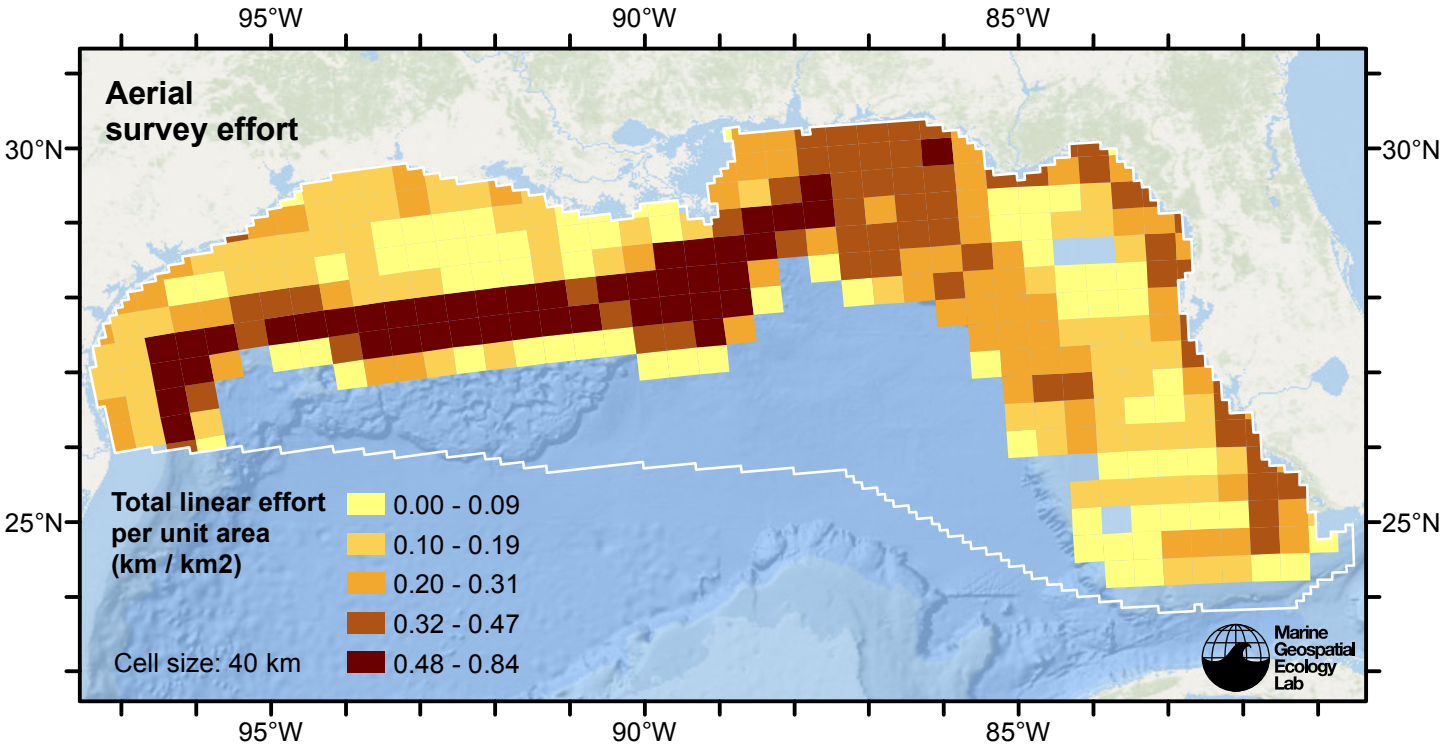

Figure 2: Aerial linear survey effort per unit area.

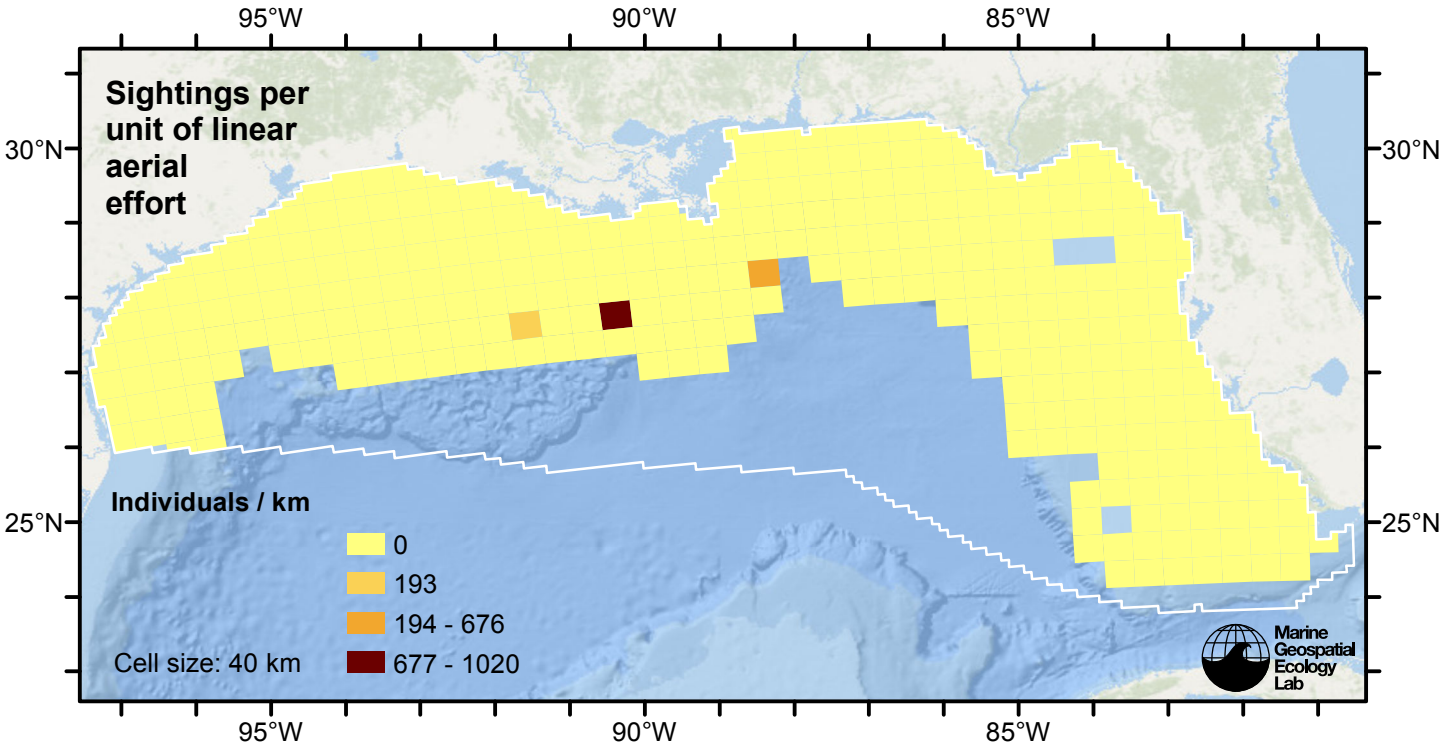

Figure 3: Melon-headed whale sightings per unit aerial linear survey effort.

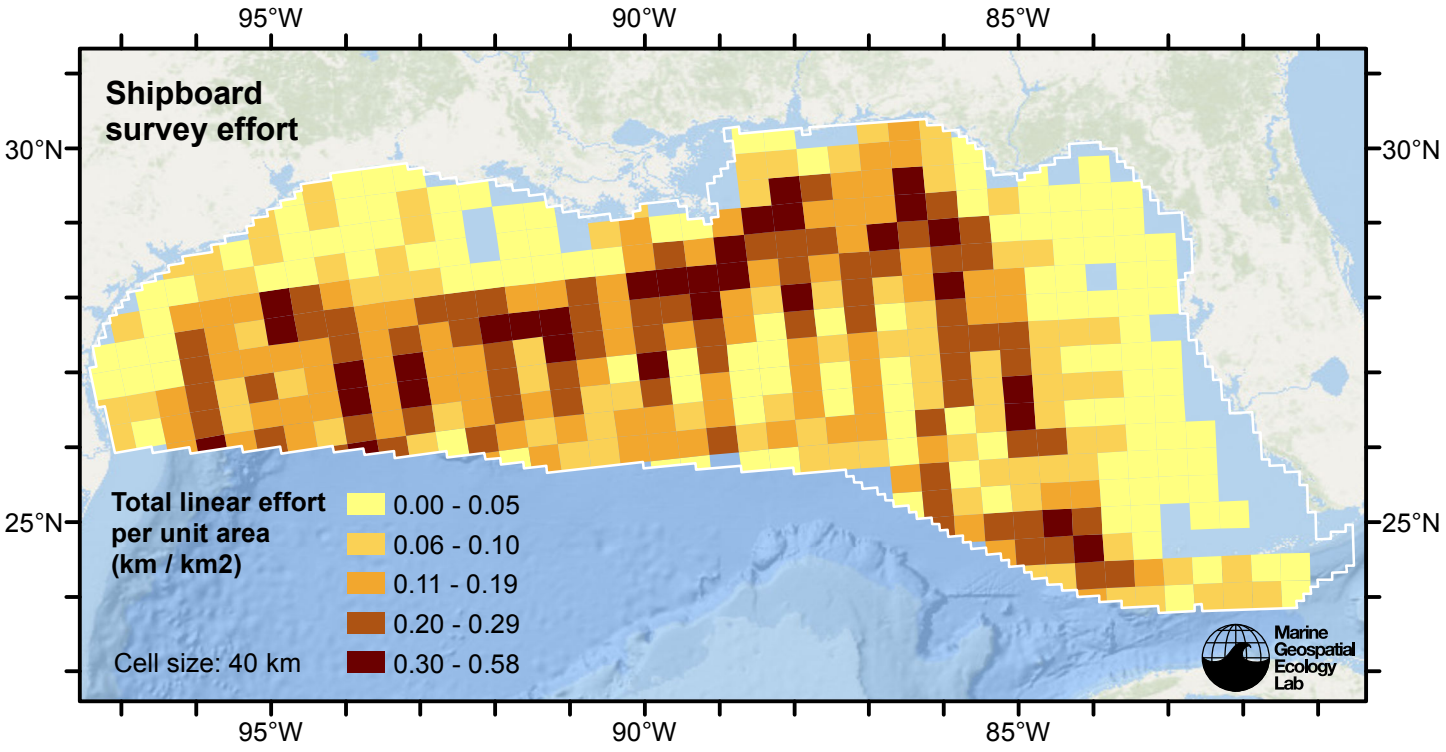

Figure 4: Shipboard linear survey effort per unit area.

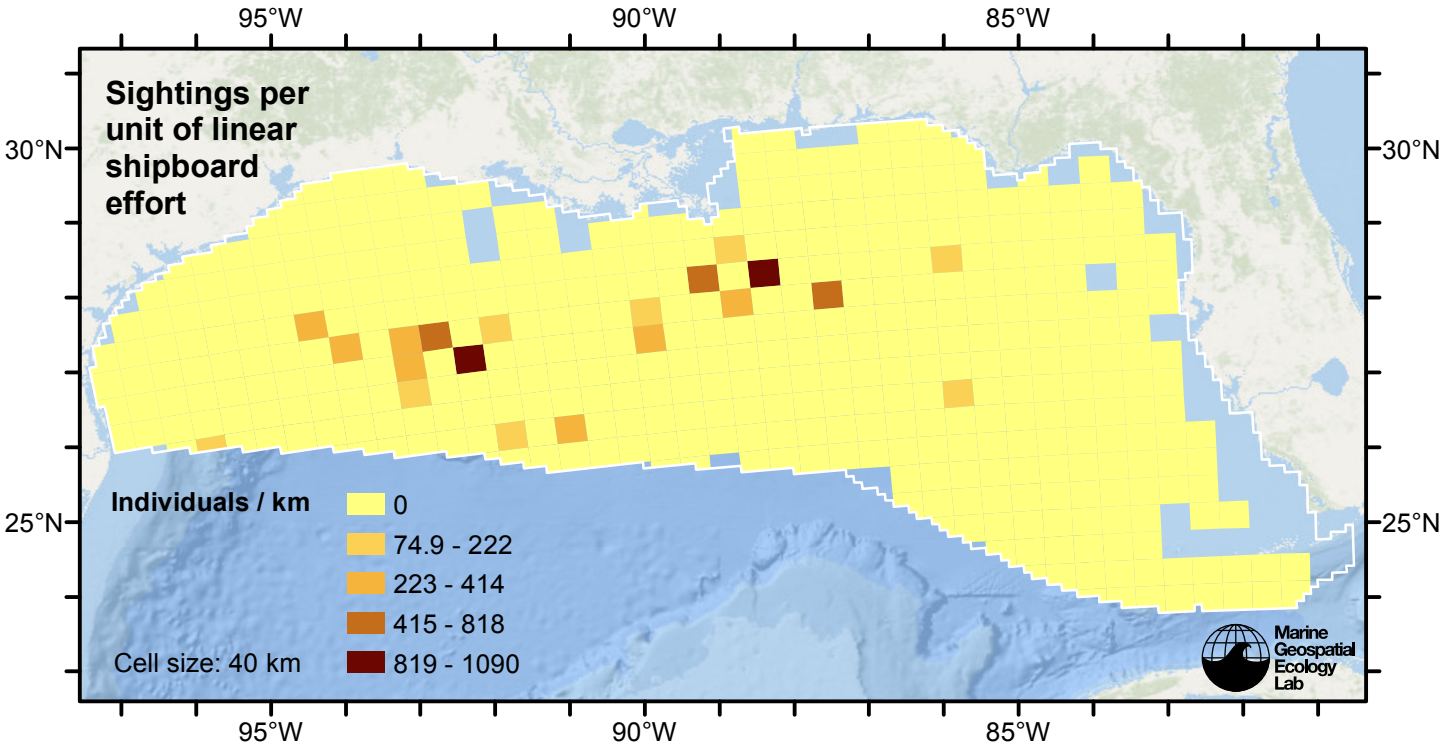

Figure 5: Melon-headed whale sightings per unit shipboard linear survey effort.

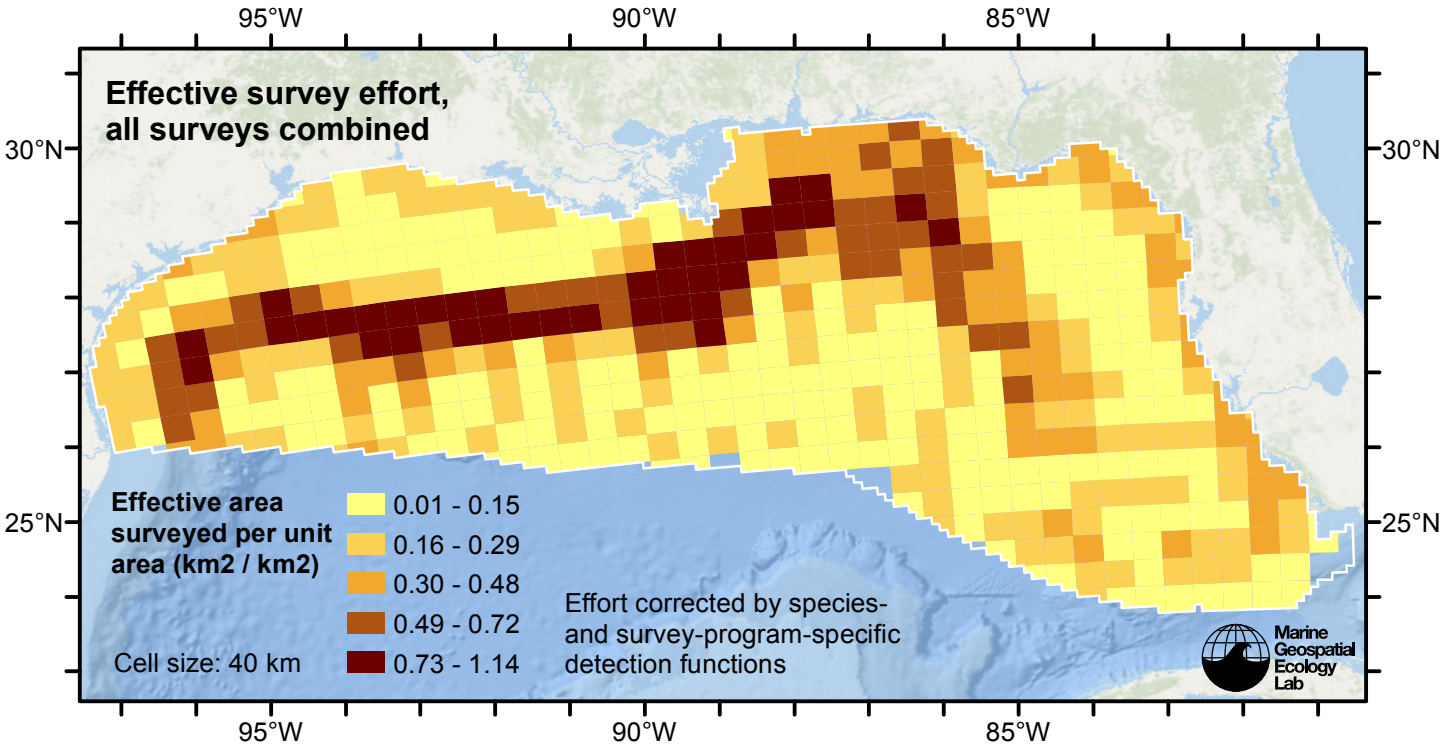

Figure 6: Effective survey effort per unit area, for all surveys combined. Here, effort is corrected by the species- and survey-program-specific detection functions used in fitting the density models.

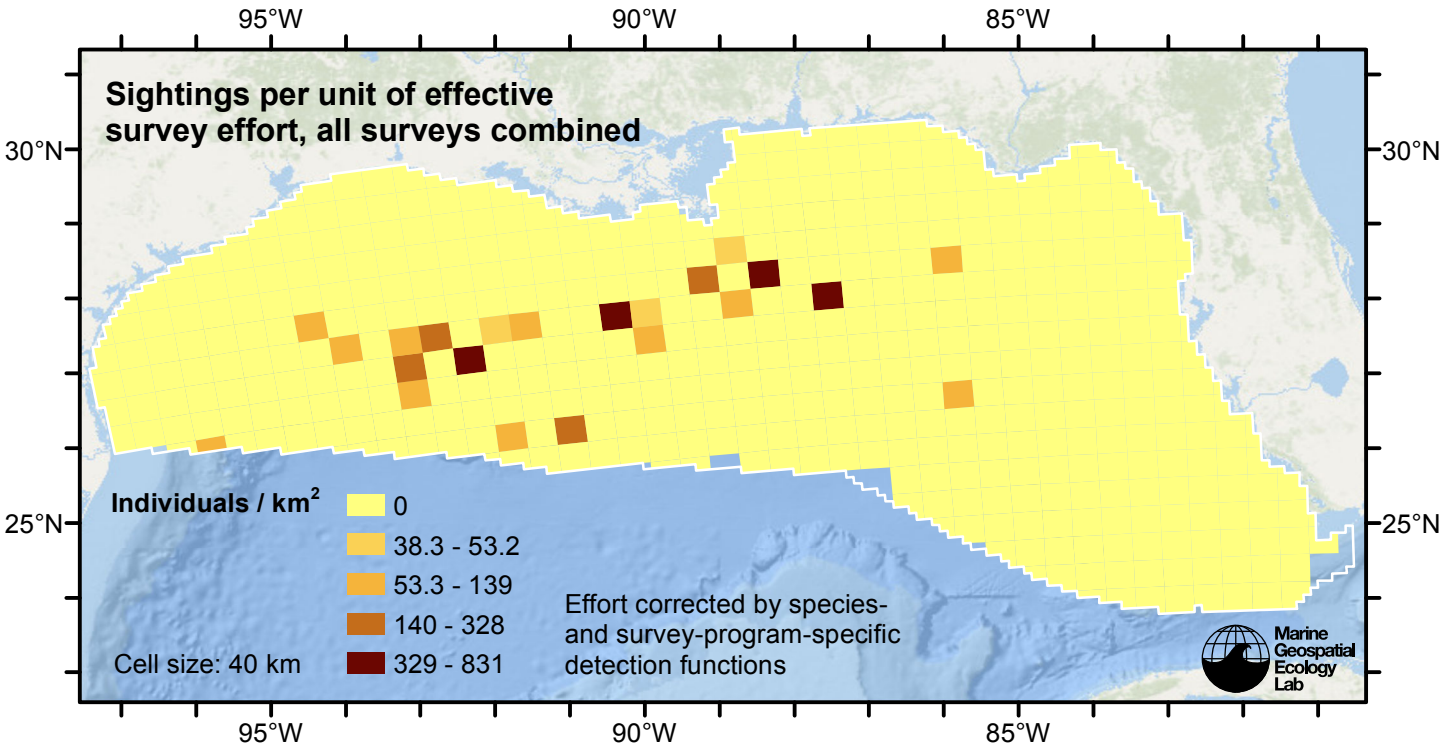

Figure 7: Melon-headed whale sightings per unit of effective survey effort, for all surveys combined. Here, effort is corrected by the species- and survey-program-specific detection functions used in fitting the density models.

Reclassification of Ambiguous Sightings

Observers occasionally experience difficulty identifying species, due to poor sighting conditions or phenotypic similarities between the possible choices. For example, observers may not always be able to distinguish fin whales from sei whales (Tim Cole, pers. comm.). When this happens, observers will report an ambiguous identification, such as "fin or sei whale".

In our density models, we handled ambiguous identifications in three ways:

1. For sightings with very generic identifications such as "large whale", we discarded the sightings. These sightings represented a clear minority when compared to those with definitive species identifications, but they are uncounted animals and our density models may therefore underestimate density to some degree.
2. For sightings of certain taxa in which a large majority of identifications were ambiguous (e.g. "Globicephala spp.") rather than specific (e.g. "Globicephala melas" or "Globicephala macrorhynchus"), it was not tractable to model the individual species so we modeled the generic taxon instead.
3. For sightings that reported an ambiguous identification of two species (e.g. "fin or sei whale") that are known to exhibit different habitat preferences or typically occur in different group sizes, and for which we had sufficient number of definitive sightings of both species, we fitted a predictive model that classified the ambiguous sightings into one species or the other.

This section describes how we utilized the third category of ambiguous sightings in the density models presented in this report.

For the predictive model, we used the cforest classifier (Hothorn et al. 2006), an elaboration of the classic random forest classifier (Breiman, 2001). First, we trained a binary classifier using the sightings that reported definitive species identifications (e.g. "fin whale" and "sei whale"). The training data included all on-effort sightings, not just those in the focal study area. We used the species ID as the response variable and oceanographic variables or group size as predictor variables, depending on the species. We used receiver operating characteristic (ROC) curve analysis to select a threshold for classifying the probabilistic predictions of species identifications made by the model into a binary result of one species or another; for the threshold, we selected the value that maximized the Youden index (see Perkins and Schisterman, 2006).

Then, for all sightings reporting the ambiguous identification, we reclassified the sighting as either one species or the other by processing the predictor values observed for that sighting through the fitted model. We then included the reclassified sightings in the detection functions and spatial models of density. The sightings reported elsewhere in this document incorporate both the definitive sightings and the reclassified sightings.

Reclassification of "Feresa attenuata/Peponocephala electra" in the Gulf of Mexico Region

Density Histograms

These plots show the per-species distribution of each predictor variable used in the reclassification model. When a variable exhibits a substantially different distribution for each species, it is a good candidate for classifying ambiguous sightings as one species or the other.

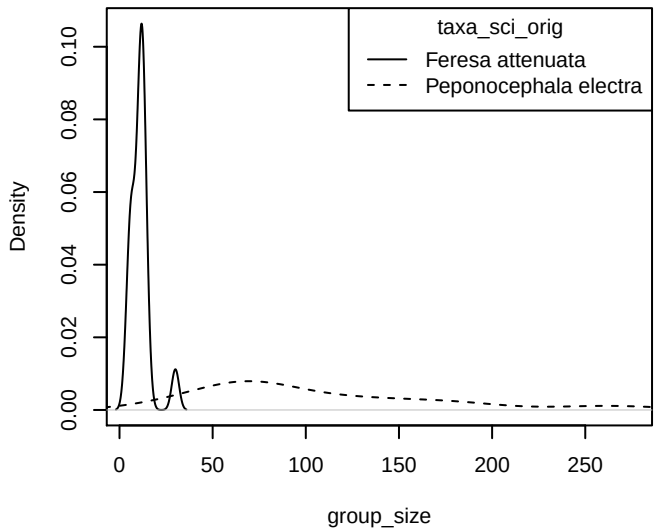

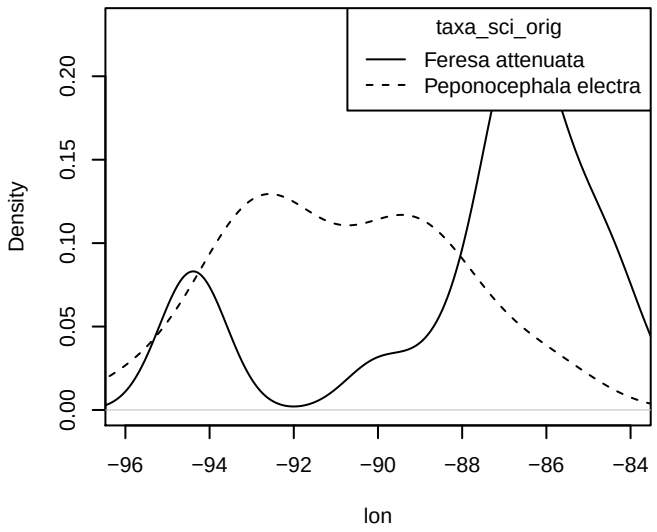

Statistical output

```
MODEL SUMMARY:
==============

     Random Forest using Conditional Inference Trees

Number of trees:  1000

Response:  factor(taxa_sci_orig)
Inputs:  group_size, lon
Number of observations:  43

Number of variables tried at each split: 5

Estimated predictor variable importance (conditional = FALSE):

           Importance
group_size    0.40973
lon           0.00633

MODEL PERFORMANCE SUMMARY:
==========================

Statistics calculated from the training data.

Area under the ROC curve (auc)           = 1.000
Mean cross-entropy (mxe)                 = 0.076
Precision-recall break-even point (prbe) = 1.000
Root-mean square error (rmse)            = 0.133

Cutoff selected by maximizing the Youden index = 0.695

Confusion matrix for that cutoff:

                              Actual Peponocephala electra  Actual Feresa attenuata  Total
Predicted Peponocephala electra                           25                        0     25
Predicted Feresa attenuata                                 0                       18     18
Total                                                     25                       18     43
```

```
Model performance statistics for that cutoff:

Accuracy (acc)                                = 1.000
Error rate (err)                              = 0.000
Rate of positive predictions (rpp)            = 0.581
Rate of negative predictions (rnp)            = 0.419

True positive rate (tpr, or sensitivity)      = 1.000
False positive rate (fpr, or fallout)         = 0.000
True negative rate (tnr, or specificity)      = 1.000
False negative rate (fnr, or miss)            = 0.000

Positive prediction value (ppv, or precision) = 1.000
Negative prediction value (npv)               = 1.000
Prediction-conditioned fallout (pcfall)       = 0.000
Prediction-conditioned miss (pcmiss)          = 0.000

Matthews correlation coefficient (mcc)        = 1.000
Odds ratio (odds)                             = Inf
SAR                                           = 0.711

Cohen's kappa (K)                             = 1.000
```

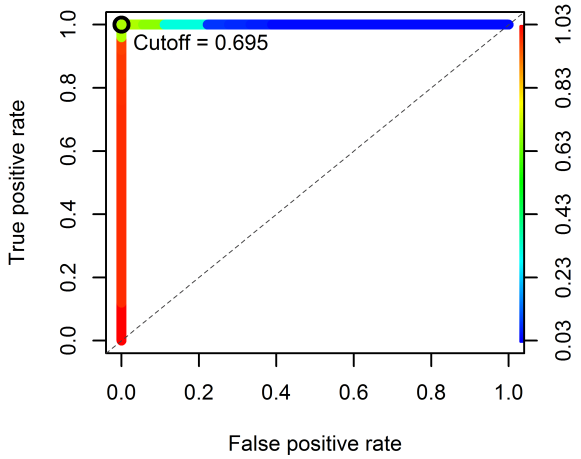

Figure 8: Receiver operating characteristic (ROC) curve illustrating the predictive performance of the model used to reclassify "Feresa attenuata/Peponocephala electra" sightings into one species or the other.

Reclassifications Performed

Survey	Definitive P. electra Sightings	Definitive F. attenuata Sightings	Ambiguous Sightings	Reclassed to P. electra	Reclassed to F. attenuata
SEFSC Gulf of Mexico Shipboard Surveys, 2003-2009	6	7	1	0	1
SEFSC GulfCet I Aerial Surveys	0	0	9	5	4
SEFSC GulfCet II Aerial Surveys	0	3	0	0	0

SEFSC Oceanic CetShip Surveys	18	8	4	0	4
SEFSC Shelf CetShip Surveys	1	0	0	0	0
Total	25	18	14	5	9

Table 4: Counts of definitive sightings, ambiguous sightings, and what the ambiguous sightings were reclassified to. Note that this analysis was performed on all on-effort sightings, not just those in the focal study area. These counts may therefore be larger than those presented in the Survey Data section of this report, which are restricted to the focal study area.

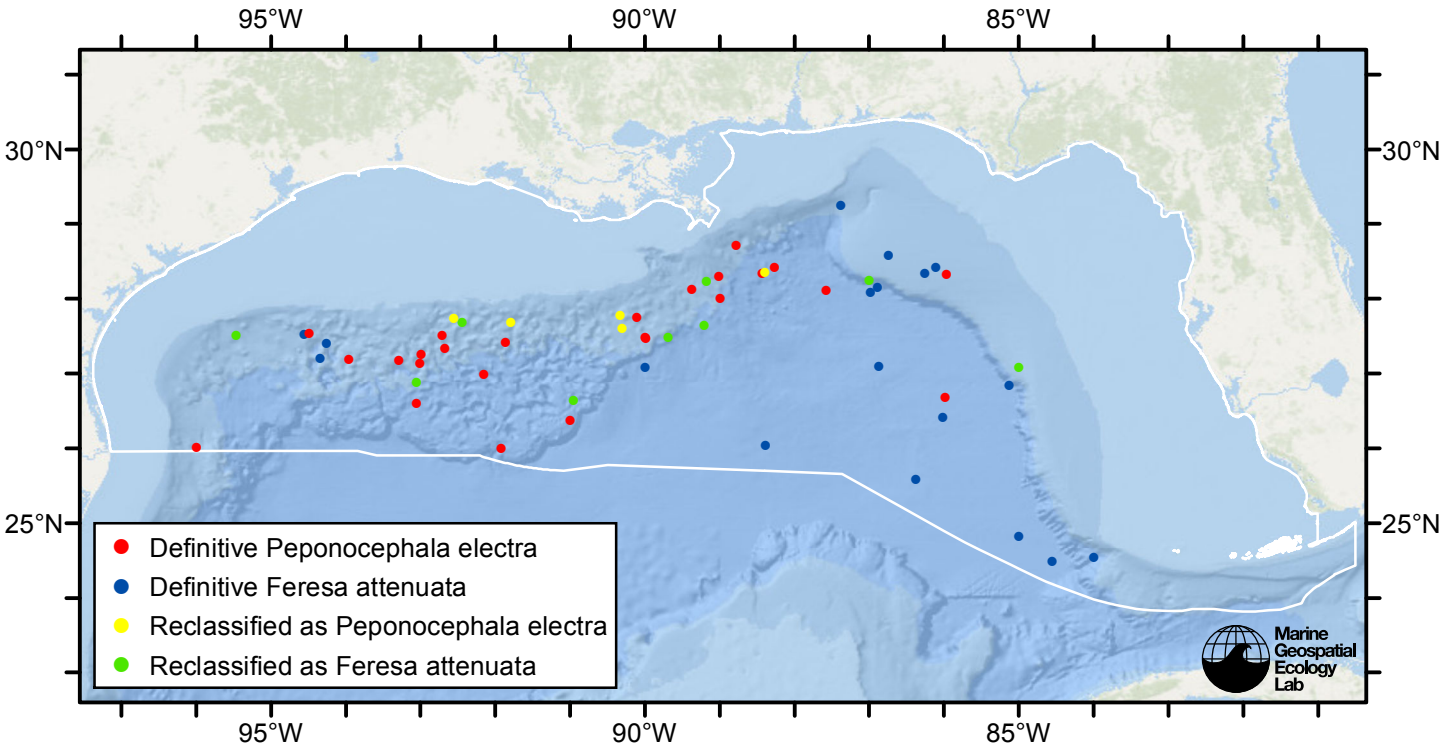

Figure 9: Definitive sightings used to train the model and ambiguous sightings reclassified by the model, by season.

Detection Functions

The detection hierarchy figures below show how sightings from multiple surveys were pooled to try to achieve Buckland et. al's (2001) recommendation that at least 60-80 sightings be used to fit a detection function. Leaf nodes, on the right, usually represent individual surveys, while the hierarchy to the left shows how they have been grouped according to how similar we believed the surveys were to each other in their detection performance.

At each node, the red or green number indicates the total number of sightings below that node in the hierarchy, and is colored green if 70 or more sightings were available, and red otherwise. If a grouping node has zero sightings–i.e. all of the surveys within it had zero sightings–it may be collapsed and shown as a leaf to save space.

Each histogram in the figure indicates a node where a detection function was fitted. The actual detection functions do not appear in this figure; they are presented in subsequent sections. The histogram shows the frequency of sightings by perpendicular sighting distance for all surveys contained by that node. Each survey (leaf node) recieves the detection function that is closest to it up the hierarchy. Thus, for common species, sufficient sightings may be available to fit detection functions deep in the hierarchy, with each function applying to only a few surveys, thereby allowing variability in detection performance between surveys to be addressed relatively finely. For rare species, so few sightings may be available that we have to pool many surveys together to try to meet Buckland's recommendation, and fit only a few coarse detection functions high in the hierarchy.

A blue Proxy Species tag indicates that so few sightings were available that, rather than ascend higher in the hierarchy to a point that we would pool grossly-incompatible surveys together, (e.g. shipboard surveys that used big-eye binoculars with those that used only naked eyes) we pooled sightings of similar species together instead. The list of species pooled is given in following sections.

Shipboard Surveys

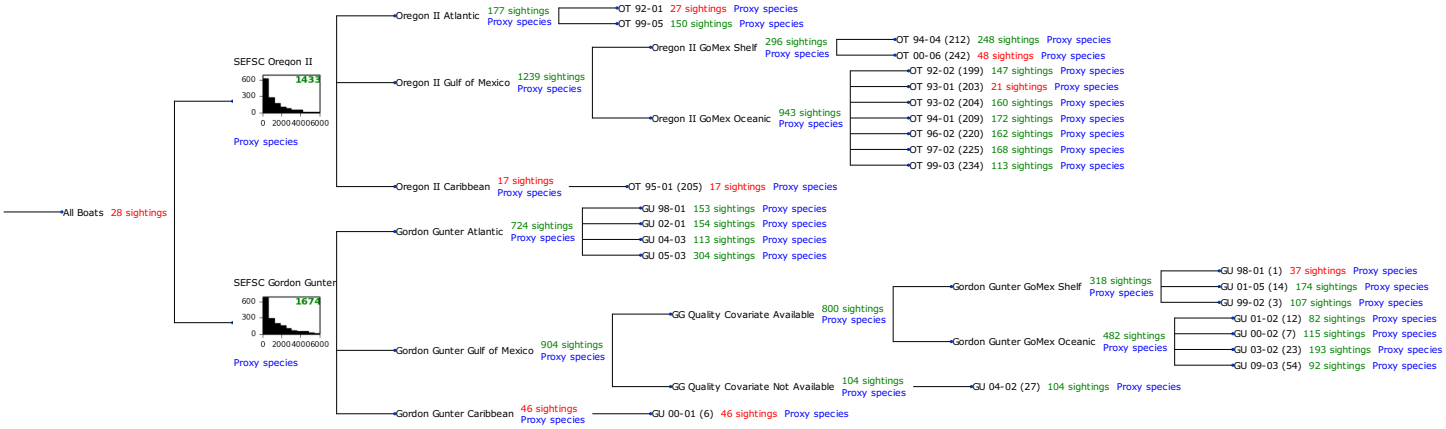

Figure 10: Detection hierarchy for shipboard surveys

SEFSC Oregon II

Because this taxon was sighted too infrequently to fit a detection function to its sightings alone, we fit a detection function to the pooled sightings of several other species that we believed would exhibit similar detectability. These "proxy species" are listed below.

Reported By Observer	Common Name	n
Delphinus capensis	Long-beaked common dolphin	0
Delphinus delphis	Short-beaked common dolphin	2
Delphinus delphis/Lagenorhynchus acutus	Short-beaked common or Atlantic white-sided dolphin	0
Delphinus delphis/Stenella	Short-beaked common dolphin or Stenella spp.	0
Delphinus delphis/Stenella coeruleoalba	Short-beaked common or striped dolphin	0
Feresa attenuata	Pygmy killer whale	11
Grampus griseus	Risso's dolphin	156
Grampus griseus/Tursiops truncatus	Risso's or Bottlenose dolphin	0
Lagenodelphis hosei	Fraser's dolphin	3
Lagenorhynchus acutus	Atlantic white-sided dolphin	0
Lagenorhynchus albirostris	White-beaked dolphin	0
Lagenorhynchus albirostris/Lagenorhynchus acutus	White-beaked or white-sided dolphin	0
Peponocephala electra	Melon-headed whale	13
Stenella	Unidentified Stenella	17
Stenella attenuata	Pantropical spotted dolphin	347
Stenella attenuata/frontalis	Pantropical or Atlantic spotted dolphin	0
Stenella clymene	Clymene dolphin	44

Stenella coeruleoalba	Striped dolphin	48
Stenella frontalis	Atlantic spotted dolphin	242
Stenella frontalis/Tursiops truncatus	Atlantic spotted or Bottlenose dolphin	0
Stenella longirostris	Spinner dolphin	38
Steno bredanensis	Rough-toothed dolphin	22
Steno bredanensis/Tursiops truncatus	Bottlenose or rough-toothed dolphin	0
Tursiops truncatus	Bottlenose dolphin	490
Total		1433

Table 5: Proxy species used to fit detection functions for SEFSC Oregon II. The number of sightings, n, is before truncation.

The sightings were right truncated at 5000m.

Covariate	Description
beaufort	Beaufort sea state.
quality	Survey-specific index of the quality of observation conditions, utilizing relevant factors other than Beaufort sea state (see methods).
size	Estimated size (number of individuals) of the sighted group.

Table 6: Covariates tested in candidate "multi-covariate distance sampling" (MCDS) detection functions.

Key	Adjustment	Order	Covariates	Succeeded	Δ AIC	Mean ESHW (m)
hr			beaufort, size	Yes	0.00	867
hr			quality, size	Yes	3.65	790
hr			size	Yes	40.44	738
hr			beaufort, quality	Yes	54.00	598
hr			quality	Yes	78.89	556
hr			beaufort	Yes	96.10	523
hr	poly	4		Yes	101.63	515
hr	poly	2		Yes	109.37	538
hr				Yes	125.96	475
hn	cos	3		Yes	346.75	1367
hn	cos	2		Yes	350.33	1525
hn			beaufort, quality, size	Yes	392.90	1971
hn			quality, size	Yes	413.78	1967
hn			beaufort, size	Yes	445.02	1998
hn			beaufort, quality	Yes	454.89	1948
hn			quality	Yes	464.32	1951
hn			size	Yes	465.68	1991

hn			beaufort	Yes	524.83	1961
hn				Yes	533.10	1963
hn	herm	4		No		
hr			beaufort, quality, size	No		

Table 7: Candidate detection functions for SEFSC Oregon II. The first one listed was selected for the density model.

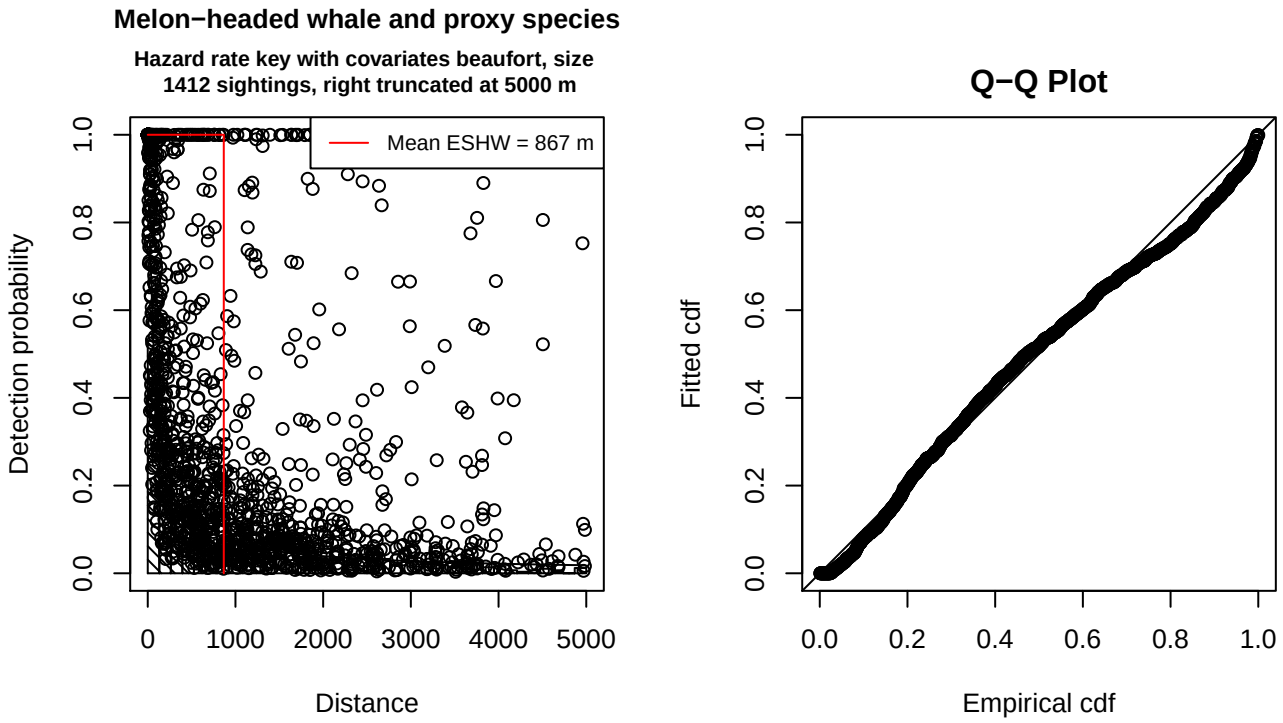

Figure 11: Detection function for SEFSC Oregon II that was selected for the density model

Statistical output for this detection function:

```
Summary for ds object
Number of observations :  1412
Distance range         :  0  -  5000
AIC                    :  22270.99

Detection function:
 Hazard-rate key function

Detection function parameters
Scale Coefficients:
             estimate         se
(Intercept)  5.1928930 0.21118617
beaufort    -0.5654155 0.06792705
size         2.3308851 0.22444978

Shape parameters:
            estimate         se
```

```
(Intercept)        0 0.03443879

                         Estimate           SE        CV
Average p            6.393312e-02 6.600196e-03 0.1032359
N in covered region 2.208558e+04 2.357900e+03 0.1067620
```

Additional diagnostic plots:

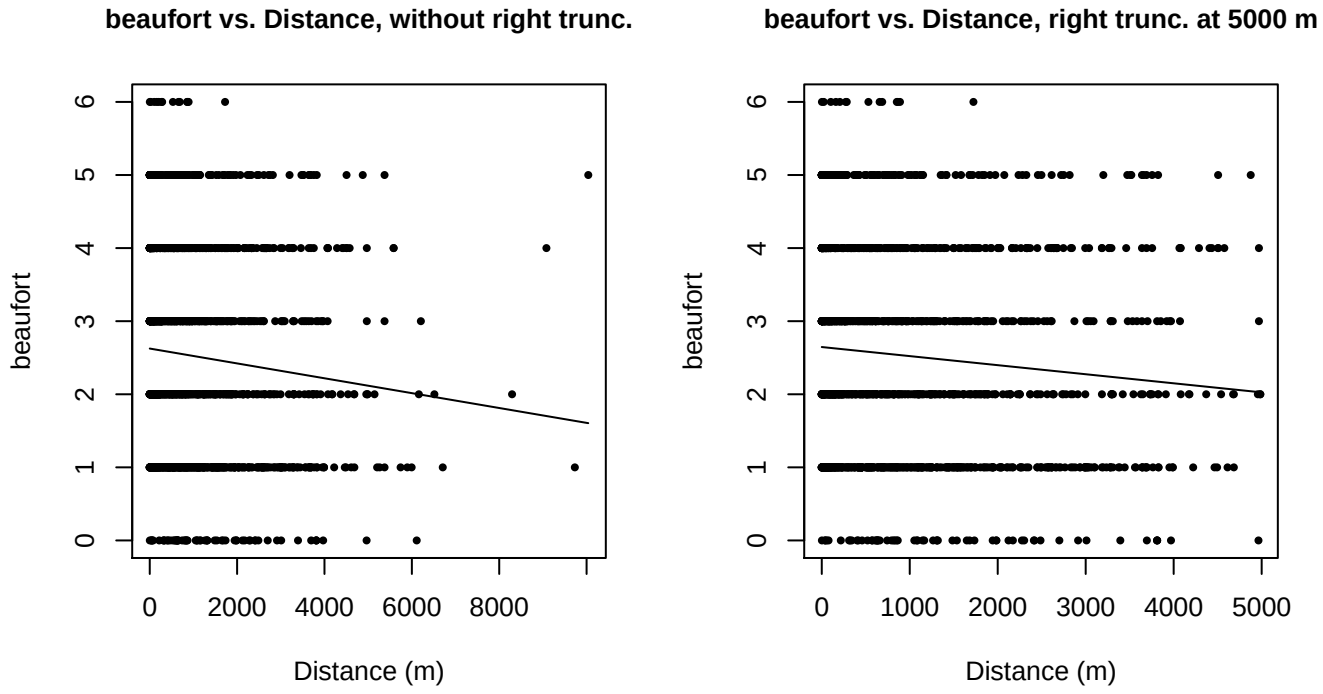

Figure 12: Scatterplots showing the relationship between Beaufort sea state and perpendicular sighting distance, for all sightings (left) and only those not right truncated (right). The line is a simple linear regression.

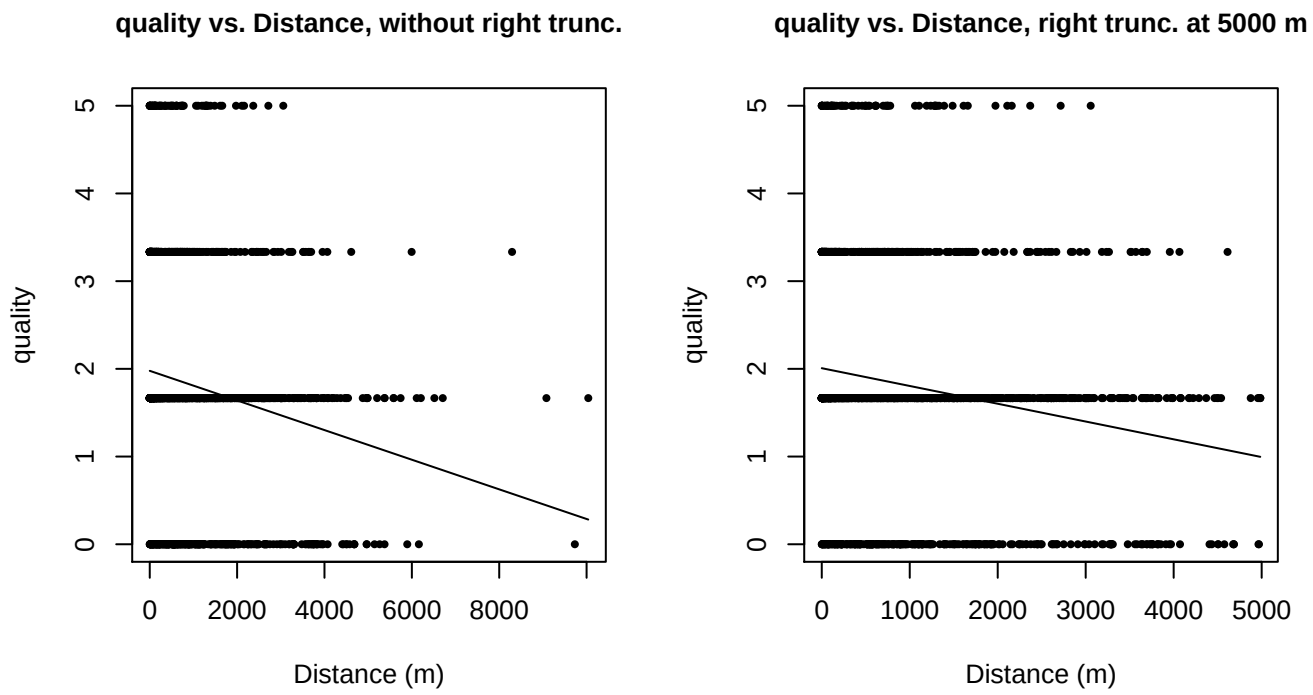

Figure 13: Scatterplots showing the relationship between the survey-specific index of the quality of observation conditions and perpendicular sighting distance, for all sightings (left) and only those not right truncated (right). Low values of the quality index correspond to better observation conditions. The line is a simple linear regression.

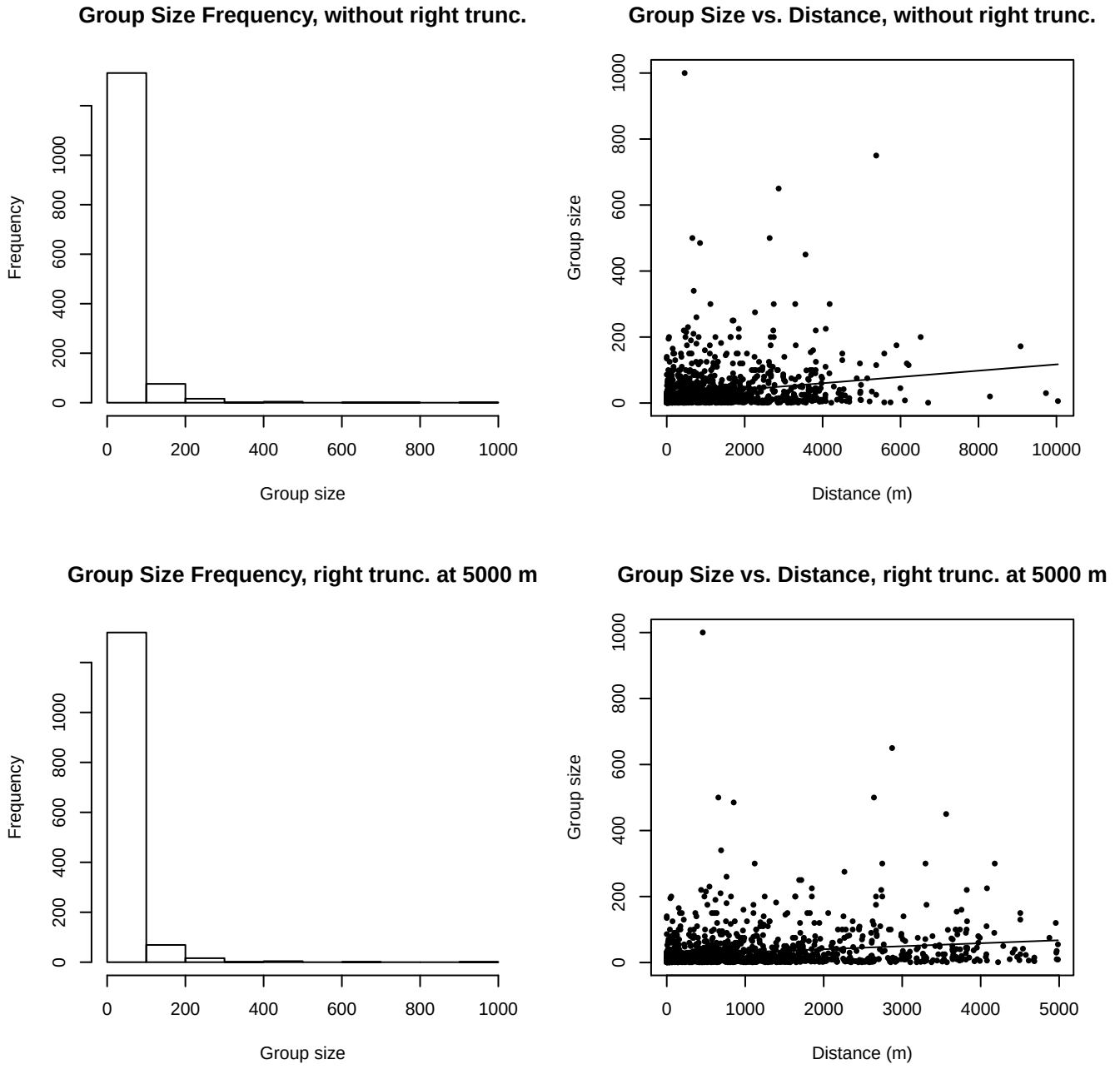

Figure 14: Histograms showing group size frequency and scatterplots showing the relationship between group size and perpendicular sighting distance, for all sightings (top row) and only those not right truncated (bottom row). In the scatterplot, the line is a simple linear regression.

SEFSC Gordon Gunter

Because this taxon was sighted too infrequently to fit a detection function to its sightings alone, we fit a detection function to the pooled sightings of several other species that we believed would exhibit similar detectability. These "proxy species" are listed below.

Reported By Observer	Common Name	n
Delphinus capensis	Long-beaked common dolphin	9
Delphinus delphis	Short-beaked common dolphin	35

Delphinus delphis/Lagenorhynchus acutus	Short-beaked common or Atlantic white-sided dolphin	0
Delphinus delphis/Stenella	Short-beaked common dolphin or Stenella spp.	0
Delphinus delphis/Stenella coeruleoalba	Short-beaked common or striped dolphin	0
Feresa attenuata	Pygmy killer whale	14
Grampus griseus	Risso's dolphin	129
Grampus griseus/Tursiops truncatus	Risso's or Bottlenose dolphin	0
Lagenodelphis hosei	Fraser's dolphin	1
Lagenorhynchus acutus	Atlantic white-sided dolphin	0
Lagenorhynchus albirostris	White-beaked dolphin	0
Lagenorhynchus albirostris/Lagenorhynchus acutus	White-beaked or white-sided dolphin	0
Peponocephala electra	Melon-headed whale	15
Stenella	Unidentified Stenella	30
Stenella attenuata	Pantropical spotted dolphin	303
Stenella attenuata/frontalis	Pantropical or Atlantic spotted dolphin	0
Stenella clymene	Clymene dolphin	29
Stenella coeruleoalba	Striped dolphin	78
Stenella frontalis	Atlantic spotted dolphin	376
Stenella frontalis/Tursiops truncatus	Atlantic spotted or Bottlenose dolphin	1
Stenella longirostris	Spinner dolphin	24
Steno bredanensis	Rough-toothed dolphin	24
Steno bredanensis/Tursiops truncatus	Bottlenose or rough-toothed dolphin	0
Tursiops truncatus	Bottlenose dolphin	606
Total		1674

Table 8: Proxy species used to fit detection functions for SEFSC Gordon Gunter. The number of sightings, n, is before truncation.

The sightings were right truncated at 6000m.

Covariate	Description
beaufort	Beaufort sea state.
size	Estimated size (number of individuals) of the sighted group.

Table 9: Covariates tested in candidate "multi-covariate distance sampling" (MCDS) detection functions.

Key	Adjustment	Order	Covariates	Succeeded	Δ AIC	Mean ESHW (m)
hr			beaufort, size	Yes	0.00	1151
hr			beaufort	Yes	104.83	844
hr			size	Yes	161.58	836
hr	poly	4		Yes	217.30	671

hr	poly	2		Yes	229.20	705
hn			beaufort, size	Yes	471.12	2367
hn	cos	2		Yes	483.53	1850
hn	cos	3		Yes	485.63	1668
hn			beaufort	Yes	560.18	2337
hn			size	Yes	607.82	2400
hn				Yes	679.46	2360
hn	herm	4		No		
hr				No		

Table 10: Candidate detection functions for SEFSC Gordon Gunter. The first one listed was selected for the density model.

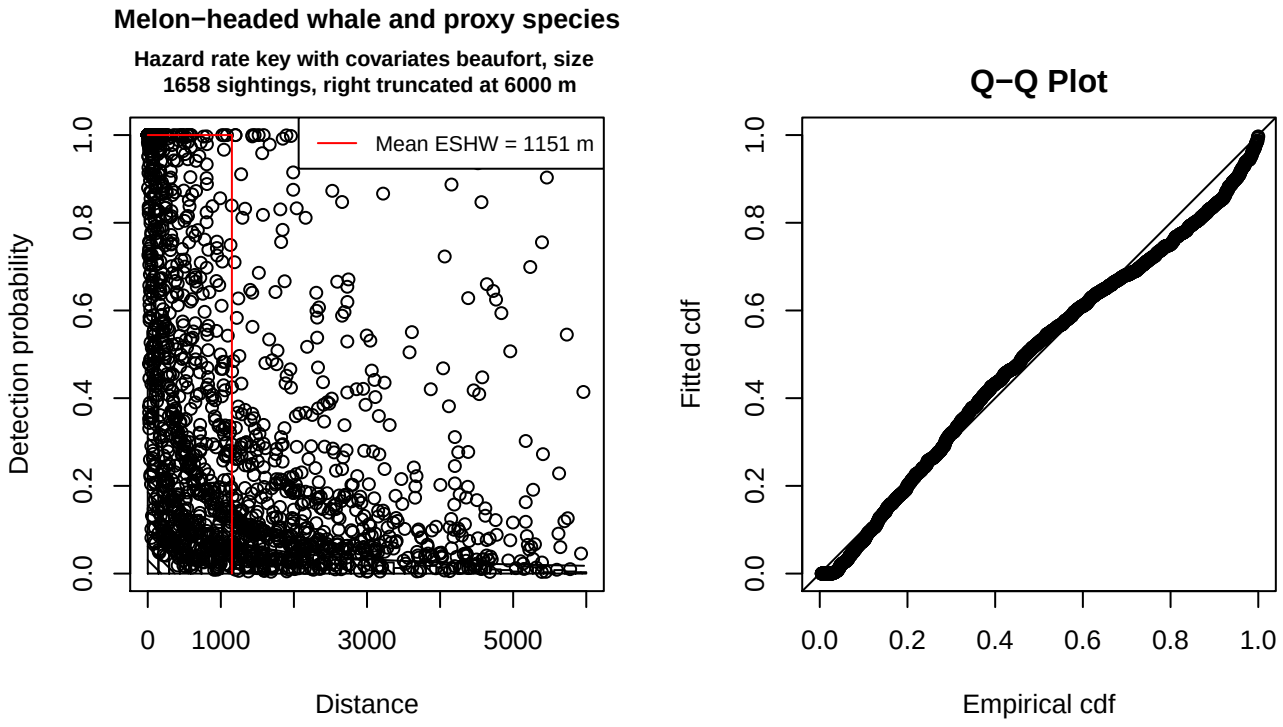

Figure 15: Detection function for SEFSC Gordon Gunter that was selected for the density model

Statistical output for this detection function:

```
Summary for ds object
Number of observations :  1658
Distance range         :  0  -  6000
AIC                    :  26706.73

Detection function:
 Hazard-rate key function

Detection function parameters
Scale Coefficients:
```

```
              estimate         se
(Intercept)  6.9027963 0.19321982
beaufort    -0.9581653 0.06908393
size         2.0895966 0.20600540

Shape parameters:
              estimate         se
(Intercept) 0.04310494 0.03374639

                         Estimate           SE        CV
Average p           6.449727e-02 6.631113e-03 0.1028123
N in covered region 2.570651e+04 2.721911e+03 0.1058841
```

Additional diagnostic plots:

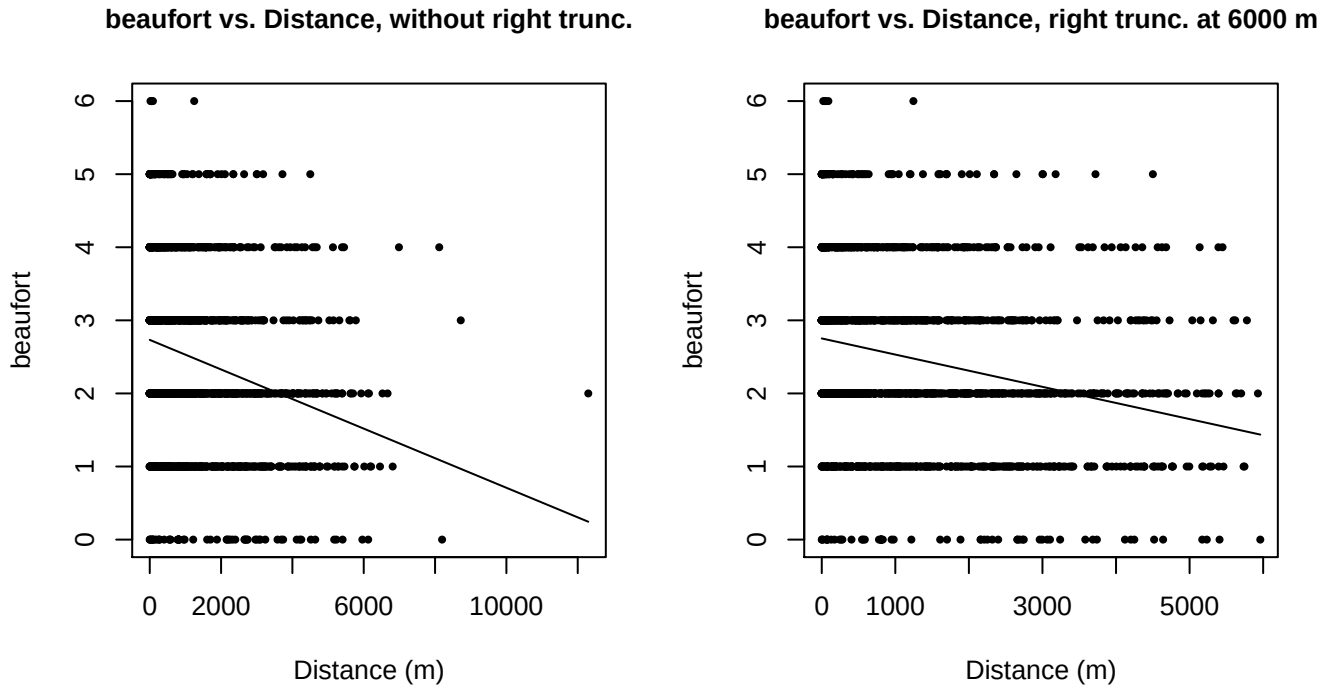

Figure 16: Scatterplots showing the relationship between Beaufort sea state and perpendicular sighting distance, for all sightings (left) and only those not right truncated (right). The line is a simple linear regression.

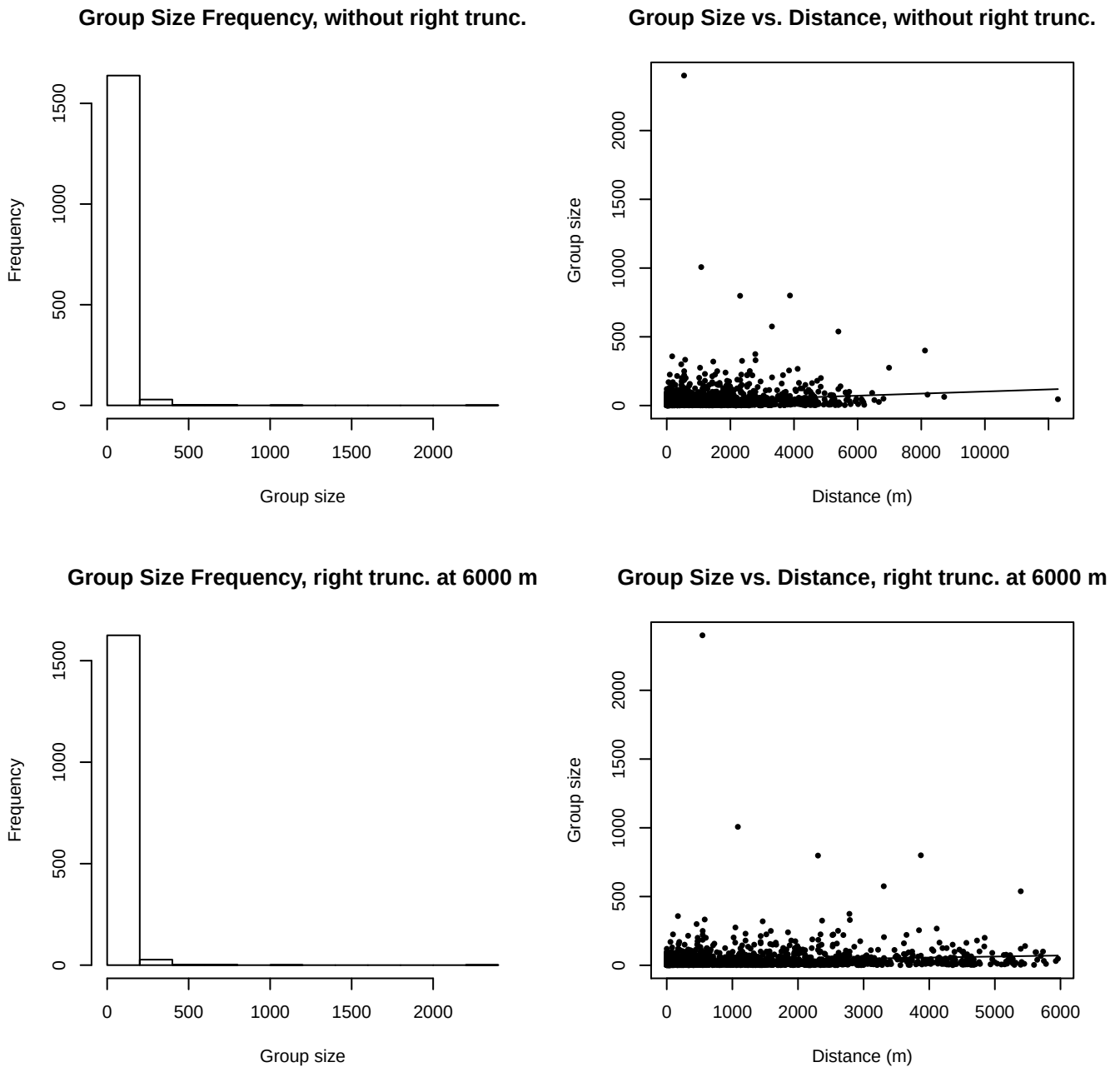

Figure 17: Histograms showing group size frequency and scatterplots showing the relationship between group size and perpendicular sighting distance, for all sightings (top row) and only those not right truncated (bottom row). In the scatterplot, the line is a simple linear regression.

Aerial Surveys

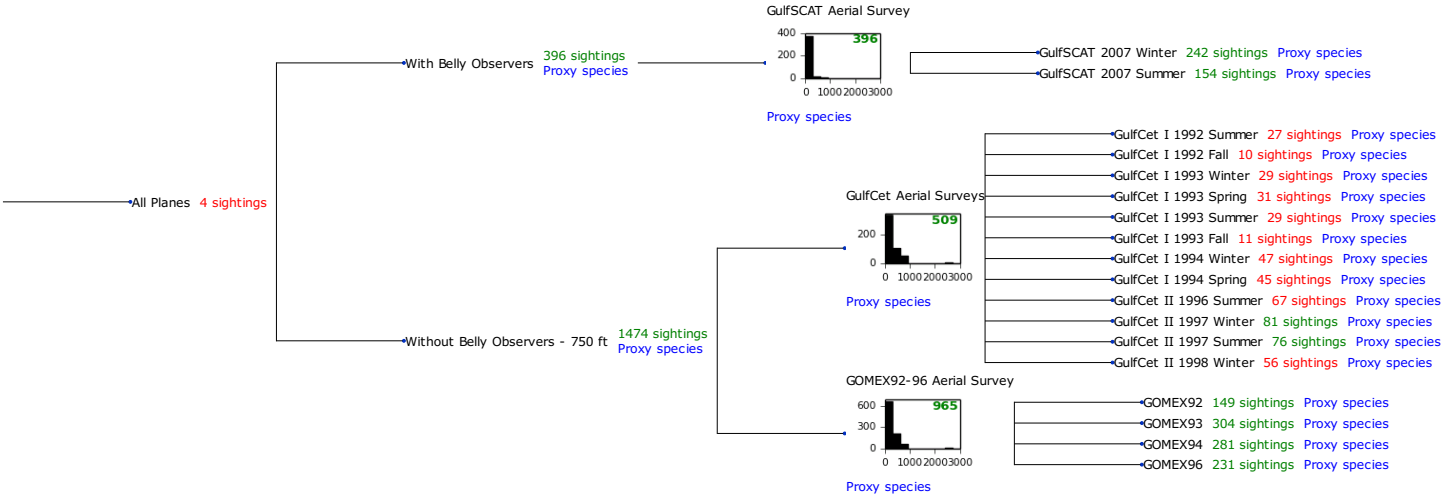

Figure 18: Detection hierarchy for aerial surveys

GulfSCAT Aerial Survey

Because this taxon was sighted too infrequently to fit a detection function to its sightings alone, we fit a detection function to the pooled sightings of several other species that we believed would exhibit similar detectability. These "proxy species" are listed below.

Reported By Observer	Common Name	n
Delphinus capensis	Long-beaked common dolphin	0
Delphinus delphis	Short-beaked common dolphin	0
Delphinus delphis/Lagenorhynchus acutus	Short-beaked common or Atlantic white-sided dolphin	0
Delphinus delphis/Stenella	Short-beaked common dolphin or Stenella spp.	0
Delphinus delphis/Stenella coeruleoalba	Short-beaked common or striped dolphin	0
Feresa attenuata	Pygmy killer whale	0
Grampus griseus	Risso's dolphin	0
Grampus griseus/Tursiops truncatus	Risso's or Bottlenose dolphin	0
Lagenodelphis hosei	Fraser's dolphin	0
Lagenorhynchus acutus	Atlantic white-sided dolphin	0
Lagenorhynchus albirostris	White-beaked dolphin	0
Lagenorhynchus albirostris/Lagenorhynchus acutus	White-beaked or white-sided dolphin	0
Peponocephala electra	Melon-headed whale	0
Stenella	Unidentified Stenella	0
Stenella attenuata	Pantropical spotted dolphin	0
Stenella attenuata/frontalis	Pantropical or Atlantic spotted dolphin	0
Stenella clymene	Clymene dolphin	0
Stenella coeruleoalba	Striped dolphin	0
Stenella frontalis	Atlantic spotted dolphin	15
Stenella frontalis/Tursiops truncatus	Atlantic spotted or Bottlenose dolphin	0

Stenella longirostris	Spinner dolphin	0
Steno bredanensis	Rough-toothed dolphin	0
Steno bredanensis/Tursiops truncatus	Bottlenose or rough-toothed dolphin	0
Tursiops truncatus	Bottlenose dolphin	381
Total		396

Table 11: Proxy species used to fit detection functions for GulfSCAT Aerial Survey. The number of sightings, n, is before truncation.

The sightings were right truncated at 400m.

Covariate	Description
beaufort	Beaufort sea state.
quality	Survey-specific index of the quality of observation conditions, utilizing relevant factors other than Beaufort sea state (see methods).
size	Estimated size (number of individuals) of the sighted group.

Table 12: Covariates tested in candidate "multi-covariate distance sampling" (MCDS) detection functions.

Key	Adjustment	Order	Covariates	Succeeded	Δ AIC	Mean ESHW (m)
hn	herm	4		Yes	0.00	218
hn	cos	2		Yes	0.09	221
hn				Yes	0.90	199
hn			size	Yes	2.21	199
hn	cos	3		Yes	2.37	209
hr	poly	2		Yes	2.39	218
hr	poly	4		Yes	2.47	223
hr				Yes	4.46	230
hr			size	Yes	5.04	232
hn			beaufort	No		
hr			beaufort	No		
hn			quality	No		
hr			quality	No		
hn			beaufort, quality	No		
hr			beaufort, quality	No		
hn			beaufort, size	No		
hr			beaufort, size	No		
hn			quality, size	No		
hr			quality, size	No		
hn			beaufort, quality, size	No		
hr			beaufort, quality, size	No		

Table 13: Candidate detection functions for GulfSCAT Aerial Survey. The first one listed was selected for the density model.

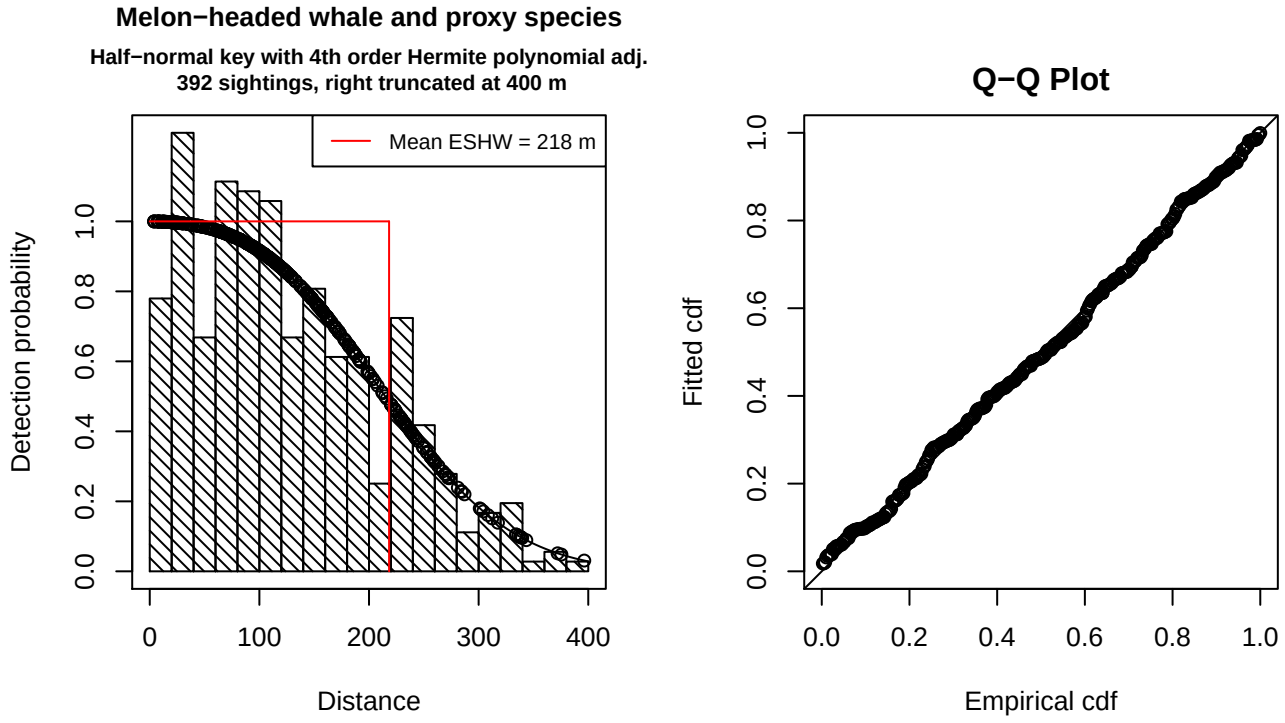

Figure 19: Detection function for GulfSCAT Aerial Survey that was selected for the density model

Statistical output for this detection function:

```
Summary for ds object
Number of observations :  392
Distance range         :  0  -  400
AIC                    :  4505.917

Detection function:
 Half-normal key function with Hermite polynomial adjustment term of order 4

Detection function parameters
Scale Coefficients:
            estimate         se
(Intercept) 4.855654 0.07415704

Adjustment term parameter(s):
                 estimate         se
herm, order 4 -0.04126215 0.01270402


Monotonicity constraints were enforced.
                       Estimate         SE         CV
Average p             0.5457903  0.0420189 0.07698725
N in covered region 718.2245780 60.4578547 0.08417681
```

```
Monotonicity constraints were enforced.
```

Additional diagnostic plots:

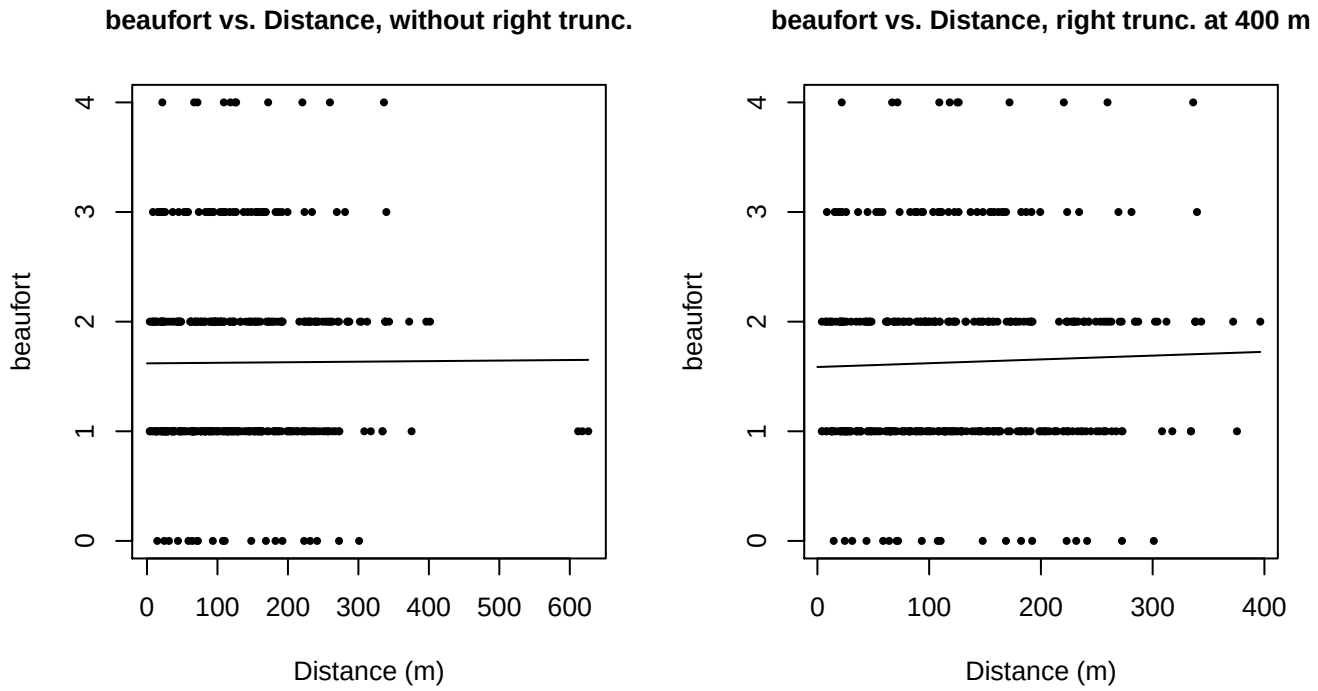

Figure 20: Scatterplots showing the relationship between Beaufort sea state and perpendicular sighting distance, for all sightings (left) and only those not right truncated (right). The line is a simple linear regression.

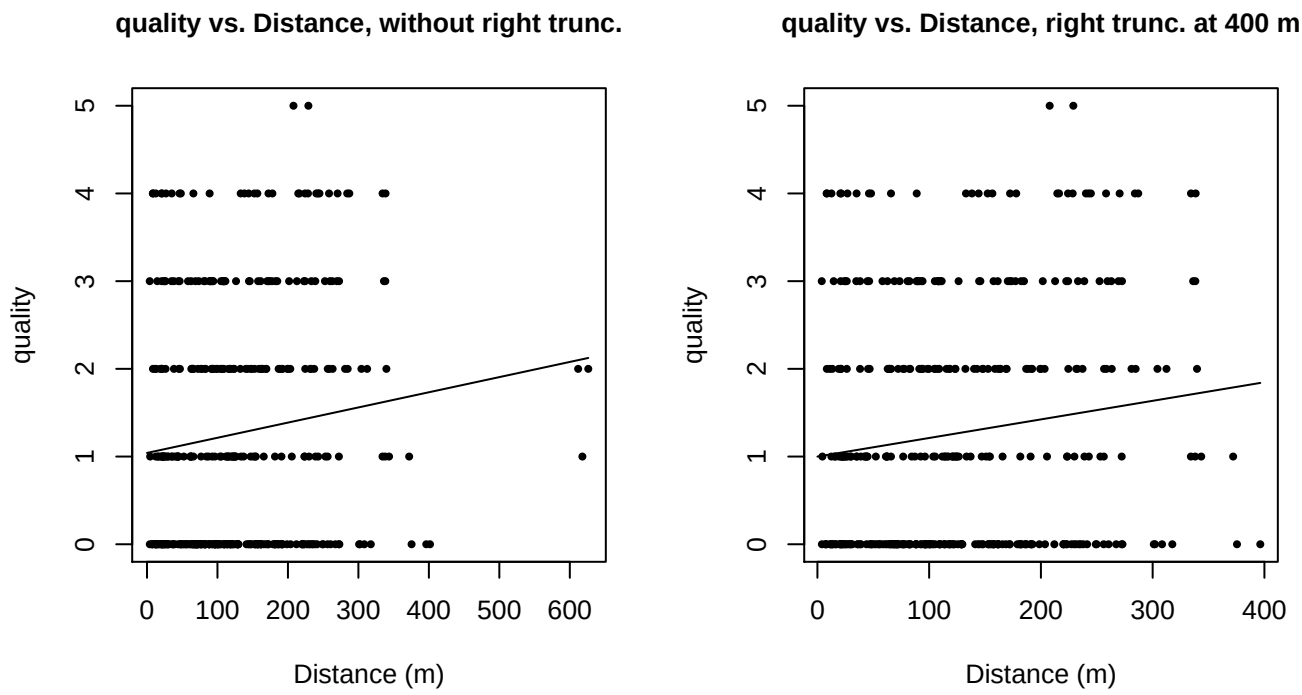

Figure 21: Scatterplots showing the relationship between the survey-specific index of the quality of observation conditions and perpendicular sighting distance, for all sightings (left) and only those not right truncated (right). Low values of the quality index correspond to better observation conditions. The line is a simple linear regression.

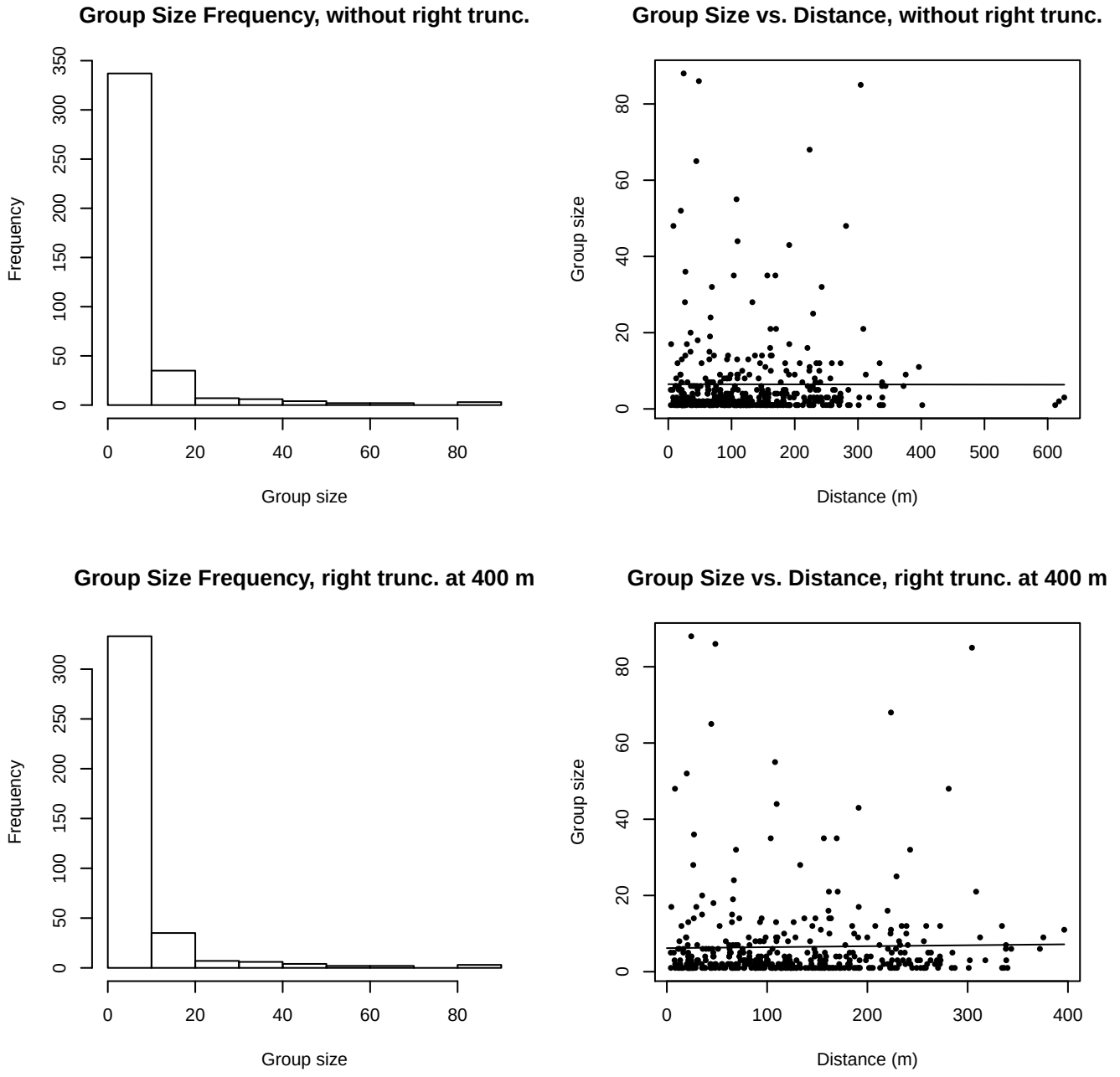

Figure 22: Histograms showing group size frequency and scatterplots showing the relationship between group size and perpendicular sighting distance, for all sightings (top row) and only those not right truncated (bottom row). In the scatterplot, the line is a simple linear regression.

GulfCet Aerial Surveys

Because this taxon was sighted too infrequently to fit a detection function to its sightings alone, we fit a detection function to the pooled sightings of several other species that we believed would exhibit similar detectability. These "proxy species" are listed below.

Reported By Observer	Common Name	n
Delphinus capensis	Long-beaked common dolphin	0
Delphinus delphis	Short-beaked common dolphin	0

Delphinus delphis/Lagenorhynchus acutus	Short-beaked common or Atlantic white-sided dolphin	0
Delphinus delphis/Stenella	Short-beaked common dolphin or Stenella spp.	0
Delphinus delphis/Stenella coeruleoalba	Short-beaked common or striped dolphin	0
Feresa attenuata	Pygmy killer whale	7
Grampus griseus	Risso's dolphin	71
Grampus griseus/Tursiops truncatus	Risso's or Bottlenose dolphin	0
Lagenodelphis hosei	Fraser's dolphin	2
Lagenorhynchus acutus	Atlantic white-sided dolphin	0
Lagenorhynchus albirostris	White-beaked dolphin	0
Lagenorhynchus albirostris/Lagenorhynchus acutus	White-beaked or white-sided dolphin	0
Peponocephala electra	Melon-headed whale	4
Stenella	Unidentified Stenella	10
Stenella attenuata	Pantropical spotted dolphin	94
Stenella attenuata/frontalis	Pantropical or Atlantic spotted dolphin	0
Stenella clymene	Clymene dolphin	12
Stenella coeruleoalba	Striped dolphin	16
Stenella frontalis	Atlantic spotted dolphin	36
Stenella frontalis/Tursiops truncatus	Atlantic spotted or Bottlenose dolphin	0
Stenella longirostris	Spinner dolphin	11
Steno bredanensis	Rough-toothed dolphin	9
Steno bredanensis/Tursiops truncatus	Bottlenose or rough-toothed dolphin	0
Tursiops truncatus	Bottlenose dolphin	237
Total		509

Table 14: Proxy species used to fit detection functions for GulfCet Aerial Surveys. The number of sightings, n, is before truncation.

The sightings were right truncated at 1296m. The vertical sighting angles were heaped at 10 degree increments, so the candidate detection functions were fitted using linear bins scaled accordingly.

Covariate	Description
beaufort	Beaufort sea state.
quality	Survey-specific index of the quality of observation conditions, utilizing relevant factors other than Beaufort sea state (see methods).
size	Estimated size (number of individuals) of the sighted group.

Table 15: Covariates tested in candidate "multi-covariate distance sampling" (MCDS) detection functions.

Key	Adjustment	Order	Covariates	Succeeded	Δ AIC	Mean ESHW (m)
hr				Yes	0.00	393

hr	poly	4		Yes	2.00	393
hr	poly	2		Yes	2.00	393
hn	cos	2		Yes	3.05	366
hn	cos	3		Yes	9.66	340
hn			size	Yes	29.80	440
hn				Yes	34.48	438
hn	herm	4		Yes	36.24	438
hn			beaufort	No		
hr			beaufort	No		
hn			quality	No		
hr			quality	No		
hr			size	No		
hn			beaufort, quality	No		
hr			beaufort, quality	No		
hn			beaufort, size	No		
hr			beaufort, size	No		
hn			quality, size	No		
hr			quality, size	No		
hn			beaufort, quality, size	No		
hr			beaufort, quality, size	No		

Table 16: Candidate detection functions for GulfCet Aerial Surveys. The first one listed was selected for the density model.

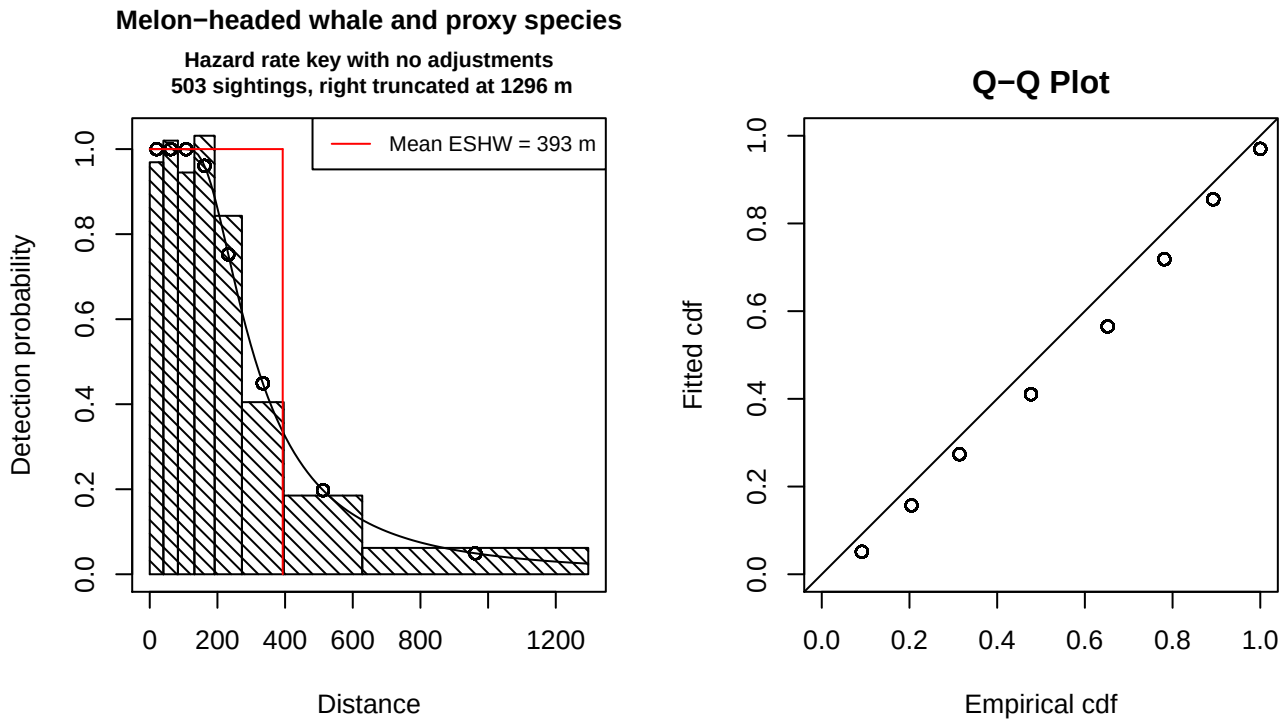

Figure 23: Detection function for GulfCet Aerial Surveys that was selected for the density model

Statistical output for this detection function:

```
Summary for ds object
Number of observations :  503
Distance range         :  0  -  1296
AIC                    :  2078.71

Detection function:
 Hazard-rate key function

Detection function parameters
Scale Coefficients:
            estimate         se
(Intercept) 5.590311 0.08294157

Shape parameters:
             estimate         se
(Intercept) 0.8474162 0.08116411

                         Estimate           SE         CV
Average p                0.3032173   0.01648324 0.05436115
N in covered region 1658.8765467 109.28948122 0.06588162
```

Additional diagnostic plots:

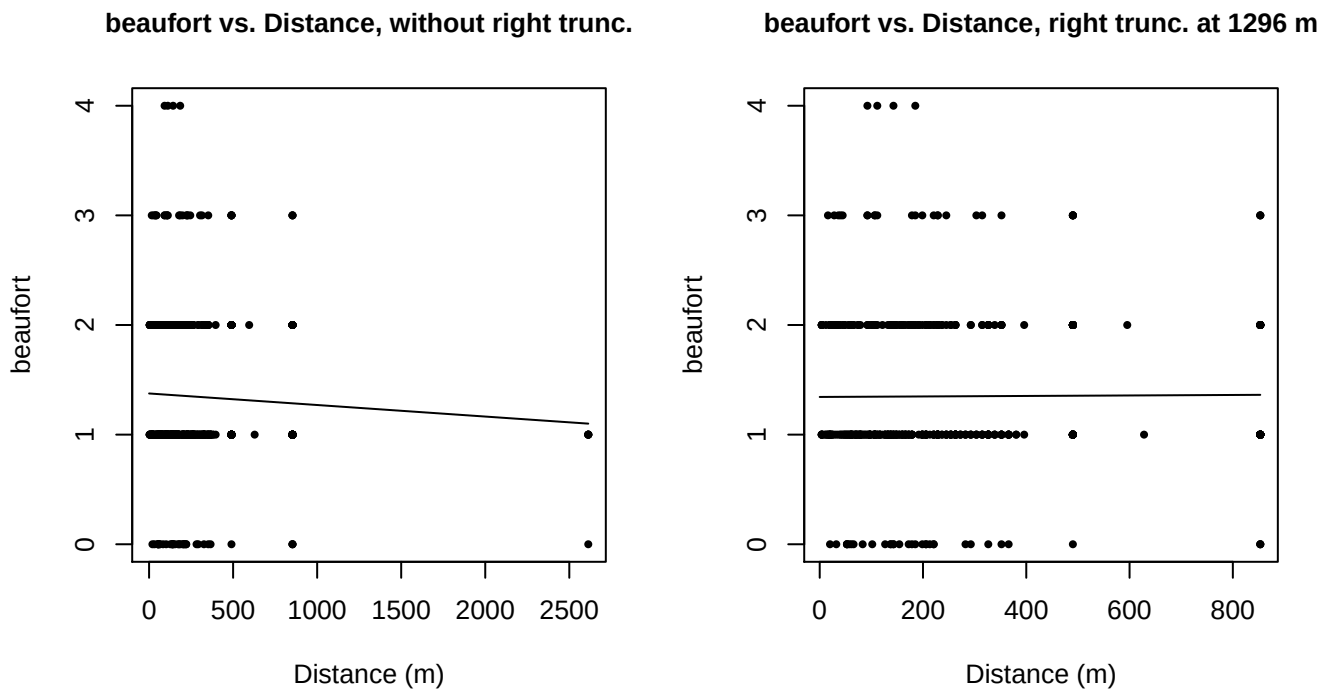

Figure 24: Scatterplots showing the relationship between Beaufort sea state and perpendicular sighting distance, for all sightings (left) and only those not right truncated (right). The line is a simple linear regression.

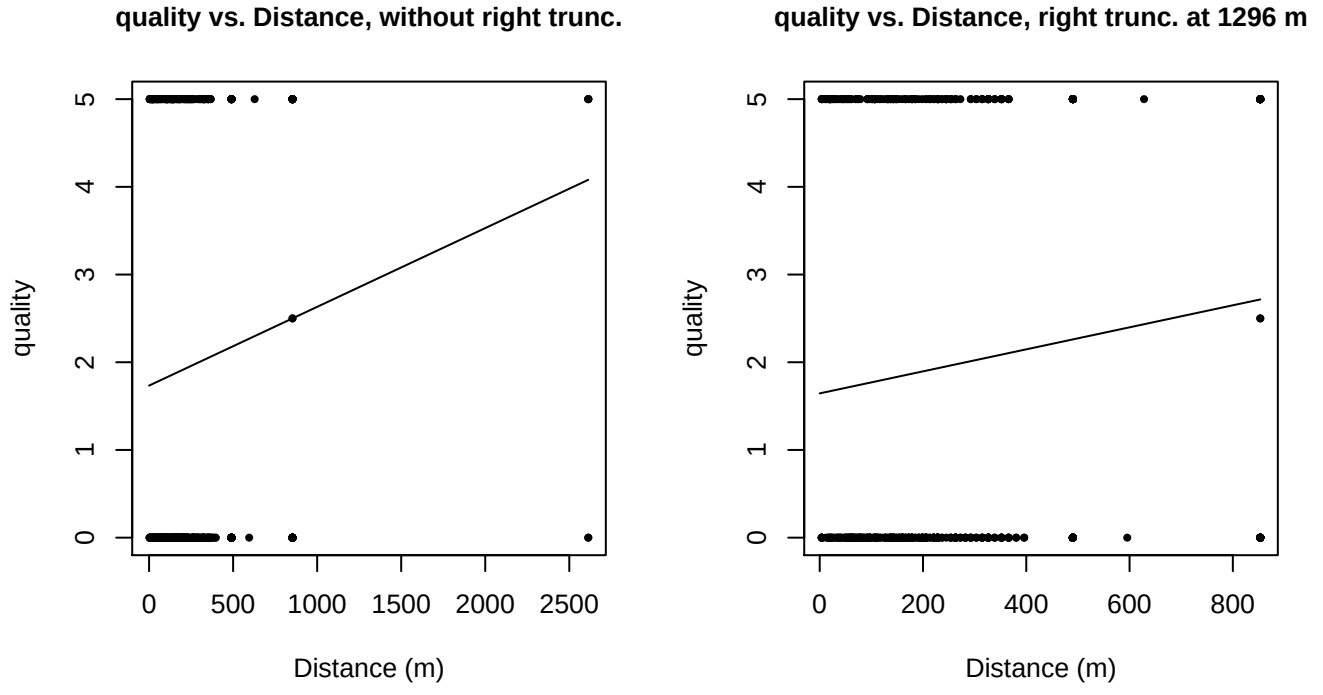

Figure 25: Scatterplots showing the relationship between the survey-specific index of the quality of observation conditions and perpendicular sighting distance, for all sightings (left) and only those not right truncated (right). Low values of the quality index correspond to better observation conditions. The line is a simple linear regression.

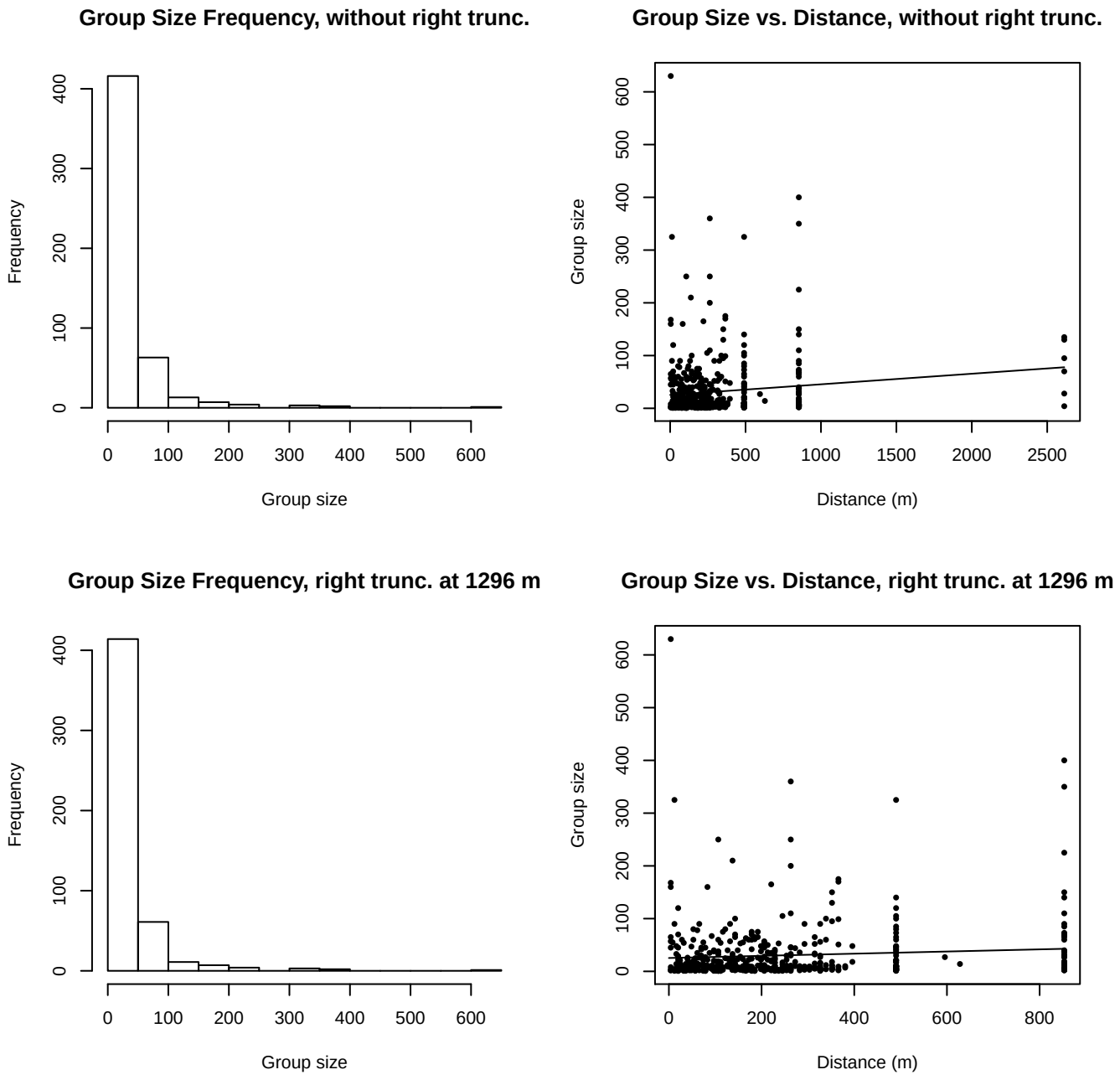

Figure 26: Histograms showing group size frequency and scatterplots showing the relationship between group size and perpendicular sighting distance, for all sightings (top row) and only those not right truncated (bottom row). In the scatterplot, the line is a simple linear regression.

GOMEX92-96 Aerial Survey

Because this taxon was sighted too infrequently to fit a detection function to its sightings alone, we fit a detection function to the pooled sightings of several other species that we believed would exhibit similar detectability. These "proxy species" are listed below.

Reported By Observer	Common Name	n
Delphinus capensis	Long-beaked common dolphin	0
Delphinus delphis	Short-beaked common dolphin	0

Delphinus delphis/Lagenorhynchus acutus	Short-beaked common or Atlantic white-sided dolphin	0
Delphinus delphis/Stenella	Short-beaked common dolphin or Stenella spp.	0
Delphinus delphis/Stenella coeruleoalba	Short-beaked common or striped dolphin	0
Feresa attenuata	Pygmy killer whale	0
Grampus griseus	Risso's dolphin	4
Grampus griseus/Tursiops truncatus	Risso's or Bottlenose dolphin	0
Lagenodelphis hosei	Fraser's dolphin	0
Lagenorhynchus acutus	Atlantic white-sided dolphin	0
Lagenorhynchus albirostris	White-beaked dolphin	0
Lagenorhynchus albirostris/Lagenorhynchus acutus	White-beaked or white-sided dolphin	0
Peponocephala electra	Melon-headed whale	0
Stenella	Unidentified Stenella	1
Stenella attenuata	Pantropical spotted dolphin	0
Stenella attenuata/frontalis	Pantropical or Atlantic spotted dolphin	0
Stenella clymene	Clymene dolphin	0
Stenella coeruleoalba	Striped dolphin	0
Stenella frontalis	Atlantic spotted dolphin	24
Stenella frontalis/Tursiops truncatus	Atlantic spotted or Bottlenose dolphin	0
Stenella longirostris	Spinner dolphin	0
Steno bredanensis	Rough-toothed dolphin	0
Steno bredanensis/Tursiops truncatus	Bottlenose or rough-toothed dolphin	0
Tursiops truncatus	Bottlenose dolphin	936
Total		965

Table 17: Proxy species used to fit detection functions for GOMEX92-96 Aerial Survey. The number of sightings, n, is before truncation.

The sightings were right truncated at 1296m. Due to a reduced frequency of sightings close to the trackline that plausibly resulted from the behavior of the observers and/or the configuration of the survey platform, the sightings were left truncted as well. Sightings closer than 83 m to the trackline were omitted from the analysis, and it was assumed that the the area closer to the trackline than this was not surveyed. This distance was estimated by inspecting histograms of perpendicular sighting distances. The vertical sighting angles were heaped at 10 degree increments, so the candidate detection functions were fitted using linear bins scaled accordingly.

Covariate	Description
beaufort	Beaufort sea state.
quality	Survey-specific index of the quality of observation conditions, utilizing relevant factors other than Beaufort sea state (see methods).
size	Estimated size (number of individuals) of the sighted group.

Table 18: Covariates tested in candidate "multi-covariate distance sampling" (MCDS) detection functions.

Key	Adjustment	Order	Covariates	Succeeded	Δ AIC	Mean ESHW (m)
hr			size	Yes	0.00	281
hr	poly	4		Yes	4.73	273
hn	cos	3		Yes	4.85	220
hr				Yes	4.90	278
hr	poly	2		Yes	5.13	269
hn	cos	2		Yes	12.07	259
hn			size	Yes	39.53	304
hn				Yes	41.94	304
hn	herm	4		Yes	43.71	304
hn			beaufort	No		
hr			beaufort	No		
hn			quality	No		
hr			quality	No		
hn			beaufort, quality	No		
hr			beaufort, quality	No		
hn			beaufort, size	No		
hr			beaufort, size	No		
hn			quality, size	No		
hr			quality, size	No		
hn			beaufort, quality, size	No		
hr			beaufort, quality, size	No		

Table 19: Candidate detection functions for GOMEX92-96 Aerial Survey. The first one listed was selected for the density model.

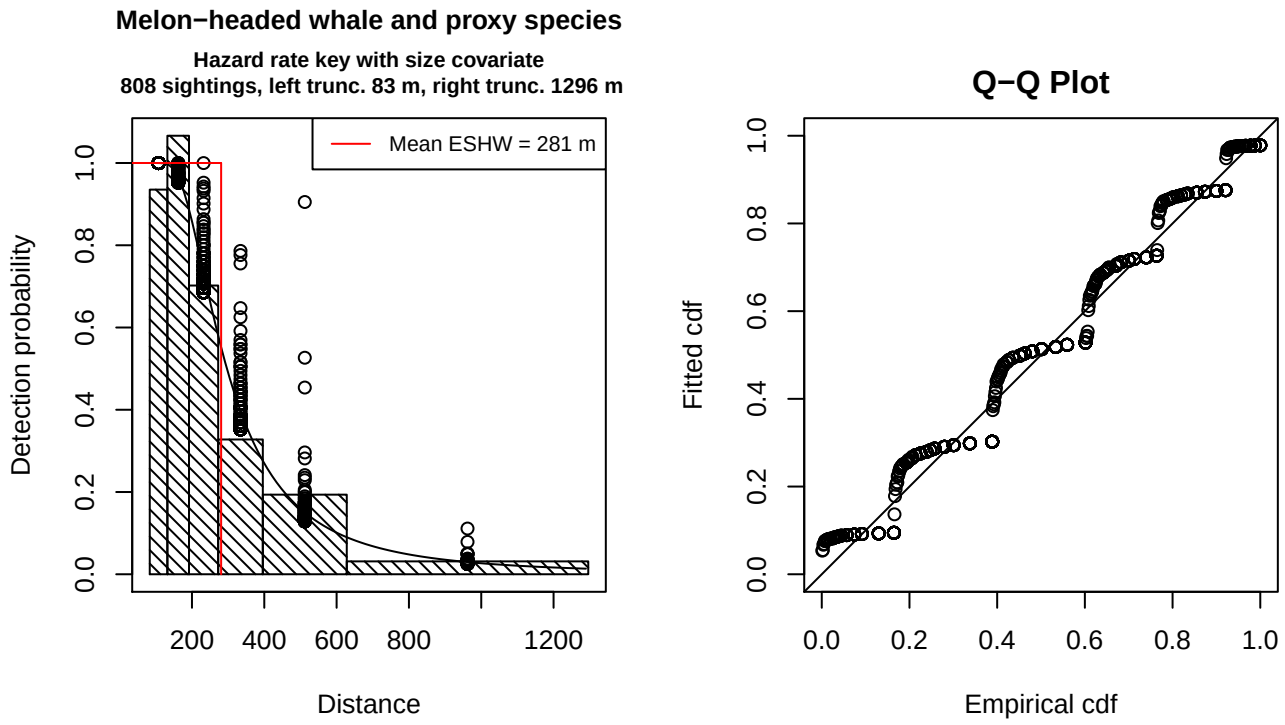

Figure 27: Detection function for GOMEX92-96 Aerial Survey that was selected for the density model

Statistical output for this detection function:

```
Summary for ds object
Number of observations :  808
Distance range         :  83.2036  -  1296
AIC                    :  2832.217

Detection function:
 Hazard-rate key function

Detection function parameters
Scale Coefficients:
             estimate         se
(Intercept) 5.49007390 0.06761203
size        0.09577309 0.04016336

Shape parameters:
            estimate         se
(Intercept) 0.9893445 0.05859387

                         Estimate           SE         CV
Average p                0.2138621   0.01146898 0.05362795
N in covered region 3778.1360570 234.49525749 0.06206639
```

Additional diagnostic plots:

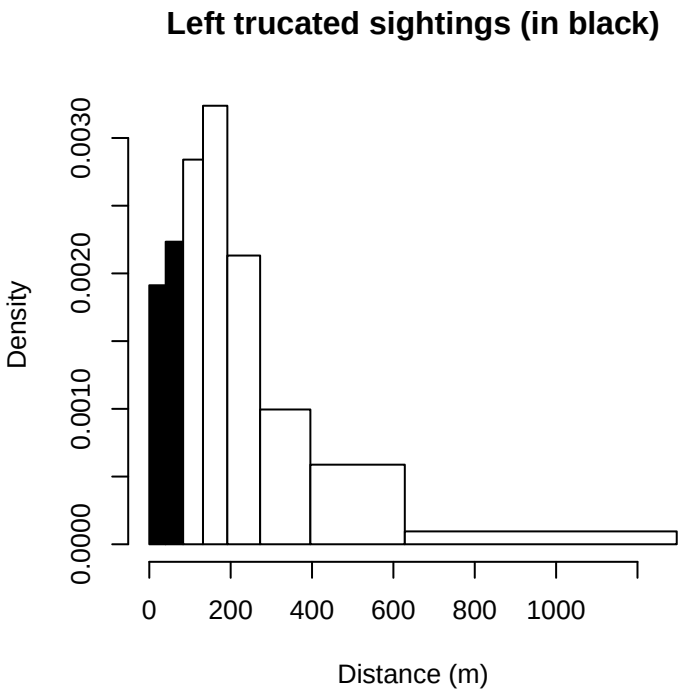

Figure 28: Density of sightings by perpendicular distance for GOMEX92-96 Aerial Survey. Black bars on the left show sightings that were left truncated.

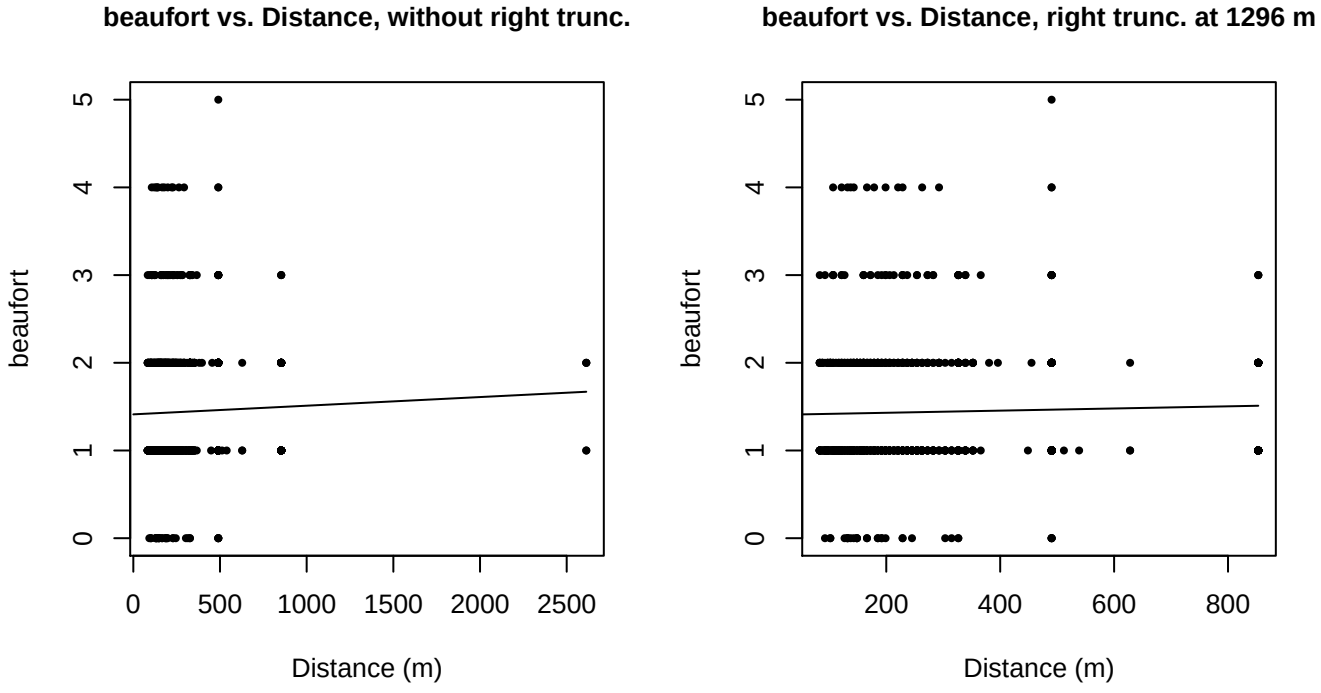

Figure 29: Scatterplots showing the relationship between Beaufort sea state and perpendicular sighting distance, for all sightings (left) and only those not right truncated (right). The line is a simple linear regression.

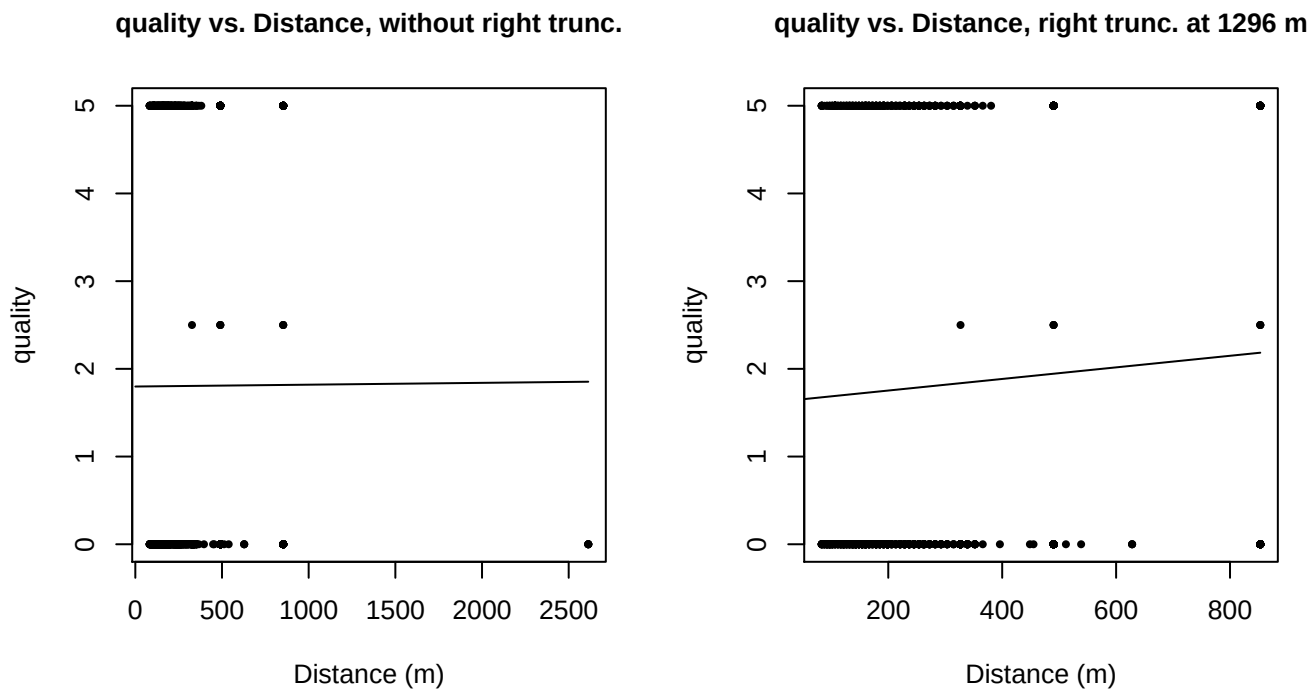

Figure 30: Scatterplots showing the relationship between the survey-specific index of the quality of observation conditions and perpendicular sighting distance, for all sightings (left) and only those not right truncated (right). Low values of the quality index correspond to better observation conditions. The line is a simple linear regression.

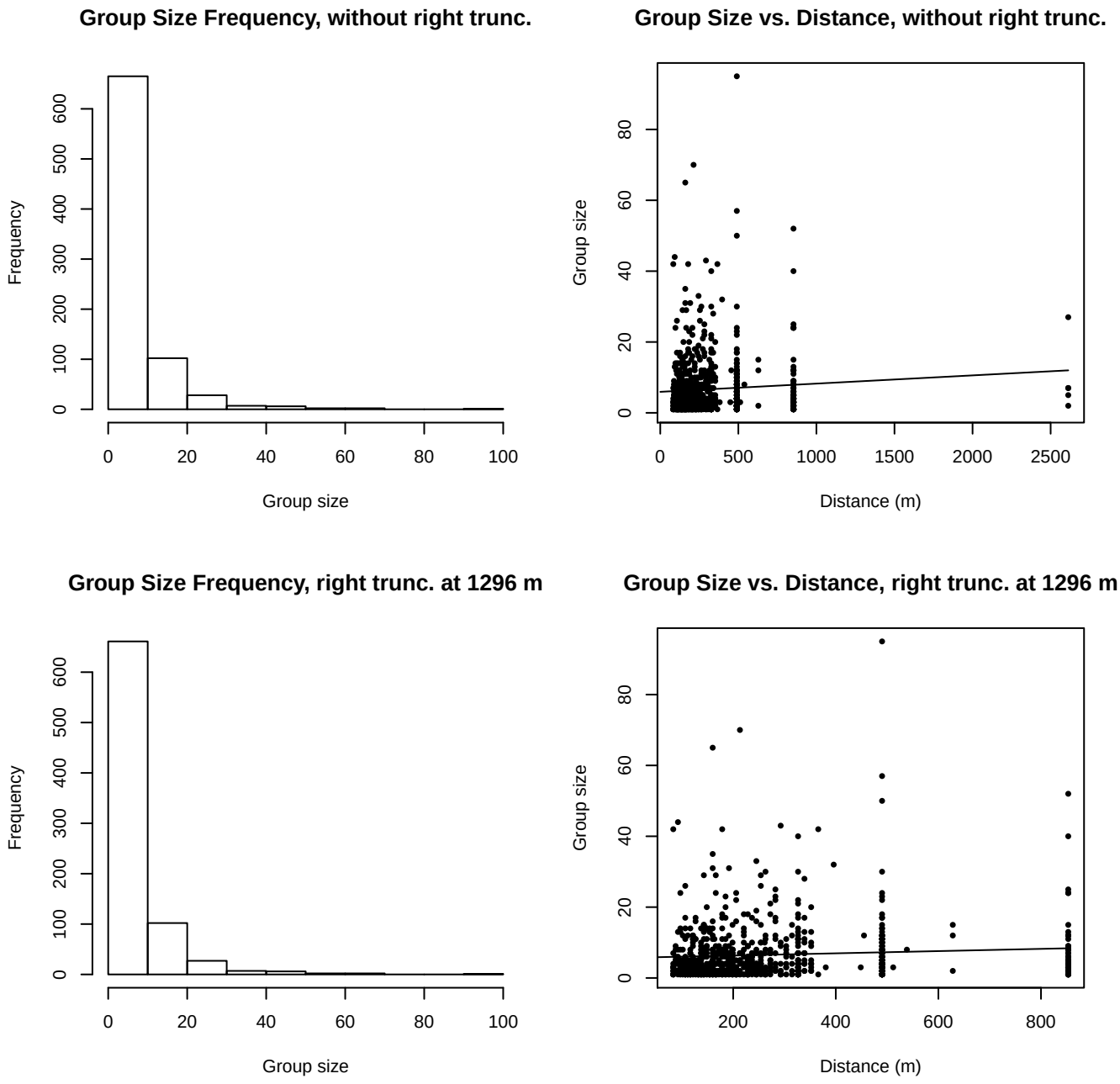

Figure 31: Histograms showing group size frequency and scatterplots showing the relationship between group size and perpendicular sighting distance, for all sightings (top row) and only those not right truncated (bottom row). In the scatterplot, the line is a simple linear regression.

g(0) Estimates

Platform	Surveys	Group Size	*g(0)*	Biases Addressed	Source
Shipboard	All	1-20	0.856	Perception	Barlow and Forney (2007)
		>20	0.970	Perception	Barlow and Forney (2007)
Aerial	All	1-5	0.43	Both	Palka (2006)
		>5	0.960	Both	Carretta et al. (2000)

Table 20: Estimates of *g(0)* used in this density model.

For shipboard surveys, we were unable to find a species-specific g(0) estimate for melon-headed whales in the literature. Barlow (2006) estimated g(0)=0.77 (CV=0.14) for groups of 1-20 individuals of 11 species of small delphinids pooled together, including melon-headed whales, produced from several years of dual-team surveys that used bigeye binoculars and similar protocols to the surveys in our study. This analysis was based on Barlow's (1995) analysis of cetaceans observed by shipboard surveys in California waters. Barlow and Forney (2007) reported an updated estimate of g(0)=0.856, incorporating additional surveys from the California Current ecosystem (CCE) and yielding a lower CV (0.056). Although Barlow and Forney did not apply the updated estimate to melon- headed whales (they reported no observations in the CCE), we favored the updated estimate because it was more recent, incorporated more data, and had a lower CV.

Barlow and Forney's estimate accounted for perception bias but not availability bias. For long diving cetaceans such as sperm whales, Kogia spp., and beaked whales, the authors used Barlow's (1999) model of g(0) that incorporated dive behavior to address availability bias. We could not find any reports of the diving behavior of melon-headed whales in the literature. Our best guess is that they exhibit behavior similar to other smaller "blackfish" species, which are not reported to be particularly long divers. Also, melon-headed whales often occur in large groups (10s or 100s of animals); the presence of so many animals increases the chance that some will be available at the surface.

For aerial surveys, we were also unable to find a species-specific g(0) estimate for melon-headed whales in the literature. For small groups, defined here as 1-5 individuals, we used Palka's (2006) estimate of g(0) for groups of 1-5 small cetaceans, estimated from two years of aerial surveys using the Hiby (1999) circle-back method. This estimate accounted for both availability and perception bias, but pooled sightings of several species together to provide a generic estimate for all delphinids, due to sample-size limitations. For large groups, defined here as greater than 5 individuals, Palka (2006) assumed that g(0) was 1. When we discussed this with NOAA SWFSC reviewers, they agreed that it was safe to assume that the availability bias component of g(0) was 1 but insisted that perception bias should be slightly less than 1, because it was possible to miss large groups. We agreed to take a conservative approach and obtained our g(0) for large groups from Carretta et al. (2000), who estimated g(0) for both small and large groups of delphinids. We used Carretta et al.'s g(0) estimate for groups of 1-25 individuals (0.960), rather than their larger one for more than 25 individuals (0.994), to account for the fact that we were using Palka's definition of large groups as those with more than 5 individuals.

Density Models

Melon-headed whales are found in tropical and subtropical waters worldwide, and occasionally at higher latitudes often in association with incursions of warm water currents (Perryman 2008). In our east coast study area, which is generally beyond the area described as primary melon-headed whale habitat, the surveys in our database reported only four sightings, all in the Gulf Stream near Cape Hatteras, North Carolina. In contrast, in the Gulf of Mexico, which is probably better habitat due to its consistently warm waters, the surveys reported 25 definitive sightings.

Melon-headed whales can be difficult for observers to distinguish from pygmy killer whales and false killer whales (Mullin et al. 1994). The surveys in our database reported 14 ambiguous "melon-headed or pygmy killer whale" sightings, but no "melon-headed or false killer whale" sightings. The definitive melon-headed whale and pygmy killer whale sightings showed distinct differences in distributions of group size and latitude, with melon-headed whales occurring in larger groups mainly on the western side of the Gulf of Mexico, and pygmy killer whales occurring in smaller groups mainly on the eastern side. To avoid underestimating density by omitting these 14 ambiguous sightings, we built a classification model that classified 5 as

melon-headed whales and 9 as pygmy killer whales (see Reclassification of Ambiguous Sightings section above). We could only utilize 4 of the 5 reclassified melon-headed whale sightings, because 1 of them did not include a perpendicular sighting distance, making it unusable for distance sampling methodology.

Melon-headed whales are an oceanic species (Mullin et al. 1994); the 29 sightings utilized in our modeling project all occurred beyond the shelf break, in waters 450m or more deep. We split the study area at the shelf break, defined here as the 100m isobath, and assumed the species was absent from the shelf. With 29 sightings, we were right at the threshold we used to determine whether to fit a spatial model from environmental predictors or a stratified model that estimated mean abundance over the occupied area. Given the apparent concentration of sightings on the continental slope and in the western side of the Gulf, we fitted a limited spatial model of two covariates. We used depth as the first covariate, then tested all other covariates added the one that explained the most additional deviance over depth alone.

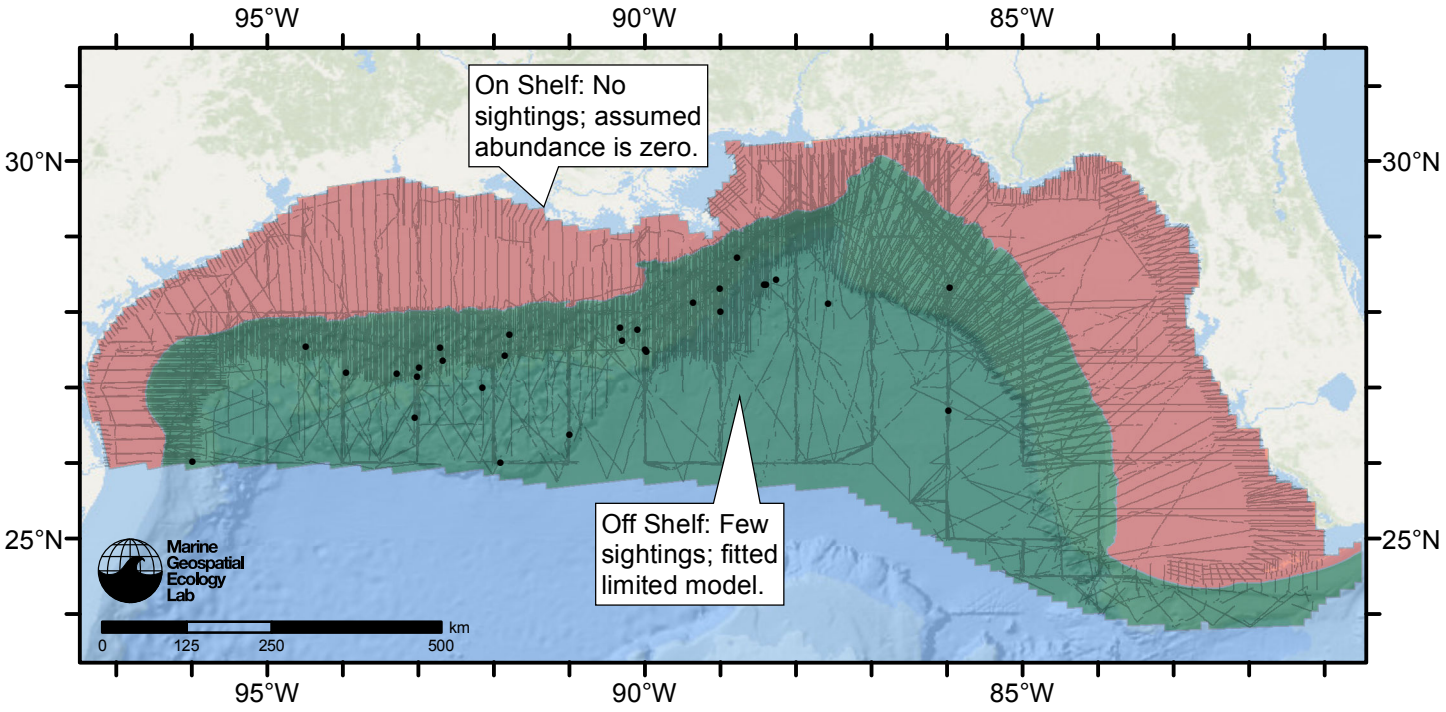

Figure 32: Melon-headed whale density model schematic. All on-effort sightings are shown, including those that were truncated when detection functions were fitted.

Climatological Model

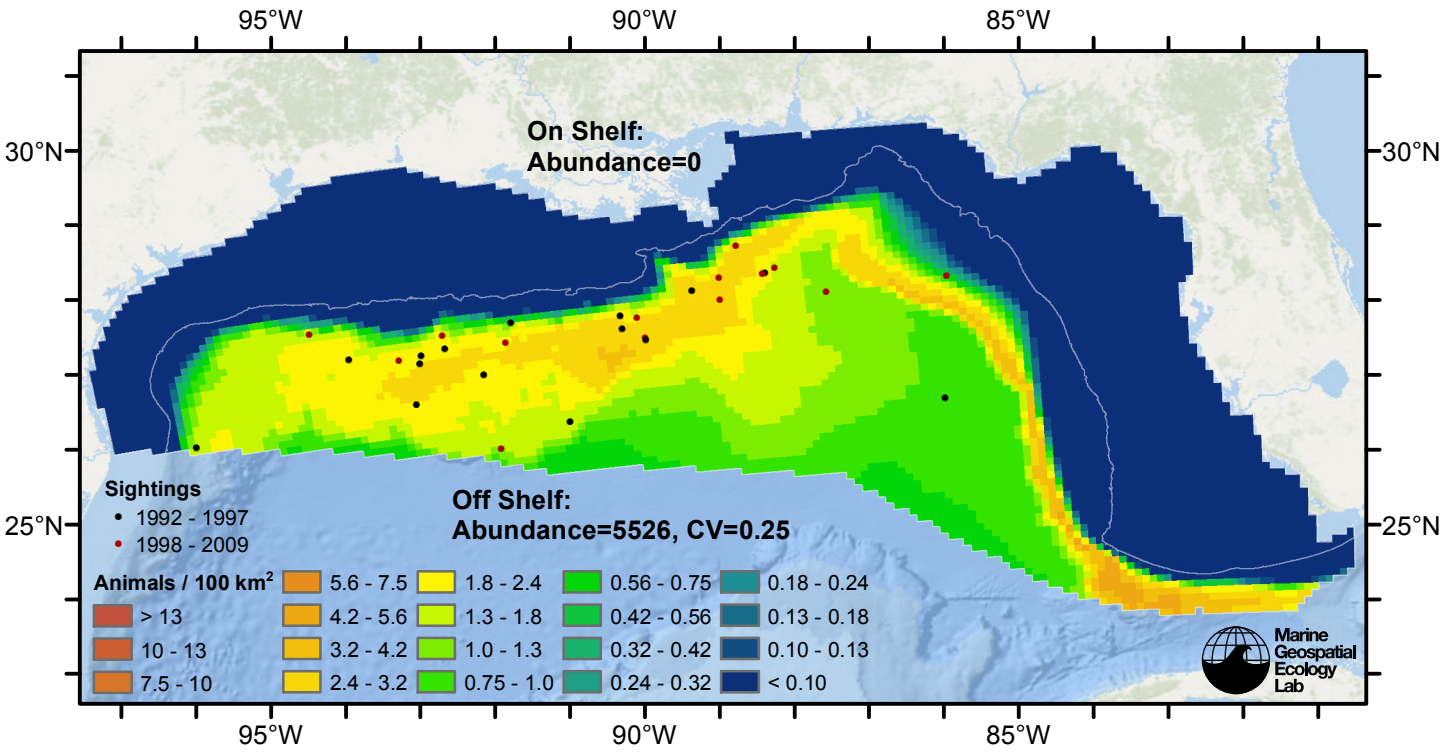

Figure 33: Melon-headed whale density predicted by the climatological model that explained the most deviance. Pixels are 10x10 km. The legend gives the estimated individuals per pixel; breaks are logarithmic. Abundance for each region was computed by summing the density cells occuring in that region.

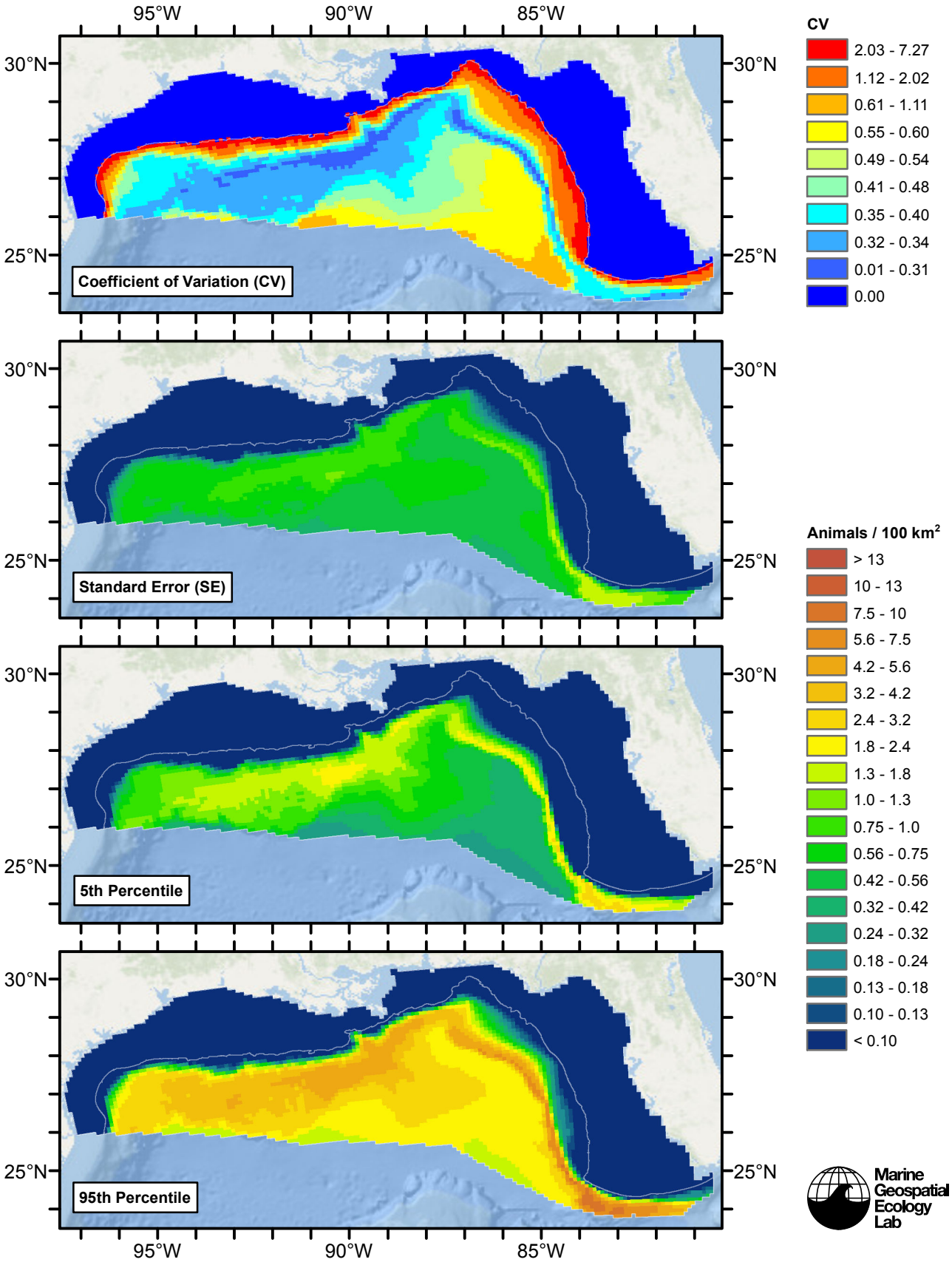

Figure 34: Estimated uncertainty for the climatological model that explained the most deviance. These estimates only incorporate the statistical uncertainty estimated for the spatial model (by the R mgcv package). They do not incorporate uncertainty in the detection functions, g(0) estimates, predictor variables, and so on.

Off Shelf

Statistical output

```
Rscript.exe: This is mgcv 1.8-2. For overview type 'help("mgcv-package")'.


Family: Tweedie(p=1.35)
Link function: log

Formula:
abundance ~ offset(log(area_km2)) + s(log10(Depth), bs = "ts",
    k = 5) + s(pmin(I(ClimDistToFront1/1000), 250), bs = "ts",
    k = 5)

Parametric coefficients:
            Estimate Std. Error t value Pr(>|t|)
(Intercept)  -5.4462     0.5194  -10.48   <2e-16 ***
---
Signif. codes:  0 '***' 0.001 '**' 0.01 '*' 0.05 '.' 0.1 ' ' 1

Approximate significance of smooth terms:
                                       edf Ref.df     F p-value
s(log10(Depth))                     2.4021      4 2.962  0.0024 **
s(pmin(I(ClimDistToFront1/1000), 250)) 0.8517      4 1.256  0.0144 *
---
Signif. codes:  0 '***' 0.001 '**' 0.01 '*' 0.05 '.' 0.1 ' ' 1

R-sq.(adj) =  0.00058   Deviance explained = 14.7%
-REML = 410.08  Scale est. = 656.89    n = 14455

All predictors were significant. This is the final model.
Creating term plots.
Diagnostic output from gam.check():

Method: REML   Optimizer: outer newton
full convergence after 11 iterations.
Gradient range [-4.547747e-05,1.580289e-06]
(score 410.0763 & scale 656.8921).
Hessian positive definite, eigenvalue range [0.3600821,90.66584].
Model rank =  9 / 9

Basis dimension (k) checking results. Low p-value (k-index<1) may
indicate that k is too low, especially if edf is close to k'.

                                       k'   edf k-index p-value
s(log10(Depth))                     4.000 2.402   0.693    0.02
s(pmin(I(ClimDistToFront1/1000), 250)) 4.000 0.852   0.729    0.00

Predictors retained during the model selection procedure: Depth, ClimDistToFront1

Predictors dropped during the model selection procedure:
```

Model term plots

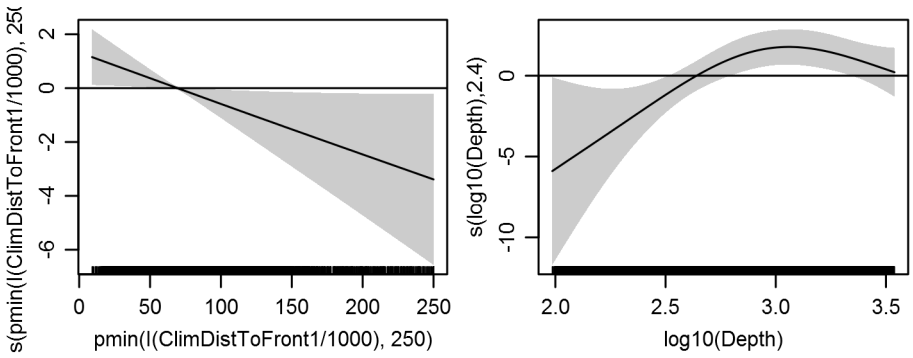

Diagnostic plots

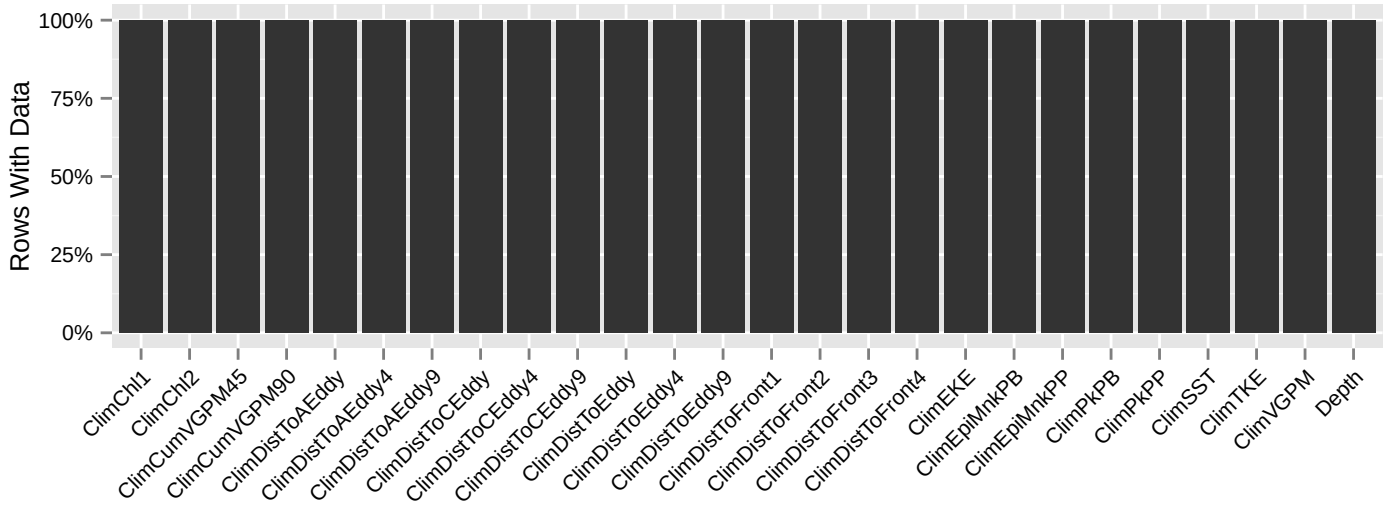

Figure 35: Segments with predictor values for the Melon-headed whale Climatological model, Off Shelf. This plot is used to assess how many segments would be lost by including a given predictor in a model.

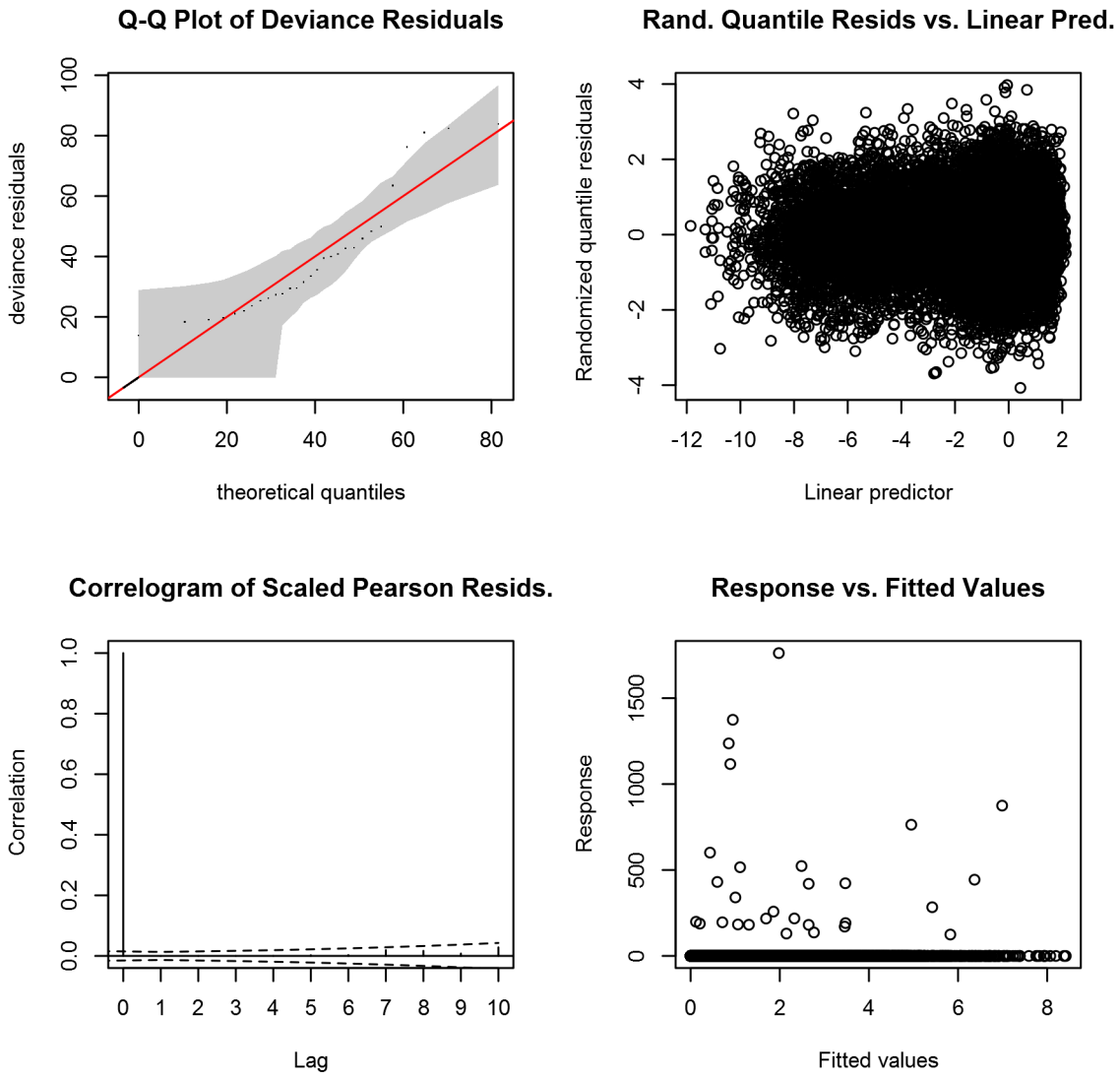

Figure 36: Statistical diagnostic plots for the Melon-headed whale Climatological model, Off Shelf.

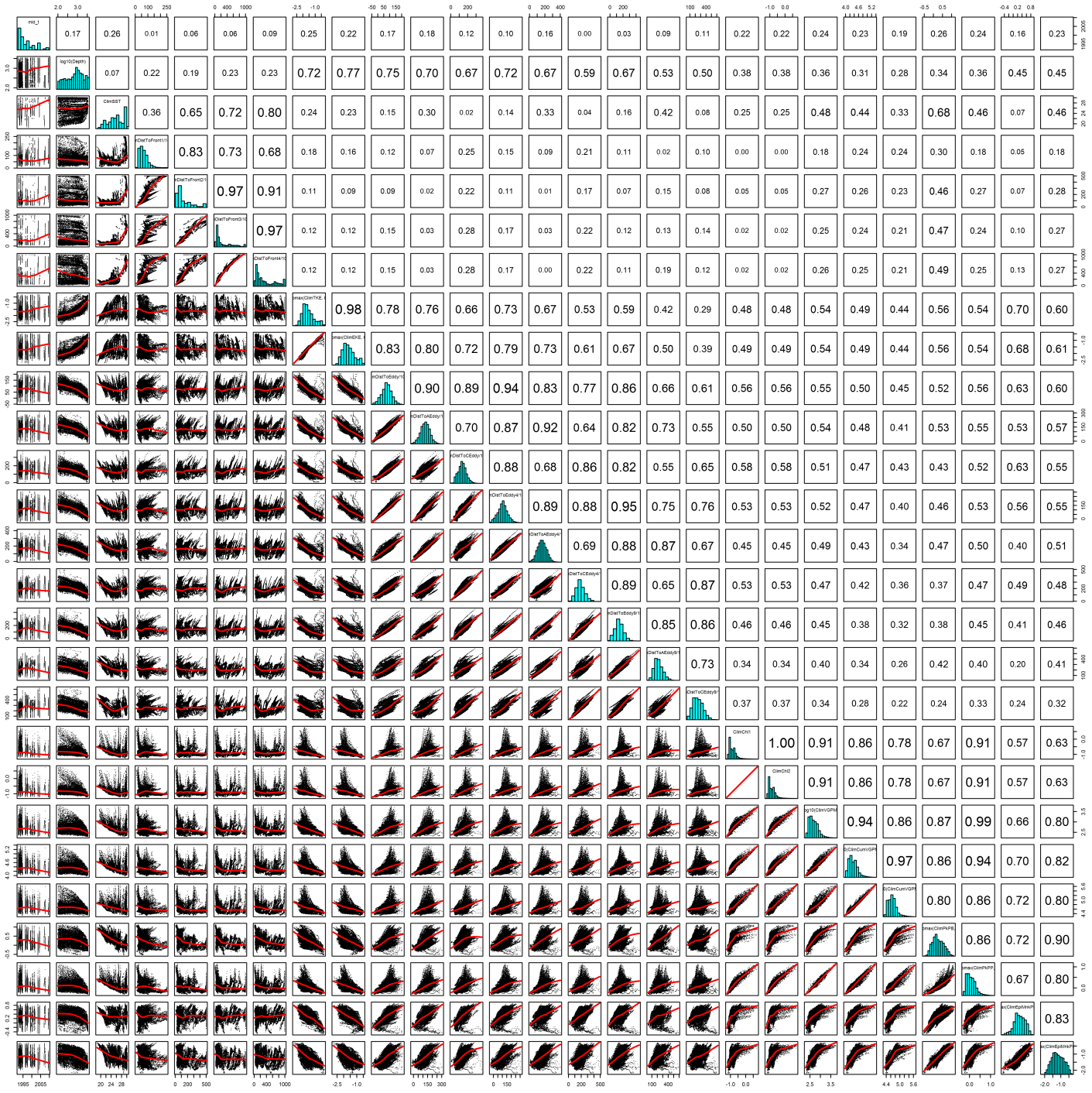

Figure 37: Scatterplot matrix for the Melon-headed whale Climatological model, Off Shelf. This plot is used to inspect the distribution of predictors (via histograms along the diagonal), simple correlation between predictors (via pairwise Pearson coefficients above the diagonal), and linearity of predictor correlations (via scatterplots below the diagonal). This plot is best viewed at high magnification.

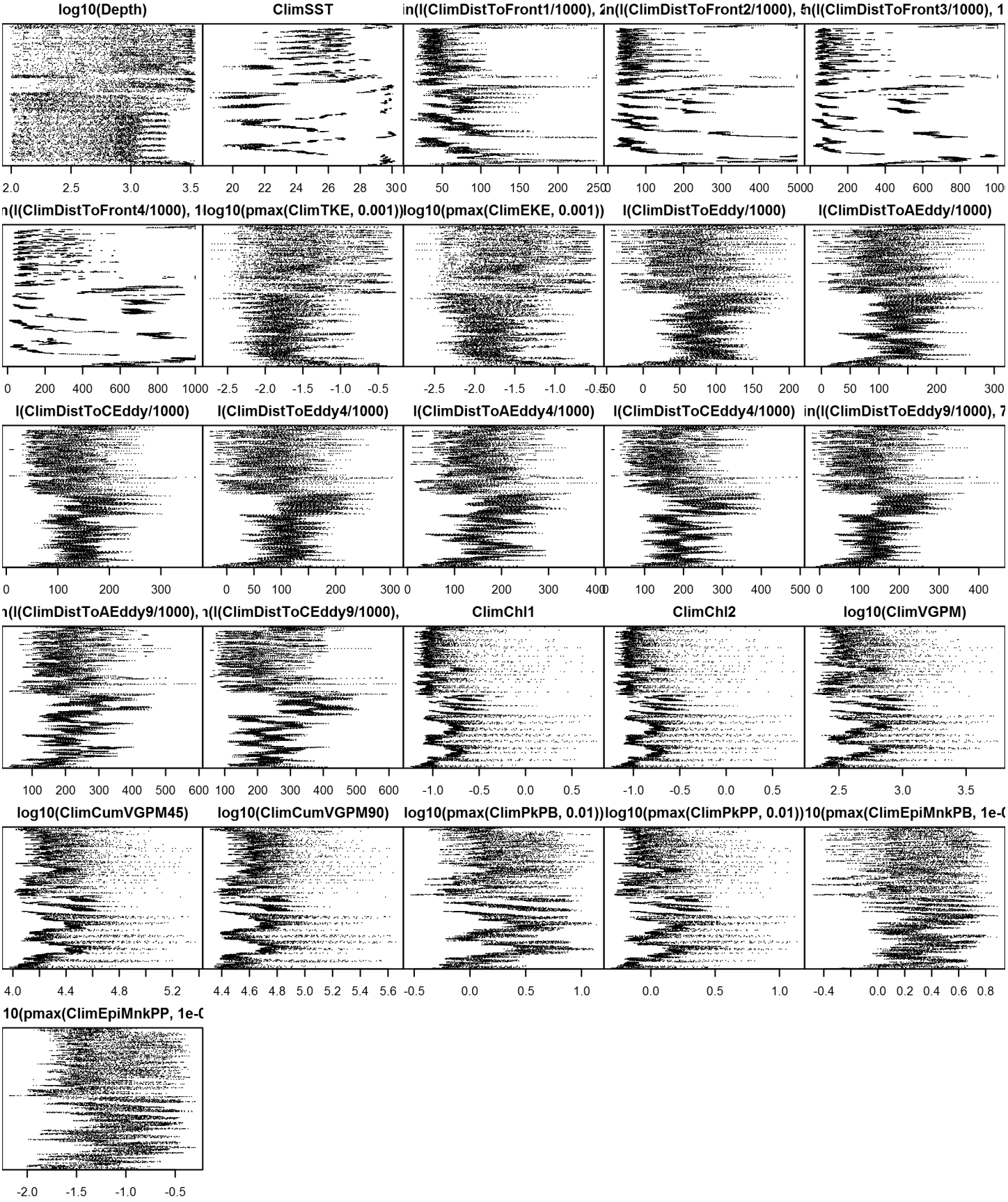

Figure 38: Dotplot for the Melon-headed whale Climatological model, Off Shelf. This plot is used to check for suspicious patterns and outliers in the data. Points are ordered vertically by transect ID, sequentially in time.

On Shelf

Density assumed to be 0 in this region.

Contemporaneous Model

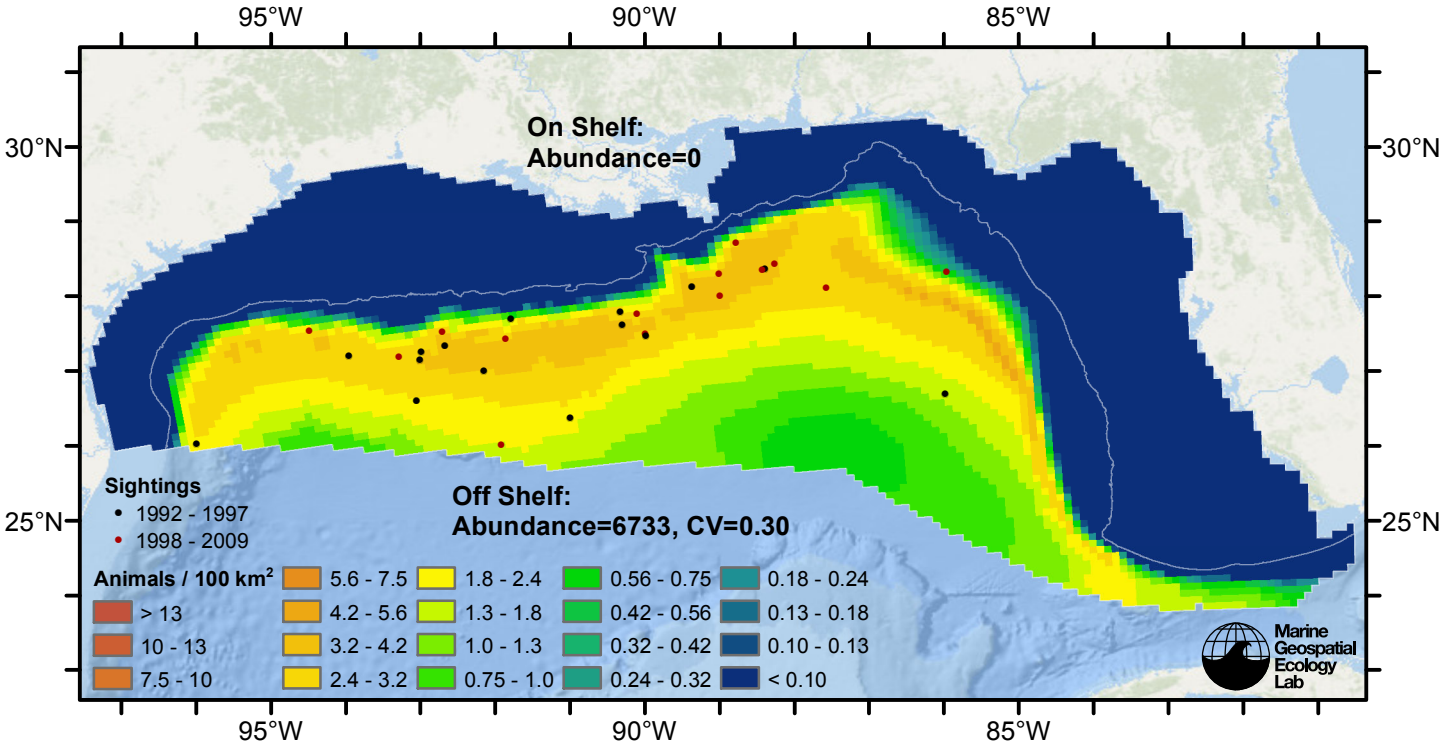

Figure 39: Melon-headed whale density predicted by the contemporaneous model that explained the most deviance. Pixels are 10x10 km. The legend gives the estimated individuals per pixel; breaks are logarithmic. Abundance for each region was computed by summing the density cells occuring in that region.

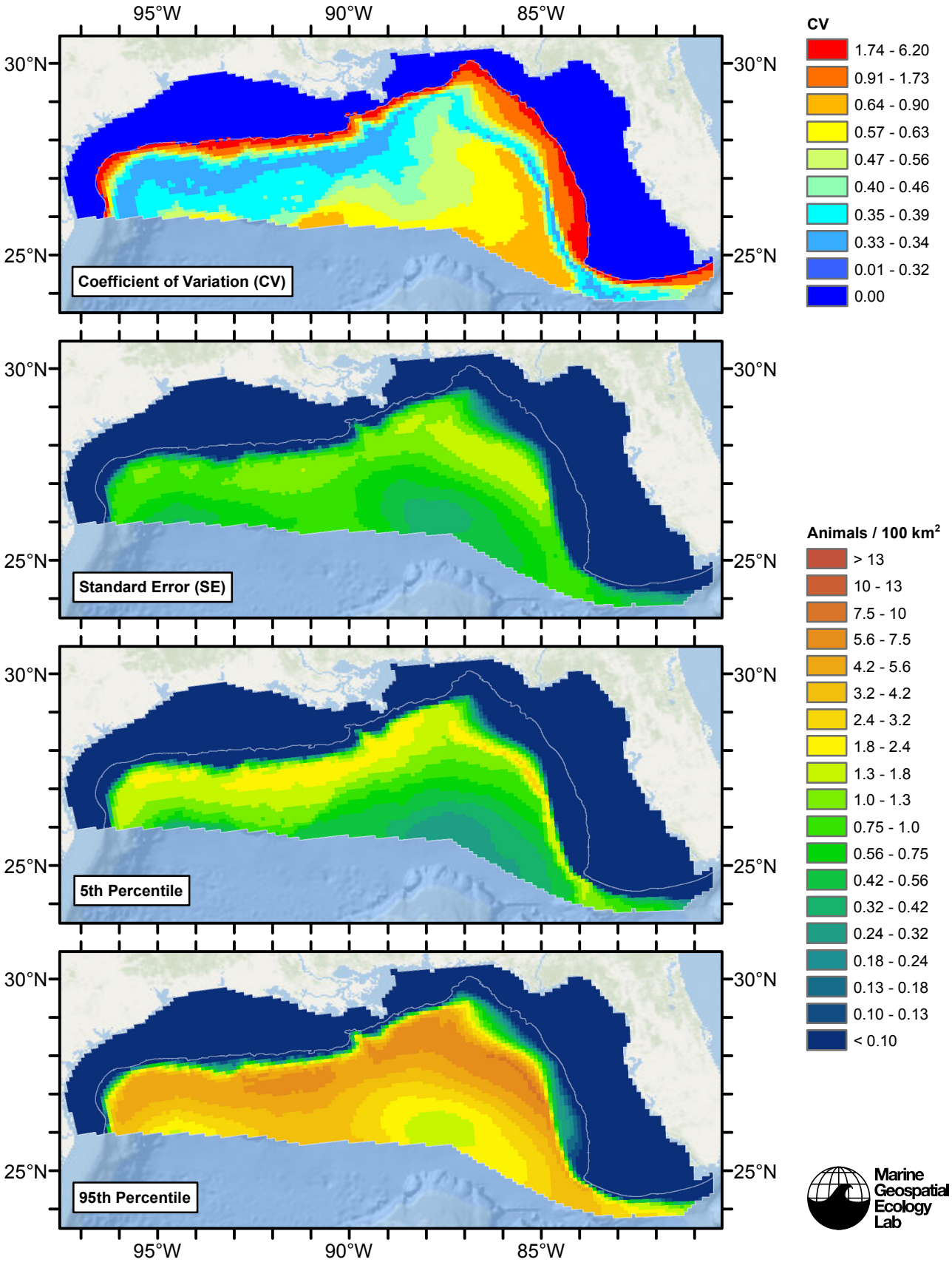

Figure 40: Estimated uncertainty for the contemporaneous model that explained the most deviance. These estimates only incorporate the statistical uncertainty estimated for the spatial model (by the R mgcv package). They do not incorporate uncertainty in the detection functions, g(0) estimates, predictor variables, and so on.

Off Shelf

Statistical output

```
Rscript.exe: This is mgcv 1.8-2. For overview type 'help("mgcv-package")'.


Family: Tweedie(p=1.346)
Link function: log

Formula:
abundance ~ offset(log(area_km2)) + s(log10(Depth), bs = "ts",
    k = 5) + s(pmin(I(DistToEddy9/1000), 700), bs = "ts", k = 5)

Parametric coefficients:
            Estimate Std. Error t value Pr(>|t|)
(Intercept)  -5.7510     0.5426   -10.6   <2e-16 ***
---
Signif. codes:  0 '***' 0.001 '**' 0.01 '*' 0.05 '.' 0.1 ' ' 1

Approximate significance of smooth terms:
                                    edf Ref.df     F  p-value
s(log10(Depth))                   2.189      4 2.355 0.006786 **
s(pmin(I(DistToEddy9/1000), 700)) 2.653      4 3.720 0.000593 ***
---
Signif. codes:  0 '***' 0.001 '**' 0.01 '*' 0.05 '.' 0.1 ' ' 1

R-sq.(adj) =  0.00189   Deviance explained = 22.9%
-REML = 353.05  Scale est. = 616.74    n = 11840

All predictors were significant. This is the final model.
Creating term plots.
Diagnostic output from gam.check():

Method: REML   Optimizer: outer newton
full convergence after 10 iterations.
Gradient range [-0.0002103954,6.315948e-07]
(score 353.051 & scale 616.7351).
Hessian positive definite, eigenvalue range [0.5076073,76.26925].
Model rank =  9 / 9

Basis dimension (k) checking results. Low p-value (k-index<1) may
indicate that k is too low, especially if edf is close to k'.

                                    k'   edf k-index p-value
s(log10(Depth))                   4.000 2.189   0.506       0
s(pmin(I(DistToEddy9/1000), 700)) 4.000 2.653   0.512       0

Predictors retained during the model selection procedure: Depth, DistToEddy9

Predictors dropped during the model selection procedure:
```

Model term plots

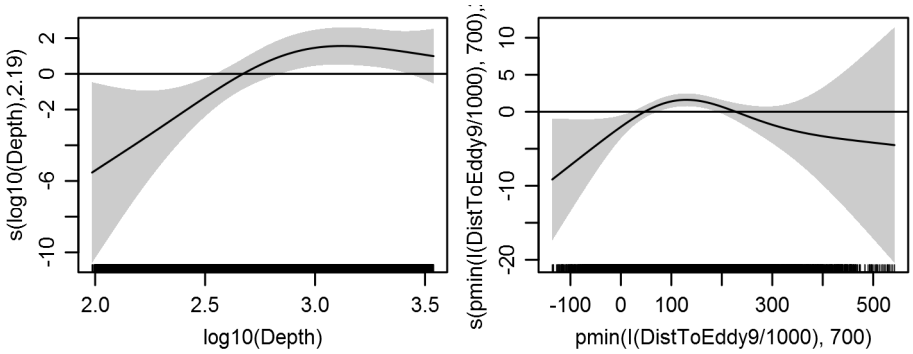

Diagnostic plots

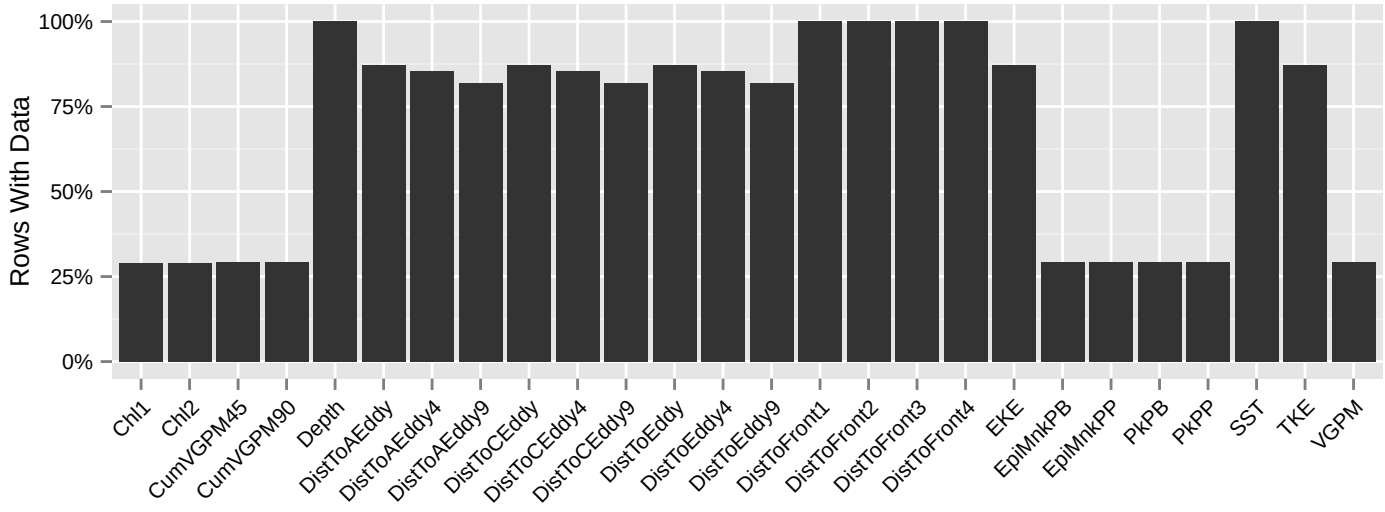

Figure 41: Segments with predictor values for the Melon-headed whale Contemporaneous model, Off Shelf. This plot is used to assess how many segments would be lost by including a given predictor in a model.

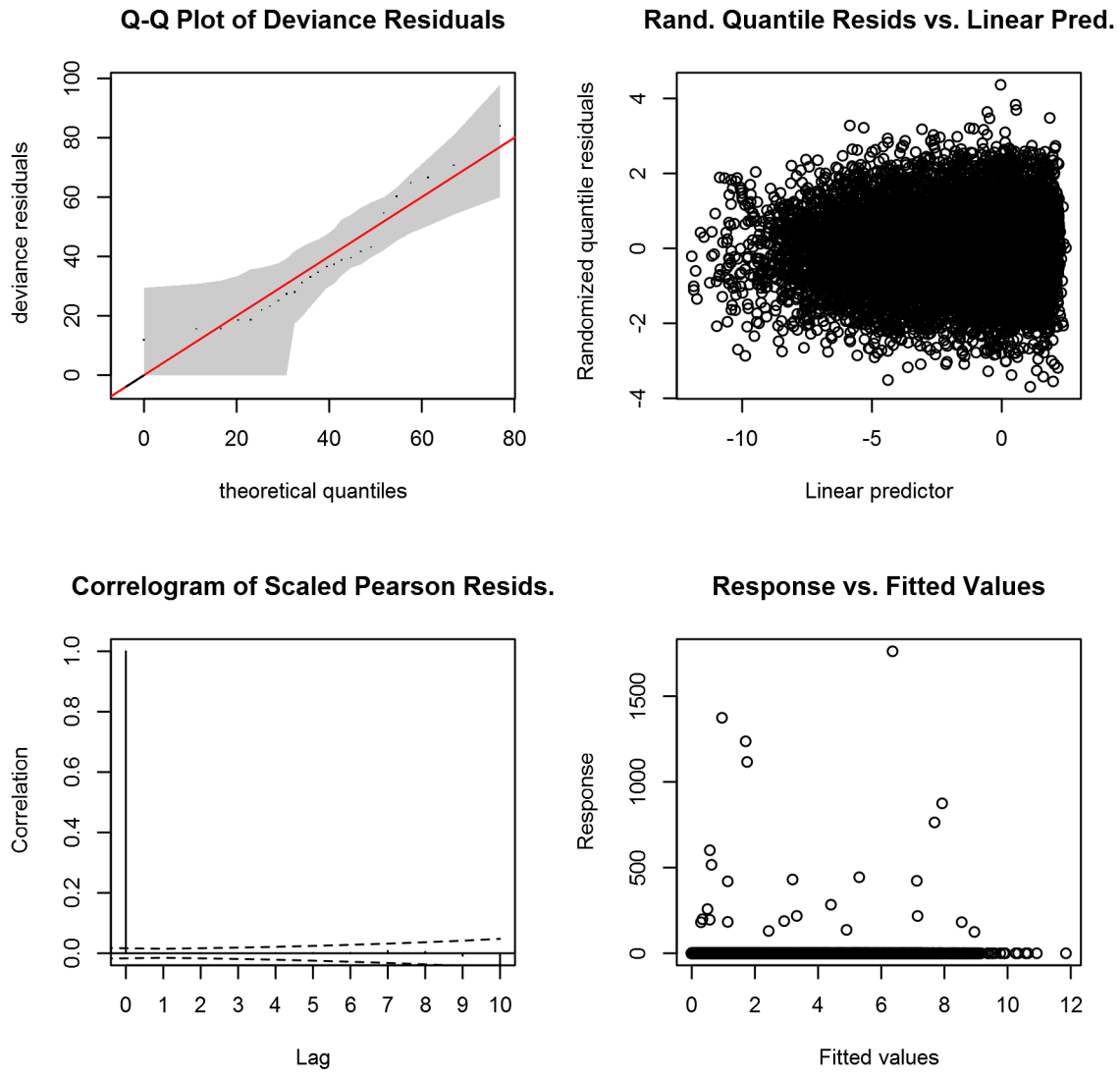

Figure 42: Statistical diagnostic plots for the Melon-headed whale Contemporaneous model, Off Shelf.

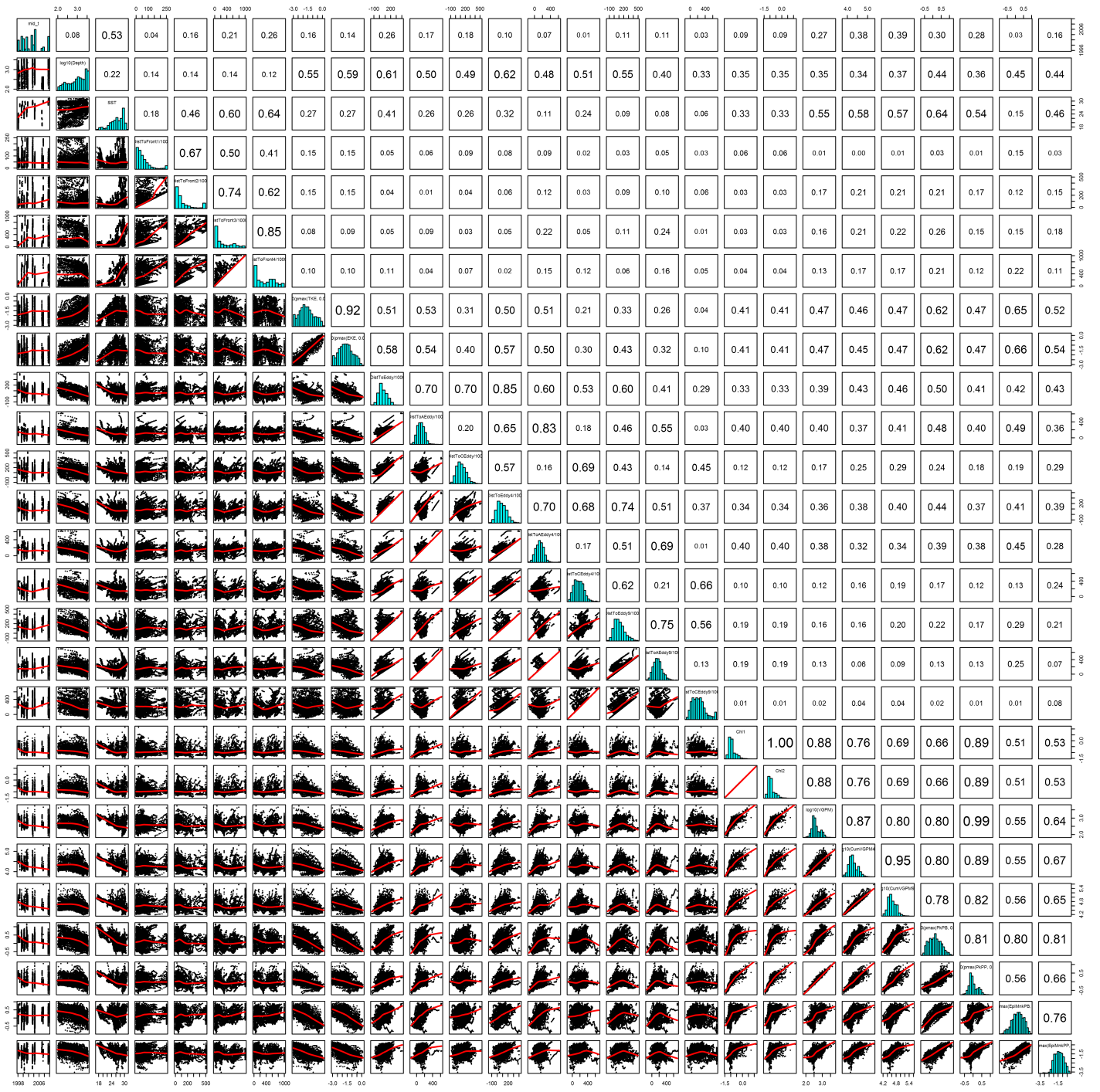

Figure 43: Scatterplot matrix for the Melon-headed whale Contemporaneous model, Off Shelf. This plot is used to inspect the distribution of predictors (via histograms along the diagonal), simple correlation between predictors (via pairwise Pearson coefficients above the diagonal), and linearity of predictor correlations (via scatterplots below the diagonal). This plot is best viewed at high magnification.

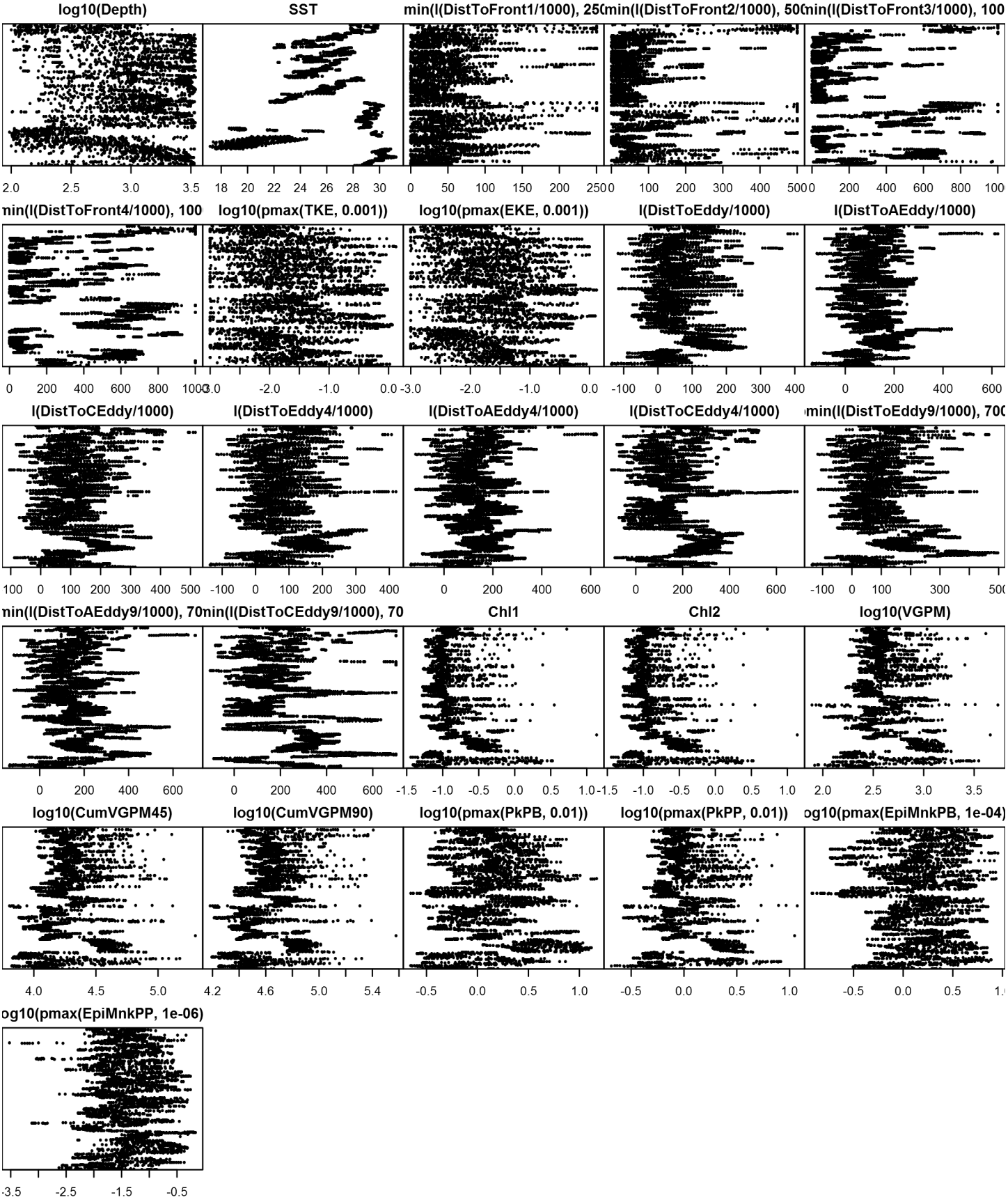

Figure 44: Dotplot for the Melon-headed whale Contemporaneous model, Off Shelf. This plot is used to check for suspicious patterns and outliers in the data. Points are ordered vertically by transect ID, sequentially in time.

On Shelf

Density assumed to be 0 in this region.

Climatological Same Segments Model

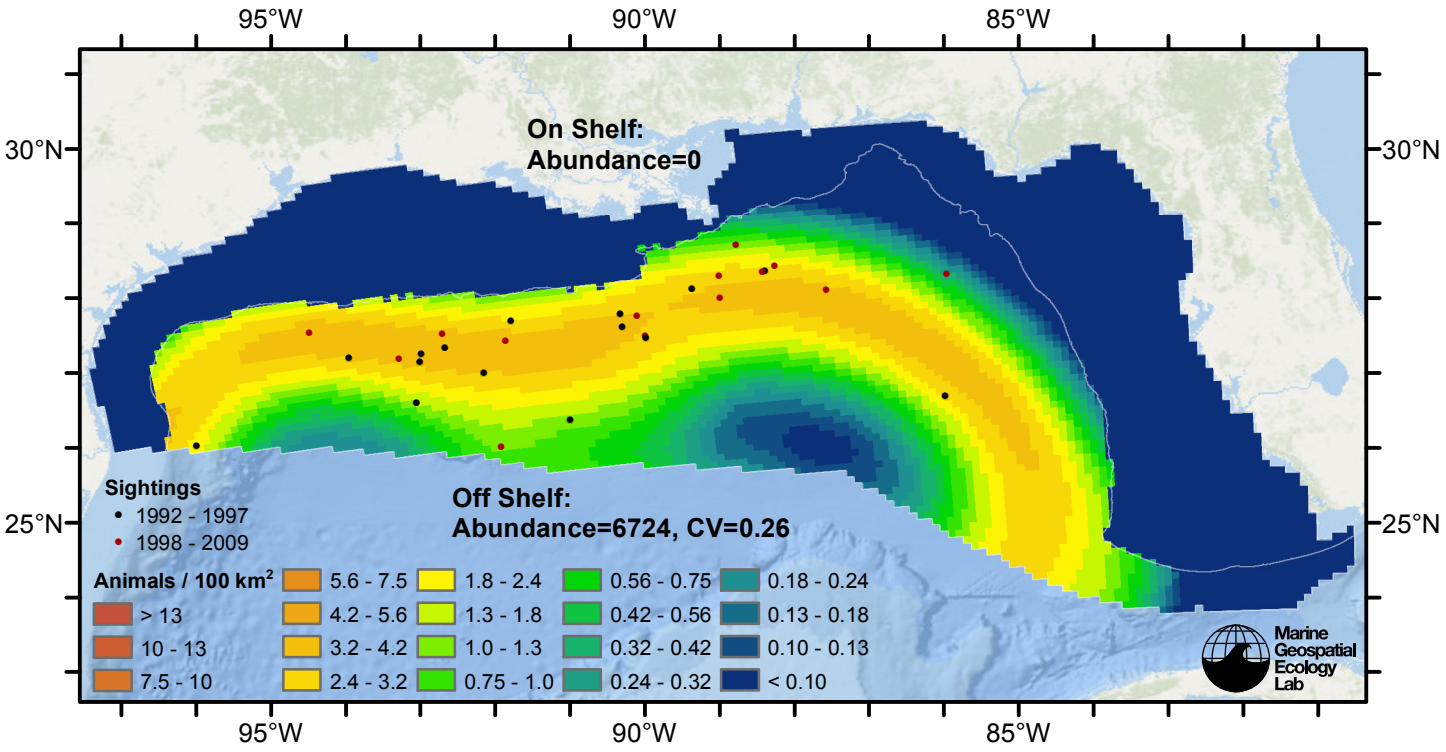

Figure 45: Melon-headed whale density predicted by the climatological same segments model that explained the most deviance. Pixels are 10x10 km. The legend gives the estimated individuals per pixel; breaks are logarithmic. Abundance for each region was computed by summing the density cells occuring in that region.

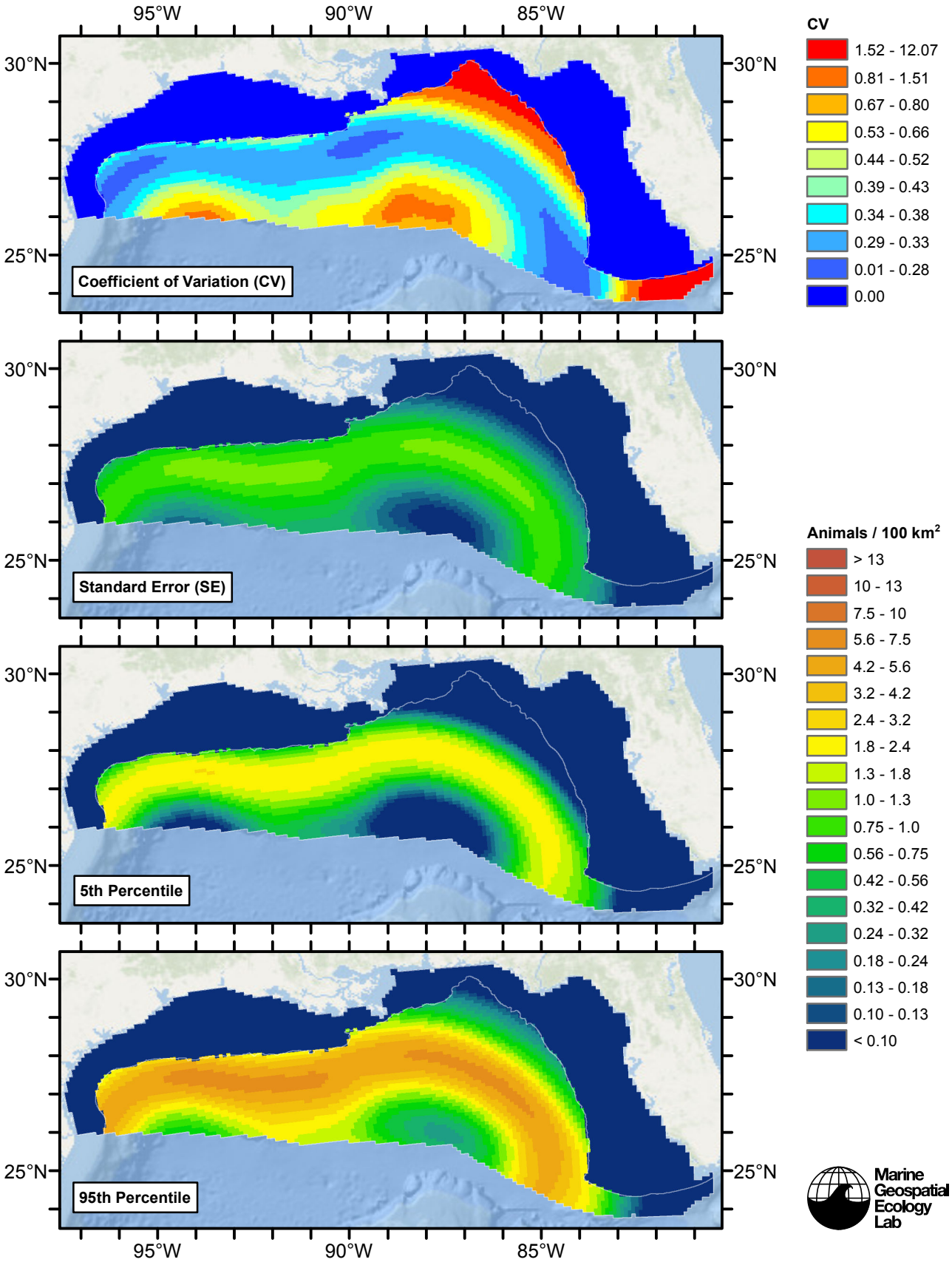

Figure 46: Estimated uncertainty for the climatological same segments model that explained the most deviance. These estimates only incorporate the statistical uncertainty estimated for the spatial model (by the R mgcv package). They do not incorporate uncertainty in the detection functions, g(0) estimates, predictor variables, and so on.

Off Shelf

Statistical output

```
Rscript.exe: This is mgcv 1.8-2. For overview type 'help("mgcv-package")'.


Family: Tweedie(p=1.36)
Link function: log

Formula:
abundance ~ offset(log(area_km2)) + s(pmin(I(ClimDistToEddy9/1000),
    700), bs = "ts", k = 5)

Parametric coefficients:
            Estimate Std. Error t value Pr(>|t|)
(Intercept)   -5.026      0.466  -10.79   <2e-16 ***
---
Signif. codes:  0 '***' 0.001 '**' 0.01 '*' 0.05 '.' 0.1 ' ' 1

Approximate significance of smooth terms:
                                       edf Ref.df     F  p-value
s(pmin(I(ClimDistToEddy9/1000), 700)) 2.575      4 3.709 0.000622 ***
---
Signif. codes:  0 '***' 0.001 '**' 0.01 '*' 0.05 '.' 0.1 ' ' 1

R-sq.(adj) =  7.43e-05   Deviance explained = 12.9%
-REML = 355.92  Scale est. = 689.95    n = 11840

All predictors were significant. This is the final model.
Creating term plots.
Diagnostic output from gam.check():

Method: REML   Optimizer: outer newton
full convergence after 11 iterations.
Gradient range [-6.727174e-05,2.093626e-05]
(score 355.918 & scale 689.9513).
Hessian positive definite, eigenvalue range [0.723024,76.10246].
Model rank =  5 / 5

Basis dimension (k) checking results. Low p-value (k-index<1) may
indicate that k is too low, especially if edf is close to k'.

                                       k'   edf k-index p-value
s(pmin(I(ClimDistToEddy9/1000), 700)) 4.000 2.575   0.566       0

Predictors retained during the model selection procedure: ClimDistToEddy9

Predictors dropped during the model selection procedure: Depth
```

Model term plots

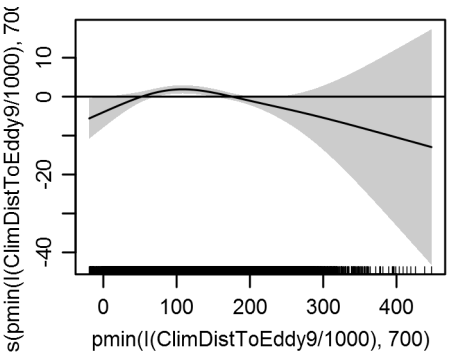

Diagnostic plots

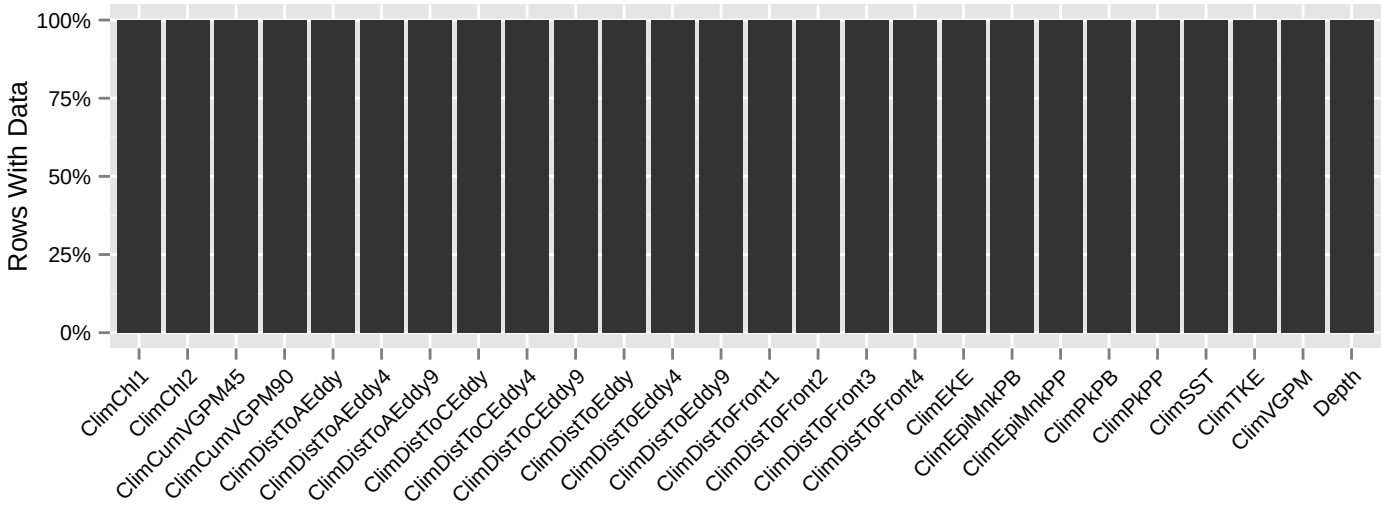

Figure 47: Segments with predictor values for the Melon-headed whale Climatological model, Off Shelf. This plot is used to assess how many segments would be lost by including a given predictor in a model.

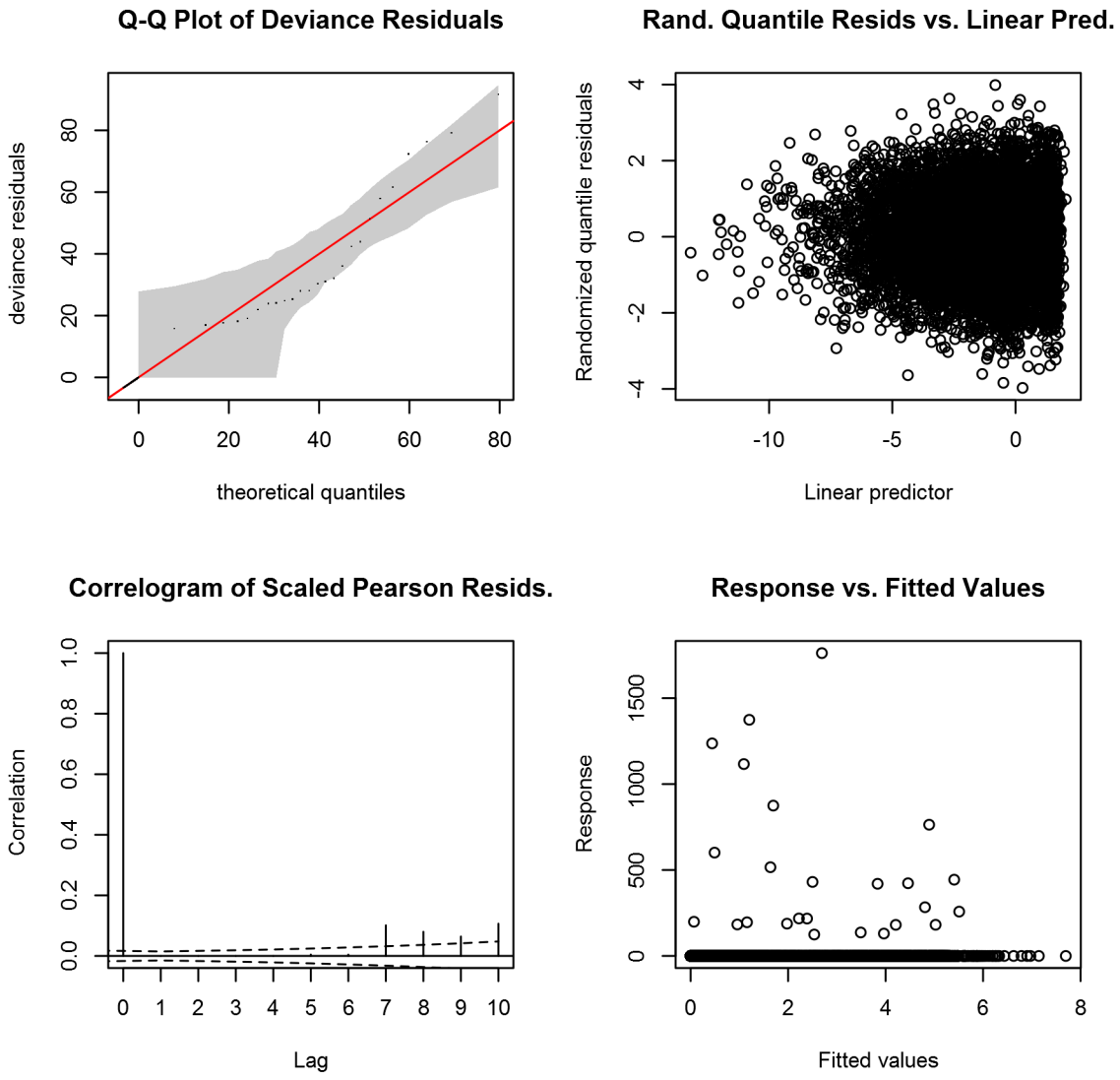

Figure 48: Statistical diagnostic plots for the Melon-headed whale Climatological model, Off Shelf.

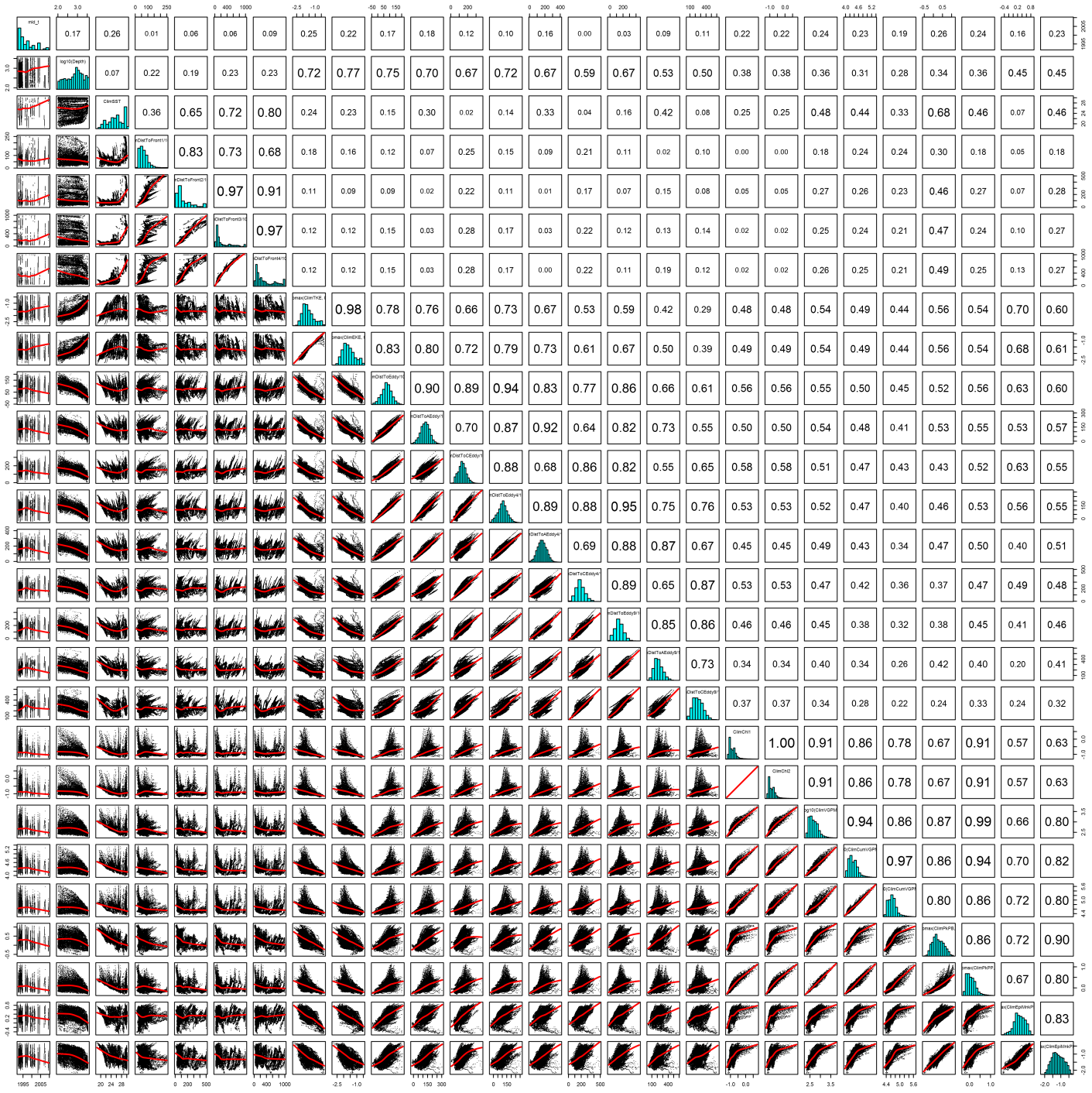

Figure 49: Scatterplot matrix for the Melon-headed whale Climatological model, Off Shelf. This plot is used to inspect the distribution of predictors (via histograms along the diagonal), simple correlation between predictors (via pairwise Pearson coefficients above the diagonal), and linearity of predictor correlations (via scatterplots below the diagonal). This plot is best viewed at high magnification.

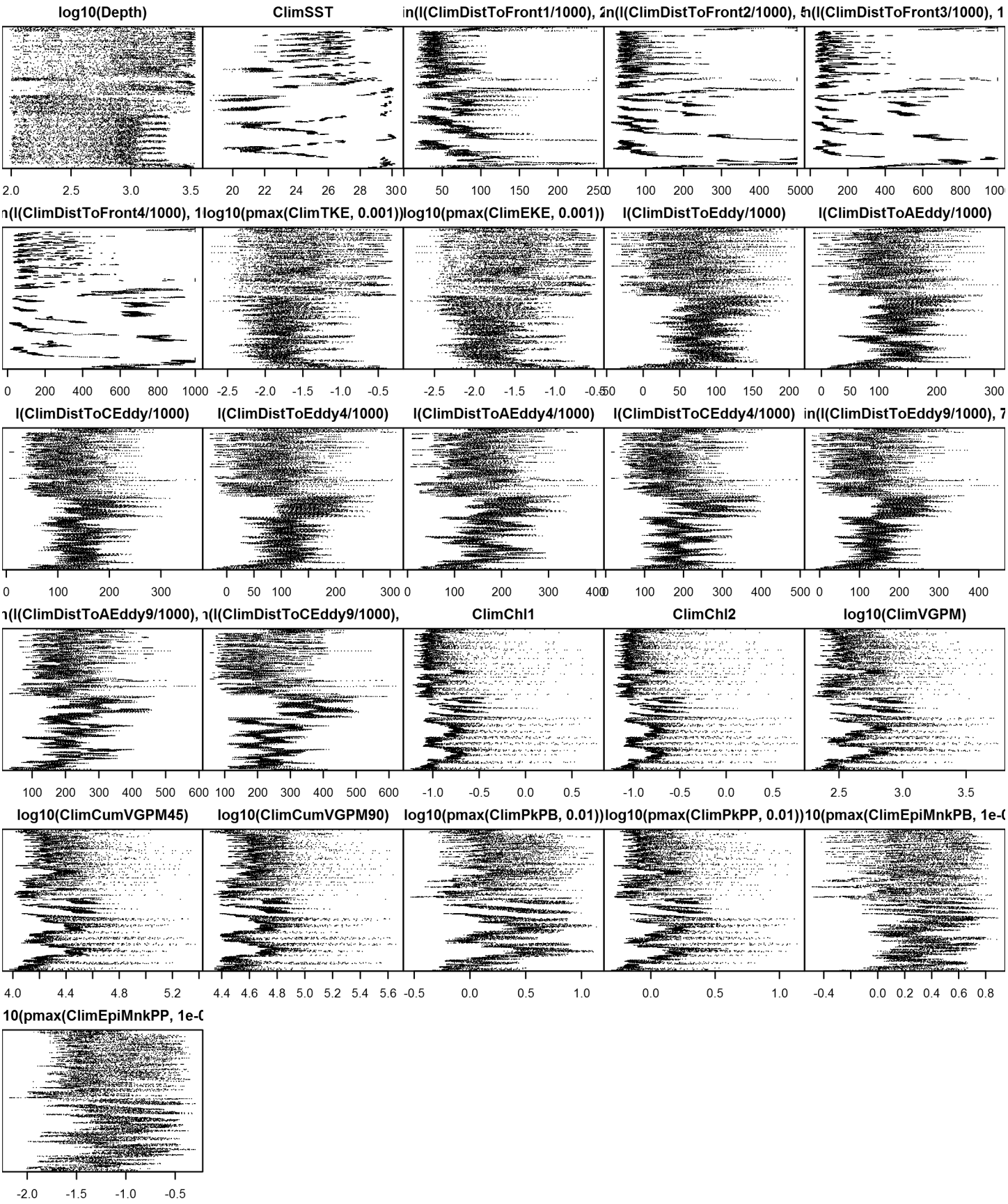

Figure 50: Dotplot for the Melon-headed whale Climatological model, Off Shelf. This plot is used to check for suspicious patterns and outliers in the data. Points are ordered vertically by transect ID, sequentially in time.

On Shelf

Density assumed to be 0 in this region.

Model Comparison

Spatial Model Performance

The table below summarizes the performance of the candidate spatial models that were tested. The first model contained only physiographic predictors. Subsequent models added additional suites of predictors of based on when they became available via remote sensing.

For each model, three versions were fitted; the % Dev Expl columns give the % deviance explained by each one. The "climatological" models were fitted to 8-day climatologies of the environmental predictors. Because the environmental predictors were always available, no segments were lost, allowing these models to consider the maximal amount of survey data. The "contemporaneous" models were fitted to day-of-sighting images of the environmental predictors; these were smoothed to reduce data loss due to clouds, but some segments still failed to retrieve environmental values and were lost. Finally, the "climatological same segments" models fitted climatological predictors to the segments retained by the contemporaneous model, so that the explantory power of the two types of predictors could be directly compared. For each of the three models, predictors were selected independently via shrinkage smoothers; thus the three models did not necessarily utilize the same predictors.

Predictors derived from ocean currents first became available in January 1993 after the launch of the TOPEX/Poseidon satellite; productivity predictors first became available in September 1997 after the launch of the SeaWiFS sensor. Contemporaneous and climatological same segments models considering these predictors usually suffered data loss. Date Range shows the years spanned by the retained segments. The Segments column gives the number of segments retained; % Lost gives the percentage lost.

Predictors	Climatol % Dev Expl	Contemp % Dev Expl	Climatol Same Segs % Dev Expl	Segments	% Lost	Date Range
Depth	10.8			14455		1992-2009
Depth+OnePredictor	14.7	22.9	12.9	11840	18.1	1993-2009

Table 21: Deviance explained by the candidate density models.

Abundance Estimates

The table below shows the estimated mean abundance (number of animals) within the study area, for the models that explained the most deviance for each model type. Mean abundance was calculated by first predicting density maps for a series of time steps, then computing the abundance for each map, and then averaging the abundances. For the climatological models, we used 8-day climatologies, resulting in 46 abundance maps. For the contemporaneous models, we used daily images, resulting in 365 predicted abundance maps per year that the prediction spanned. The Dates column gives the dates to which the estimates apply. For our models, these are the years for which both survey data and remote sensing data were available.

The Assumed g(0)=1 column specifies whether the abundance estimate assumed that detection was certain along the survey trackline. Studies that assumed this did not correct for availability or perception bias, and therefore underestimated abundance. The In our models column specifies whether the survey data from the study was also used in our models. If not, the study provides a completely independent estimate of abundance.

Dates	Model or study	Estimated abundance	CV	Assumed g(0)=1	In our models
1992-2009	Climatological model	5526	0.25	No	
1993-2009	Contemporaneous model*	6733	0.30	No	

1992-2009	Climatological same segments model	6724	0.26	No	
2009	Oceanic waters, Jun-Aug (Waring et al. 2013)	2235	0.75	Yes	Yes
2003-2004	Oceanic waters, Jun-Aug (Mullin 2007)	2283	0.76	Yes	Yes
1996-2001	Oceanic waters, Apr-Jun (Mullin and Fulling 2004)	3451	0.55	Yes	Yes
1991-1994	Oceanic waters, Apr-Jun (Hansen et al. 1995)	3965	0.39	Yes	Yes

Table 22: Estimated mean abundance within the study area. We selected the model marked with * as our best estimate of the abundance and distribution of this taxon. For comparison, independent abundance estimates from NOAA technical reports and/or the scientific literature are shown. Please see the Discussion section below for our evaluation of our models compared to the other estimates. Note that our abundance estimates are averaged over the whole year, while the other studies may have estimated abundance for specific months or seasons. Our coefficients of variation (CVs) underestimate the true uncertainty in our estimates, as they only incorporated the uncertainty of the GAM stage of our models. Other sources of uncertainty include the detection functions and g(0) estimates. It was not possible to incorporate these into our CVs without undertaking a computationally-prohibitive bootstrap; we hope to attempt that in a future version of our models.

Density Maps

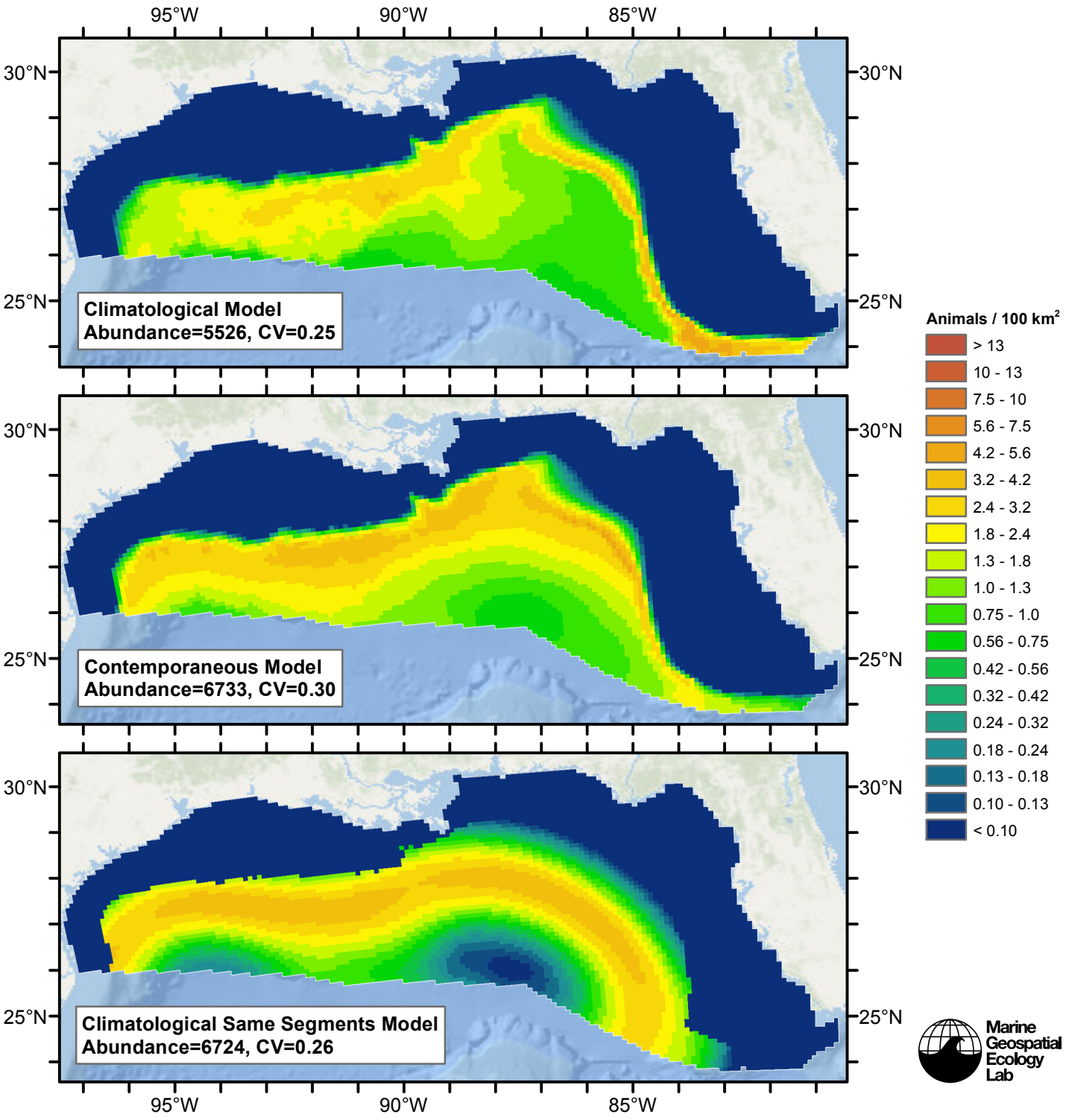

Figure 51: Melon-headed whale density and abundance predicted by the models that explained the most deviance. Regions inside the study area (white line) where the background map is visible are areas we did not model (see text).

Temporal Variability

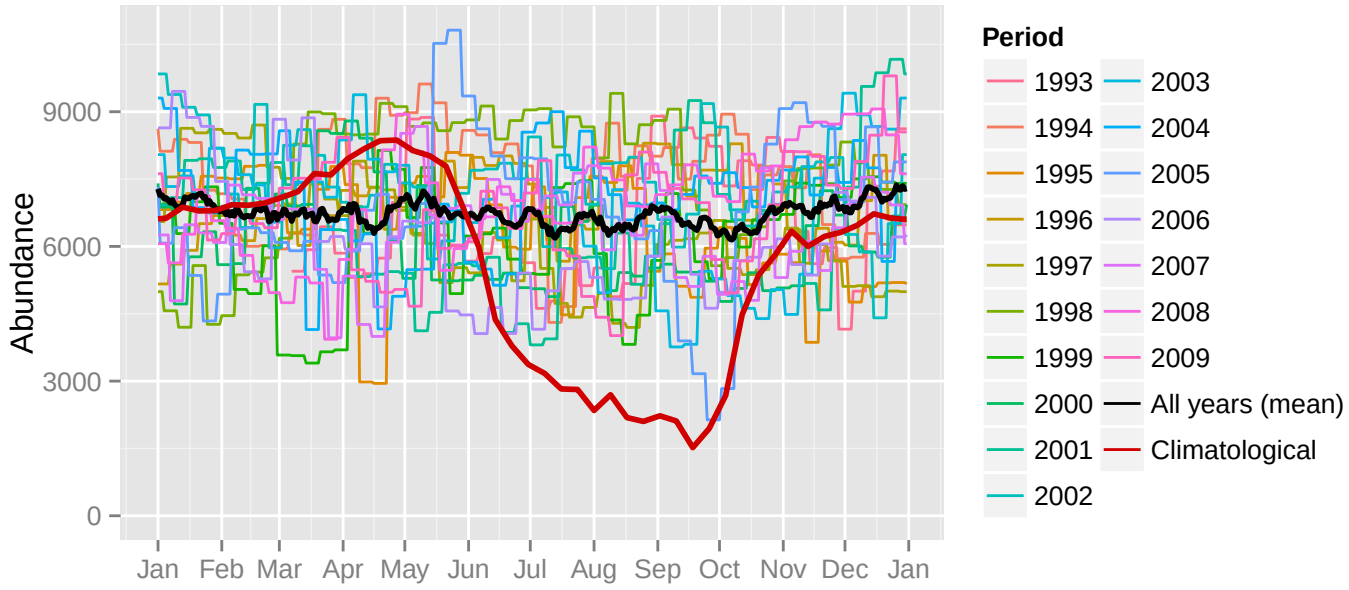

Figure 52: Comparison of Melon-headed whale abundance predicted at a daily time step for different time periods. Individual years were predicted using contemporaneous models. "All years (mean)" averages the individual years, giving the mean annual abundance of the contemporaneous model. "Climatological" was predicted using the climatological model. The results for the climatological same segments model are not shown.

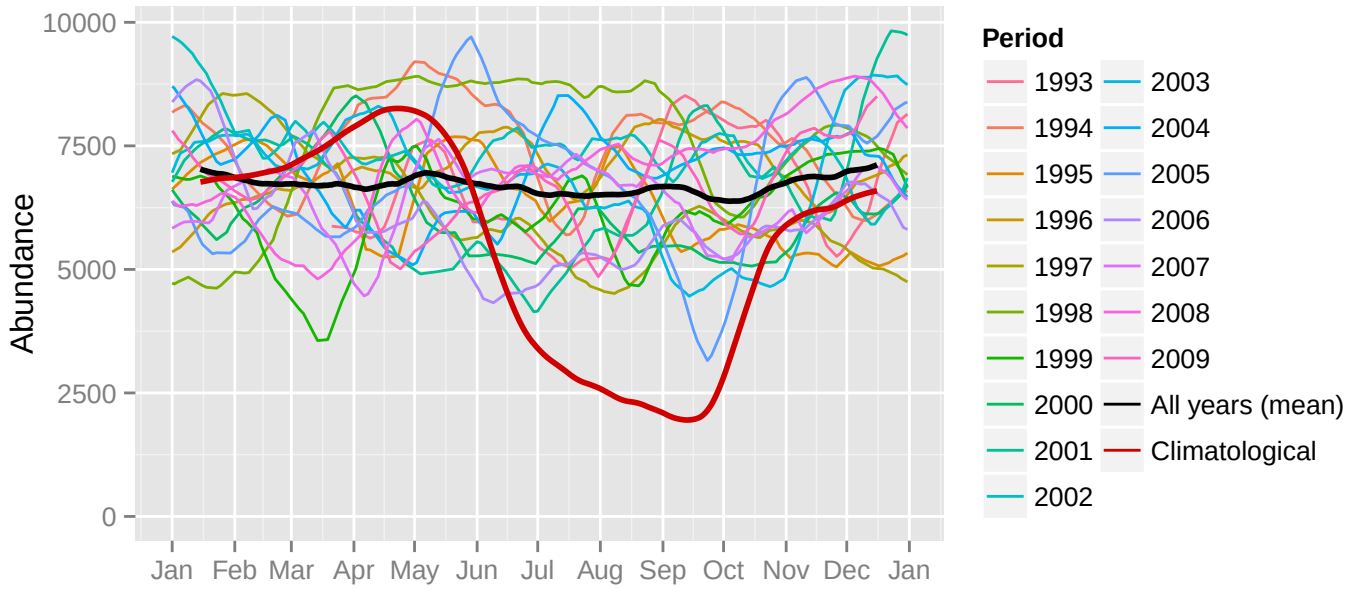

Figure 53: The same data as the preceding figure, but with a 30-day moving average applied.

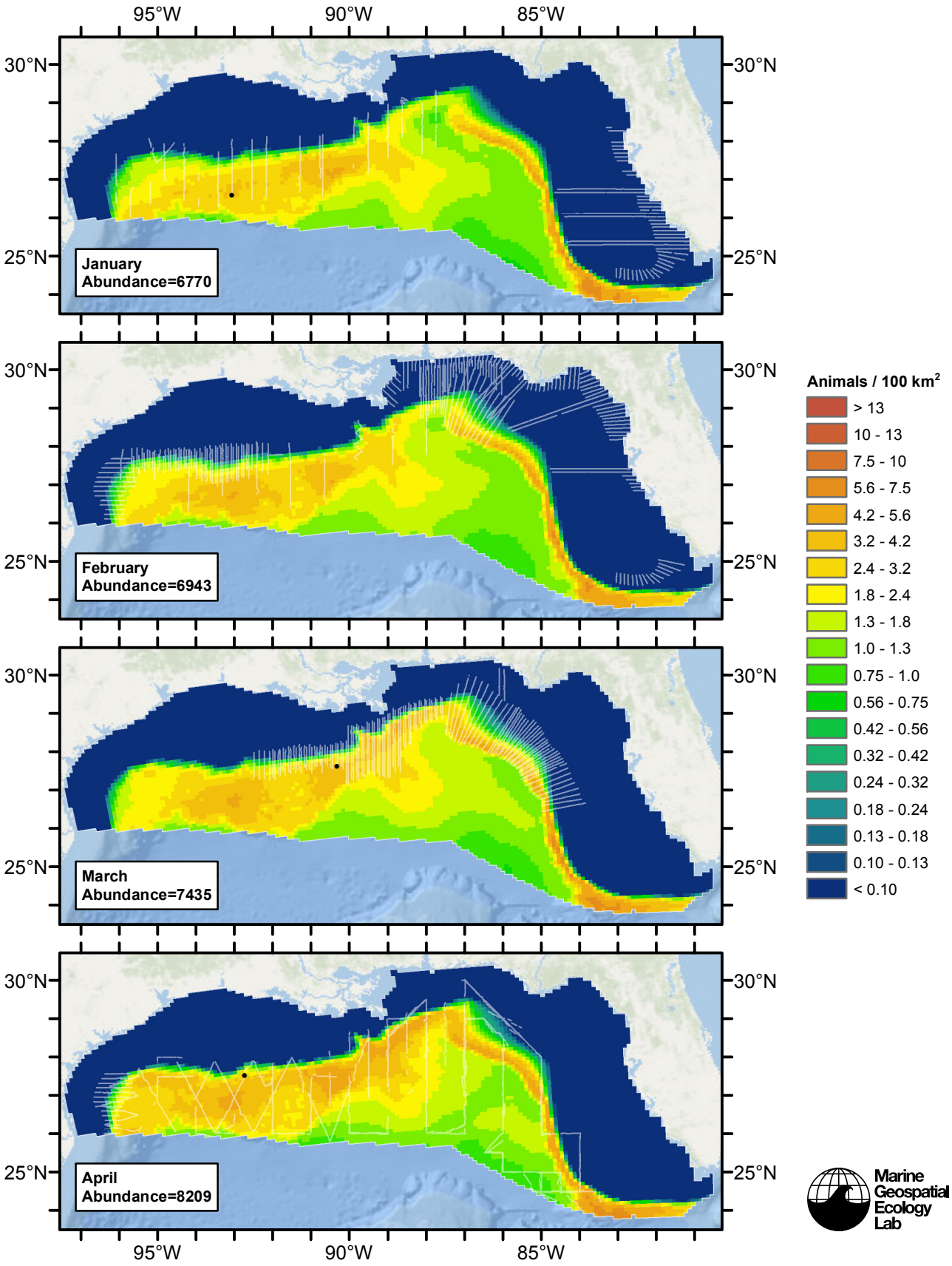
95°W
90°W
85°W
30°N
25°N
January
Abundance=6770
February
Abundance=6943
March
Abundance=7435
April
Abundance=8209
Animals / 100 km²
> 13
10 - 13
7.5 - 10
5.6 - 7.5
4.2 - 5.6
3.2 - 4.2
2.4 - 3.2
1.8 - 2.4
1.3 - 1.8
1.0 - 1.3
0.75 - 1.0
0.56 - 0.75
0.42 - 0.56
0.32 - 0.42
0.24 - 0.32
0.18 - 0.24
0.13 - 0.18
0.10 - 0.13
< 0.10
Marine
Geospatial
Ecology
Lab

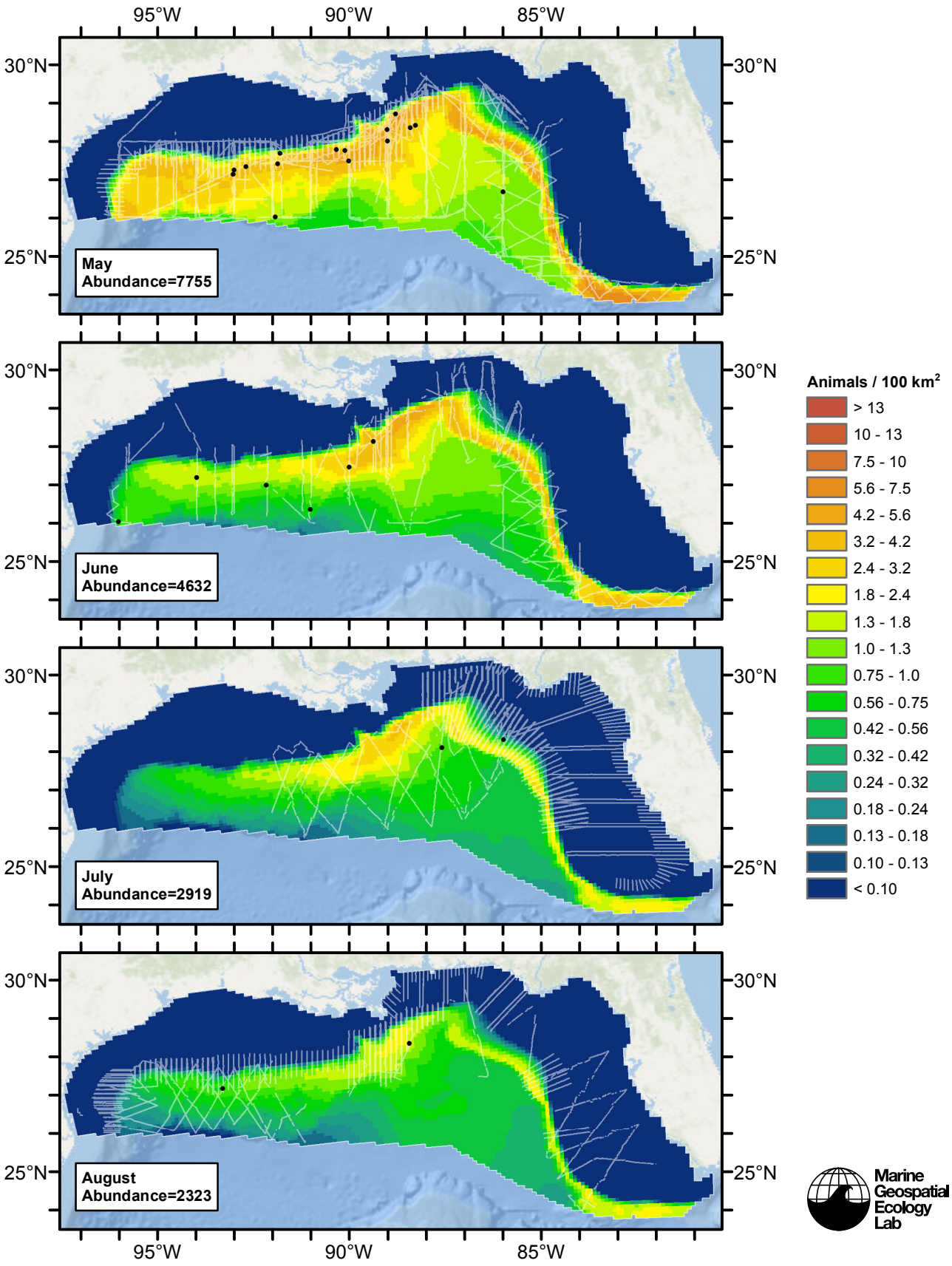
95°W
90°W
85°W
30°N
25°N
May
Abundance=7755
June
Abundance=4632
July
Abundance=2919
August
Abundance=2323
Animals / 100 km²
> 13
10 - 13
7.5 - 10
5.6 - 7.5
4.2 - 5.6
3.2 - 4.2
2.4 - 3.2
1.8 - 2.4
1.3 - 1.8
1.0 - 1.3
0.75 - 1.0
0.56 - 0.75
0.42 - 0.56
0.32 - 0.42
0.24 - 0.32
0.18 - 0.24
0.13 - 0.18
0.10 - 0.13
< 0.10
Marine
Geospatial
Ecology
Lab

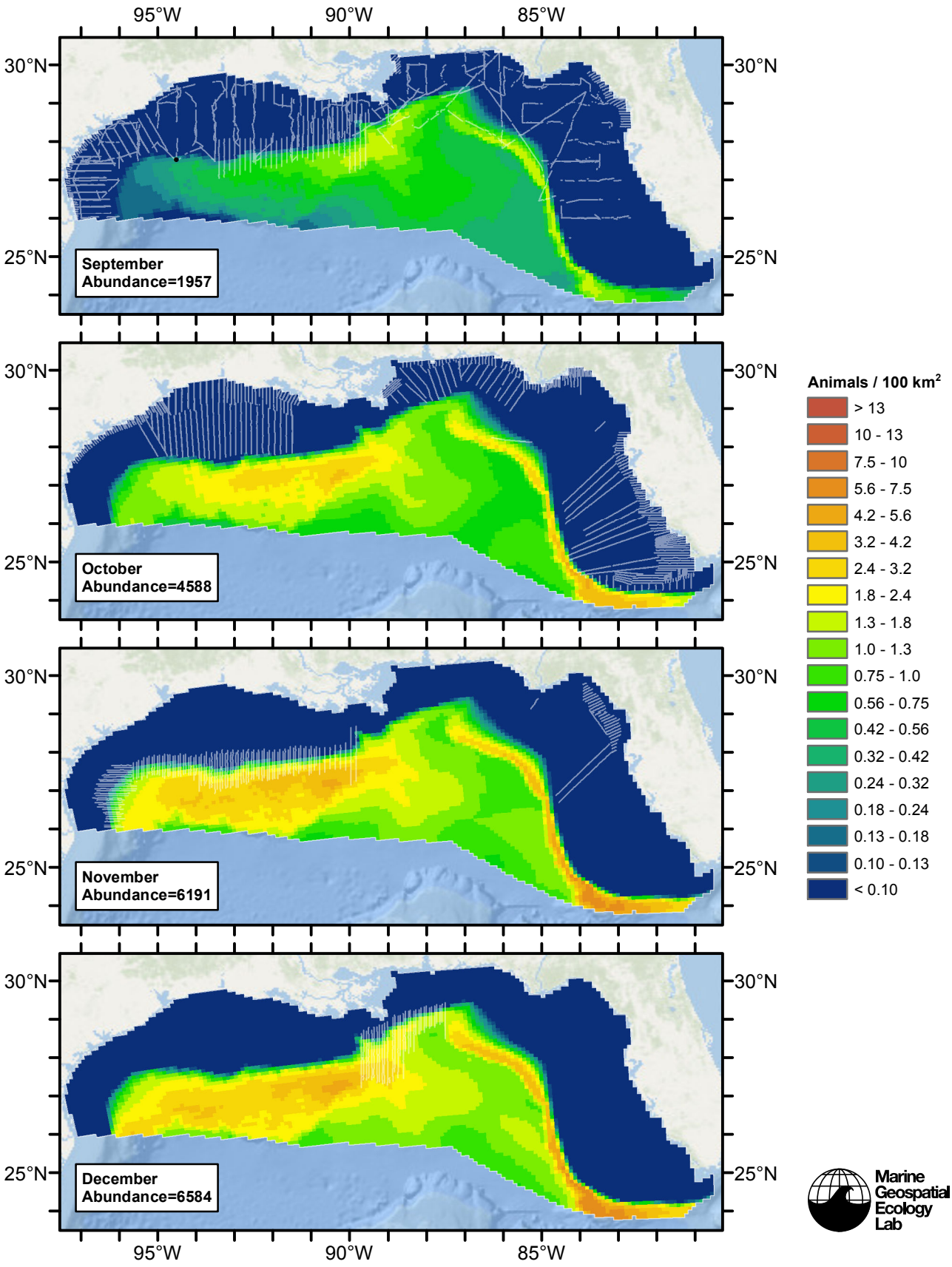
95°W
90°W
85°W
30°N
25°N
September
Abundance=1957
October
Abundance=4588
November
Abundance=6191
December
Abundance=6584
Animals / 100 km²
> 13
10 - 13
7.5 - 10
5.6 - 7.5
4.2 - 5.6
3.2 - 4.2
2.4 - 3.2
1.8 - 2.4
1.3 - 1.8
1.0 - 1.3
0.75 - 1.0
0.56 - 0.75
0.42 - 0.56
0.32 - 0.42
0.24 - 0.32
0.18 - 0.24
0.13 - 0.18
0.10 - 0.13
< 0.10
Marine
Geospatial
Ecology
Lab

Contemporaneous Model

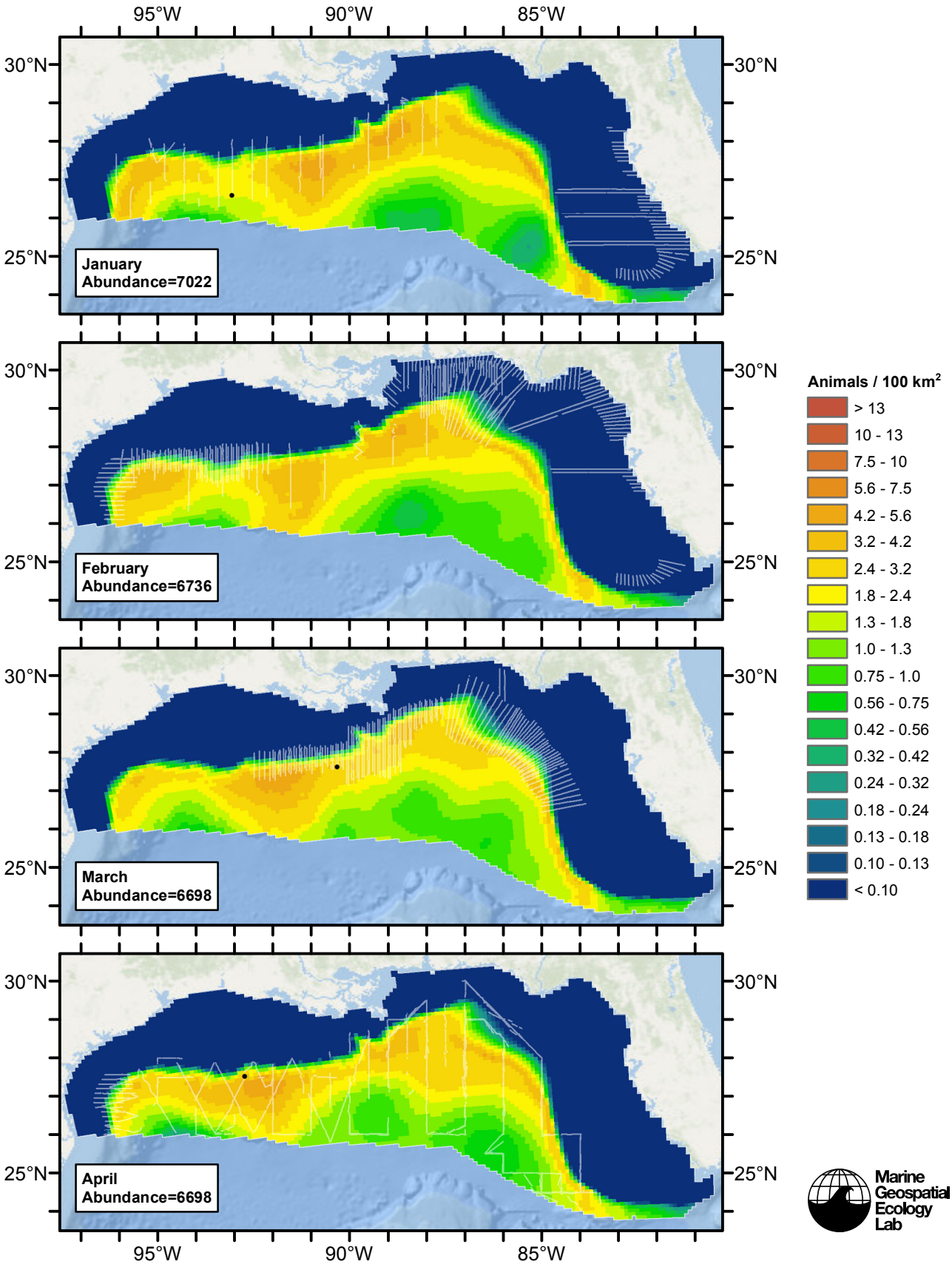

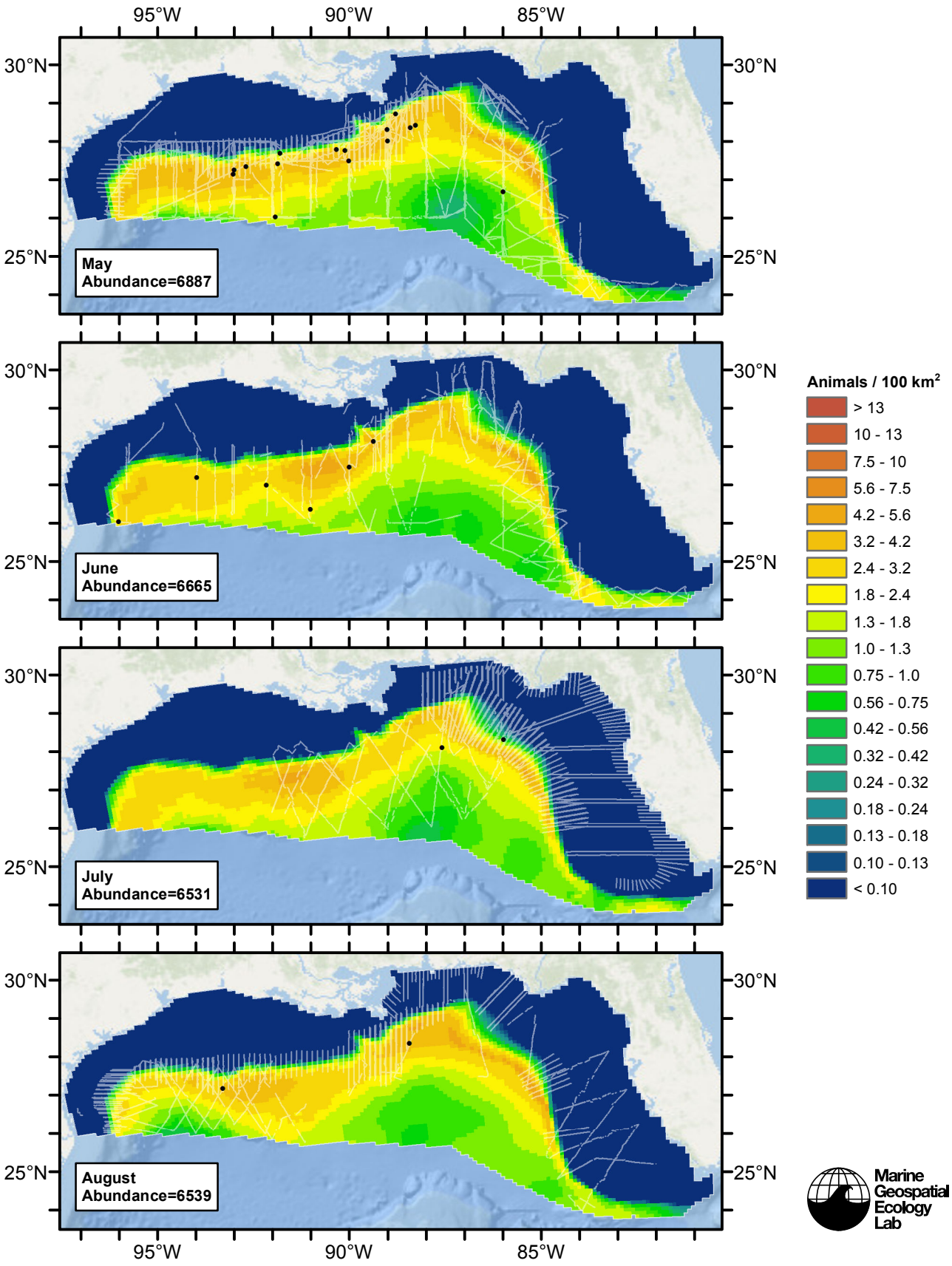
95°W
90°W
85°W
30°N
25°N
May
Abundance=6887
June
Abundance=6665
July
Abundance=6531
August
Abundance=6539
Animals / 100 km²
> 13
10 - 13
7.5 - 10
5.6 - 7.5
4.2 - 5.6
3.2 - 4.2
2.4 - 3.2
1.8 - 2.4
1.3 - 1.8
1.0 - 1.3
0.75 - 1.0
0.56 - 0.75
0.42 - 0.56
0.32 - 0.42
0.24 - 0.32
0.18 - 0.24
0.13 - 0.18
0.10 - 0.13
< 0.10
Marine
Geospatial
Ecology
Lab

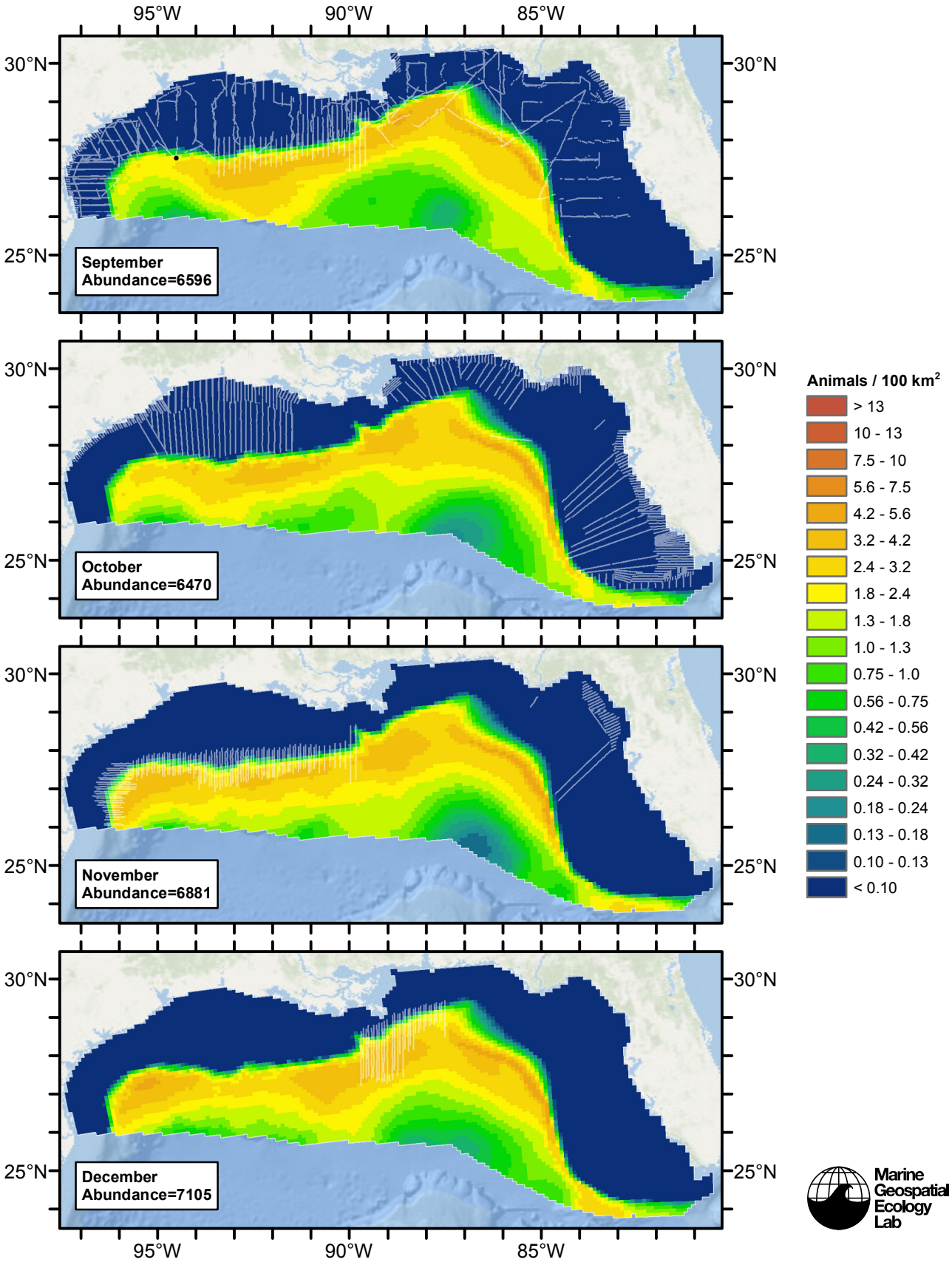
95°W
90°W
85°W
30°N
25°N
September
Abundance=6596
October
Abundance=6470
November
Abundance=6881
December
Abundance=7105
Animals / 100 km²
> 13
10 - 13
7.5 - 10
5.6 - 7.5
4.2 - 5.6
3.2 - 4.2
2.4 - 3.2
1.8 - 2.4
1.3 - 1.8
1.0 - 1.3
0.75 - 1.0
0.56 - 0.75
0.42 - 0.56
0.32 - 0.42
0.24 - 0.32
0.18 - 0.24
0.13 - 0.18
0.10 - 0.13
< 0.10
Marine
Geospatial
Ecology
Lab

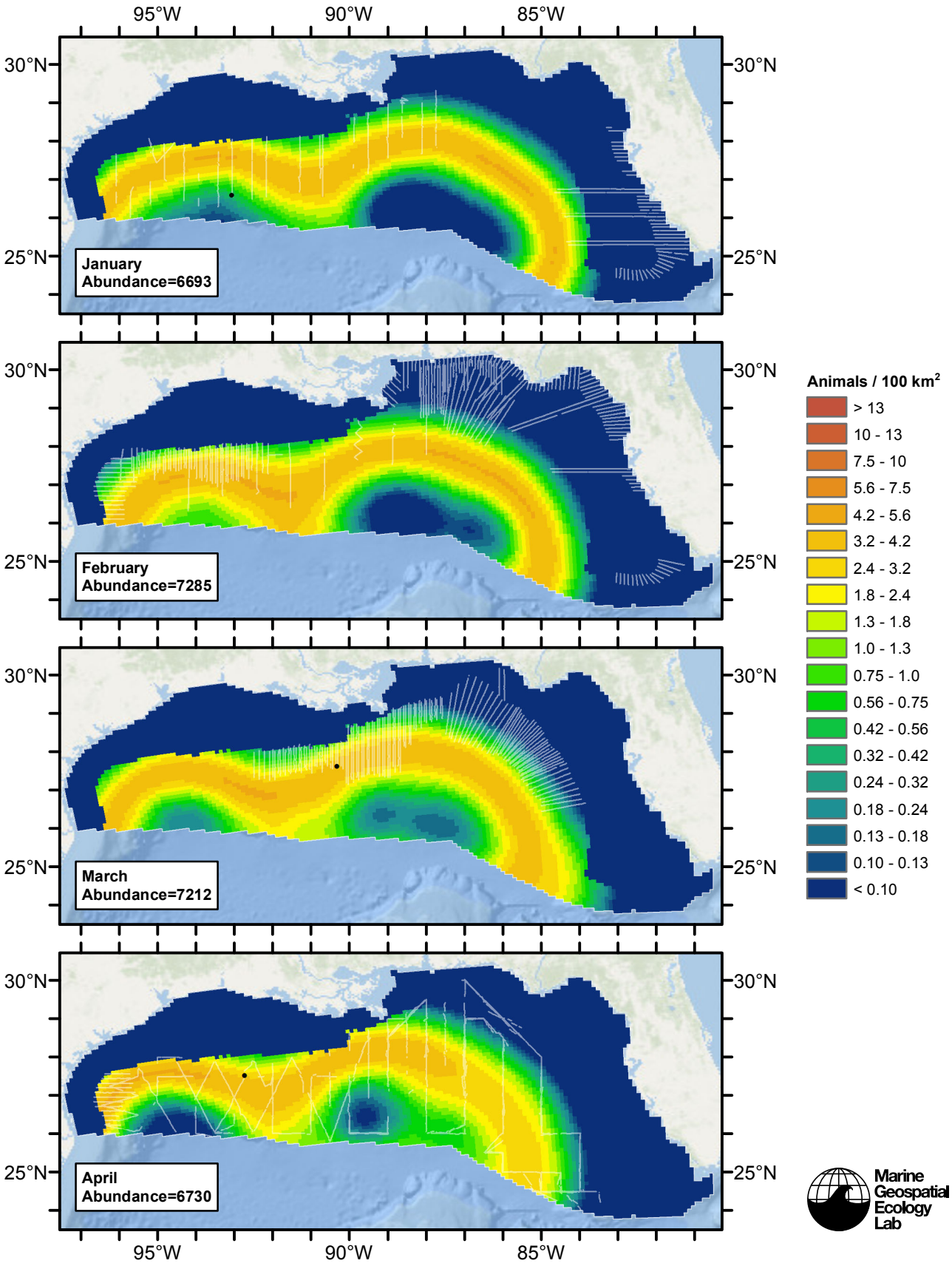
95°W
90°W
85°W
30°N
25°N
January
Abundance=6693
February
Abundance=7285
March
Abundance=7212
April
Abundance=6730
Animals / 100 km²
> 13
10 - 13
7.5 - 10
5.6 - 7.5
4.2 - 5.6
3.2 - 4.2
2.4 - 3.2
1.8 - 2.4
1.3 - 1.8
1.0 - 1.3
0.75 - 1.0
0.56 - 0.75
0.42 - 0.56
0.32 - 0.42
0.24 - 0.32
0.18 - 0.24
0.13 - 0.18
0.10 - 0.13
< 0.10
Marine
Geospatial
Ecology
Lab

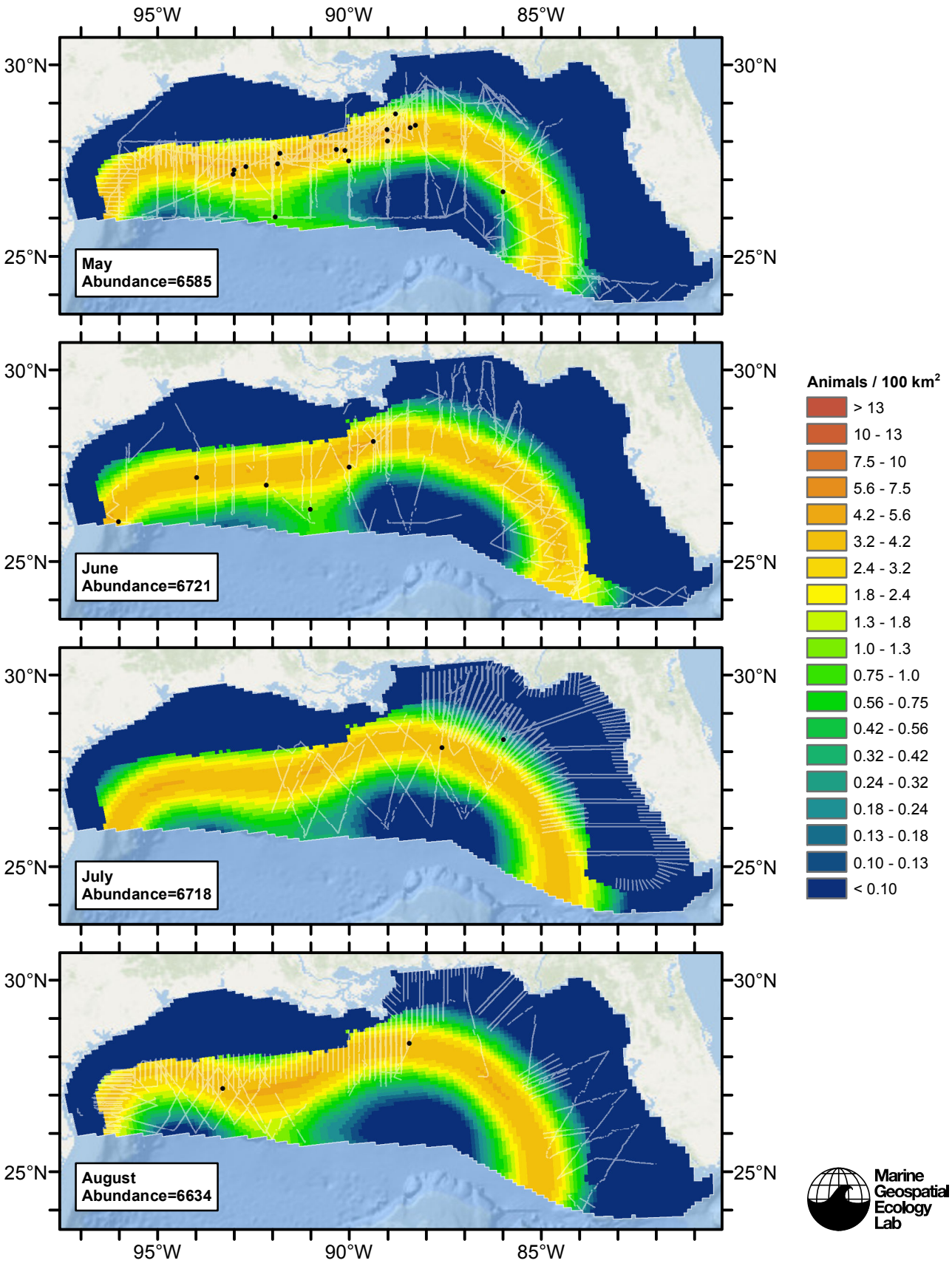
95°W
90°W
85°W
30°N
25°N
May
Abundance=6585
June
Abundance=6721
July
Abundance=6718
August
Abundance=6634
Animals / 100 km²
> 13
10 - 13
7.5 - 10
5.6 - 7.5
4.2 - 5.6
3.2 - 4.2
2.4 - 3.2
1.8 - 2.4
1.3 - 1.8
1.0 - 1.3
0.75 - 1.0
0.56 - 0.75
0.42 - 0.56
0.32 - 0.42
0.24 - 0.32
0.18 - 0.24
0.13 - 0.18
0.10 - 0.13
< 0.10
Marine
Geospatial
Ecology
Lab

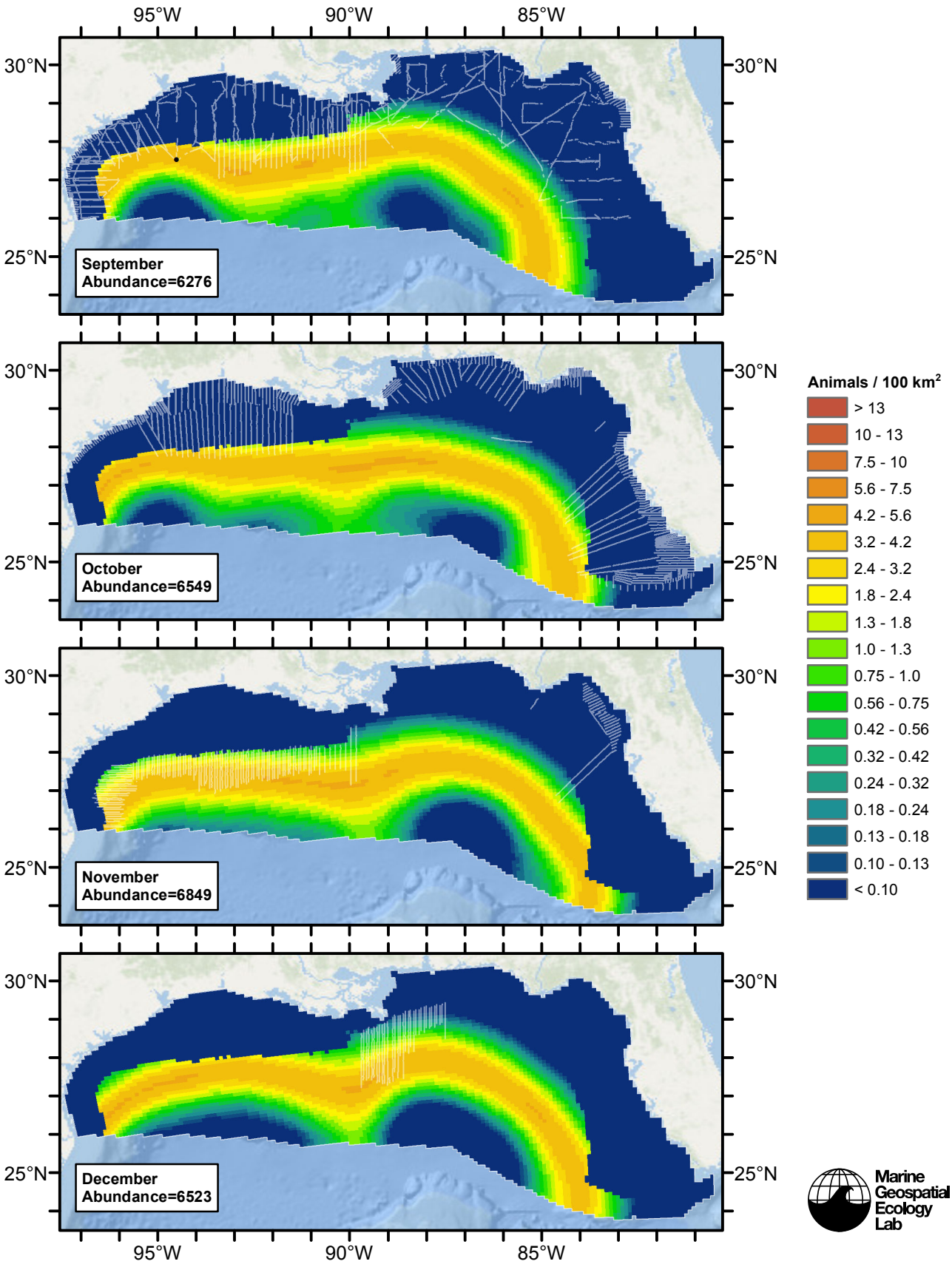
95°W
90°W
85°W
30°N
25°N
September
Abundance=6276
October
Abundance=6549
November
Abundance=6849
December
Abundance=6523
Animals / 100 km²
> 13
10 - 13
7.5 - 10
5.6 - 7.5
4.2 - 5.6
3.2 - 4.2
2.4 - 3.2
1.8 - 2.4
1.3 - 1.8
1.0 - 1.3
0.75 - 1.0
0.56 - 0.75
0.42 - 0.56
0.32 - 0.42
0.24 - 0.32
0.18 - 0.24
0.13 - 0.18
0.10 - 0.13
< 0.10
Marine
Geospatial
Ecology
Lab

Discussion

The model that included depth plus a contemporaneous predictor explained substantially more deviance than models that included depth alone or that included depth plus a climatological predictor. The contemporaneous predictor that was retained, distance to the closest eddy that was at least nine weeks old, resulted in the loss of 18.1% of the segments (from 1992 and early 1993) but explained nearly twice as much deviance as the best model with a climatological predictor. Also, the climatological model exhibited a large variation in abundance throughout the year (Fig. 52), while the average of the contemporaneous model displayed relatively stable abundance across the year. We found no reports in the literature describing large scale migrations by melon-headed whales, so we had no basis to believe the climatological model's prediction was realistic.

On the basis of clearly superior explanatory performance and stable year-round abundance, we selected the model that included the contemporaneous predictor as our best estimate of melon-headed whale distribution and abundance. This model predicted that melon-headed whales are found most often in deep waters about 150 km from geostrophic eddy cores. But because this model was based on a limited number of sightings it must be interpreted cautiously.

Because the survey effort used as input to this model was biased toward spring and summer and was spatiotemporally patchy (see maps in the Temporal Variability section above), we were not confident that any of our models could produce realistic predictions at a monthly temporal resolution. This problem affected all species that we modeled in the Gulf of Mexico, and we recommend that year-round average predictions be used for all Gulf of Mexico species.

Our best estimate of melon-headed whale abundance, 6733, is roughly 1.5-3x larger than NOAA's series of estimates, which ranged from 3965 for 1991-1994 to 2235 in 2009. Although differences between our estimates and NOAA's can sometimes be traced to NOAA's assumption that g(0)=1 and our assumption that it did not, we do not believe this played a large role with melon-headed whales. All of the sightings we utilized were of large groups, thus we assumed g(0)=0.970 or 0.960 for all of them (depending on which platform sighted them). Our best guess is that the difference results mainly from differences in detection functions. For example, in the most recent estimate for which detailed documentation is publicly available (Mullin 2007), from 2003-2004, NOAA estimated an abundance of 2283. In that analysis, NOAA's shipboard detection function had an effective strip half width (ESHW) for small dolphins of 2336m. Our shipboard detection functions had mean ESHWs of 867m and 1151m. Abundance scales inversely with ESHW, so it is not surprising that our estimate would be 3x larger when our ESHWs were 2-3x smaller.

Another contributing factor concerns the ambiguous "melon-headed or pygmy killer whale" sightings. We incorporated four of these, raising the number of sightings in our model from 25 to 29, a 16% increase. NOAA's estimates did not incorporate these ambiguous sightings, thus, all else being equal, we would expect our estimates to be 16% higher than NOAA's due to this difference.

We note that, at the time of this writing, NOAA's most recent abundance estimate of 2235 is what NOAA used to estimate stock-level parameters important to management, including the Minimum Population Estimate (Nmin) and the Potential Biological Removal (PBR). Because these estimates are low relative to the abundance we estimated, it is likely that if our results are used to estimate population-level impacts from potentially harmful human activities (i.e. "takes", as defined by the Marine Mammal Protection Act), the estimated impacts will be high relative NOAA's estimated stock size (i.e. the estimated takes will greatly exceed PBR).

There is no easy solution to this problem. One possibility is that NOAA could recalculate stock-level parameters such as Nmin and PBR using our results. But this would violate NOAA's guideline that data older than 8 years not be used to estimate stock-level parameters (Moore et al. 2011). Alternatively, impacts could be estimated using NOAA's abundance estimate of 2235, computing density by dividing this number by the total area of the off-shelf portion of the U.S. Exclusive Economic Zone in the Gulf of Mexico. But this would fail to account for the non-uniform distribution of melon-headed whales predicted by our study. Finally, in a hybrid approach, a new density surface could be obtained by apportioning NOAA's abundance estimate of 2235 proportionally according to the density surface predicted by our models. To do that, divide our density surface by our total estimated abundance (6733), then multiply every cell by 2235. To check that the result computed correctly, sum up all of the cells; the result should equal 2235. This new density surface would reflect the distribution pattern predicted by our study but use the total abundance estimate from NOAA.

Interested parties should consult with NOAA about the best way to proceed with this problem.

References

Barlow J (1995) The abundance of cetaceans in California waters. Part I: Ship surveys in summer and fall of 1991. Fishery Bulletin 93: 1-14.

Barlow J (1999) Trackline detection probability for long diving whales. In: Marine Mammal Survey and Assessment Methods (Garner GW, Amstrup SC, Laake JL, Manly BFJ, McDonald LL, Robertson DG, eds.). Balkema, Rotterdam, pp. 209-221.

Barlow J (2006) Cetacean abundance in Hawaiian waters estimated from a summer/fall survey in 2002. Marine Mammal Science 22: 446-464.

Barlow J, Forney KA (2007) Abundance and density of cetaceans in the California Current ecosystem. Fish. Bull. 105: 509-526.

Carretta JV, Lowry MS, Stinchcomb CE, Lynn MS, Cosgrove RE (2000) Distribution and abundance of marine mammals at San Clemente Island and surrounding offshore waters: results from aerial and ground surveys in 1998 and 1999. Administrative Report LJ-00-02, available from Southwest Fisheries Science Center, P.O. Box 271, La Jolla, CA USA 92038. 44 p.

Hansen LJ, Mullin KD, Roden CL (1995) Estimates of cetacean abundance in the northern Gulf of Mexico from vessel surveys. Southeast Fisheries Science Center, Miami Laboratory, Contribution No. MIA-94/95-25, 9 pp.

Hiby L (1999) The objective identification of duplicate sightings in aerial survey for porpoise. In: Marine Mammal Survey and Assessment Methods (Garner GW, Amstrup SC, Laake JL, Manly BFJ, McDonald LL, Robertson DG, eds.). Balkema, Rotterdam, pp. 179-189.

Moore JE, Merrick RL, Angliss R, Barlow J, Bettridge S, Caretta J, et al. (2011) Guidelines for Assessing Marine Mammal Stocks: Report of the GAMMS III Workshop, February 15-18, 2011, La Jolla, California. US Department of Commerce, National Oceanic and Atmospheric Administration, National Marine Fisheries Service, Office of Protected Resources.

Mullin KD (2007) Abundance of cetaceans in the oceanic Gulf of Mexico based on 2003-2004 ship surveys. 26 pp.

Mullin KD, Fulling GL (2004) Abundance of cetaceans in the oceanic northern Gulf of Mexico. Mar. Mamm. Sci. 20(4): 787-807.

Mullin KD, Jefferson TA, Hansen LJ, Hoggard W (1994) First sightings of melon-headed whales (Peponocephala electra) in the Gulf of Mexico. Mar Mamm Sci. 10(3): 342-348.

Palka DL (2006) Summer Abundance Estimates of Cetaceans in US North Atlantic Navy Operating Areas. US Dept Commer, Northeast Fish Sci Cent Ref Doc. 06-03: 41 p.

Perryman WL (2008) Melon-Headed Whale: Peponocephala electra. In: Encyclopedia of Marine Mammals, 2nd. ed. (Perrin WF, Wursig B, Thewissen JGM, eds.) Academic Press, San Diego, California. pp. 733-735.

Waring GT, Josephson E, Maze-Foley K, Rosel PE, eds. (2013) U.S. Atlantic and Gulf of Mexico Marine Mammal Stock Assessments – 2012. NOAA Tech Memo NMFS NE 223; 419 p.